

# **Establishment of a Database for Tool Life Performance**

by

Troy S. Vom Braucke

Thesis submitted for the degree  
Masters of Engineering by Research

June 2004

School of Engineering and Science  
Swinburne University of Technology  
Australia

## Abstract

The cutting tool industry has evolved over the last half century to the point where an increasing range and complexity of cutting tools are available for metal machining. This highlighted a need to provide an intelligent, user-friendly system of tool selection and recommendation that can also provide predictive economic performance data for engineers and end-users alike. Such an ‘expert system’ was developed for a local manufacturer of cutting tools in the form of a relational database to be accessed over the Internet.

A number of performance predictive models were reviewed for various machining processes, however they did not encompass the wide range of variables encountered in metal machining, thus adaptation of these existing models for an expert system was reasoned to be economically prohibitive at this time. Interrogation of published expert systems from cutting tool manufacturers, showed the *knowledge-engineered* principle to be a common approach to transferring economic and technological information to an end-user. The key advantage being the flexibility to allow further improvements as new knowledge is gained. As such, a relational database was built upon the *knowledge-engineered* principle, based on skilled craft oriented knowledge to establish an expert system for selection and performance assessment of cutting tools.

An investigation into tapping of austenitic stainless steels was undertaken to develop part of a larger expert system. The expert system was then interrogated in this specific area in order to challenge by experiment, the skilled craft oriented knowledge in this area. The experimental results were incorporated into the database where appropriate, providing a user-friendly working expert system for intelligent cutting tool selection, recommendation and performance data.

## **Acknowledgments**

I would like to thank my academic supervisors, Professor Derry Doyle and Dr. Yat Choy Wong for their advice, critique and wisdom along with Dr. Jaromir Audy. Sutton Tools Pty. Ltd. for their financial support, my industry supervisor, Robert Sutton for his encouragement and the enormous contribution of both Alan Mitchell and Jeff Boyd for their invaluable knowledge, expertise and time. Finally, thanks to my family and friends for providing me with the support network to follow my dreams.

## **Statement of original authorship**

This thesis contains no material which has been accepted for the award to the candidate of any other degree or diploma, except where due reference is made in the text of the thesis.

This thesis, to the best of my knowledge, contains no material previously published or written by any other person except where due reference has been made in the text of the thesis.

Signed .....

# Contents

---

<b>Chapter 1 Introduction.....</b>	<b>1</b>
<b>Chapter 2 Literature Review .....</b>	<b>6</b>
<b>2.1 Metal Cutting Prediction Methods.....</b>	<b>6</b>
2.1.1 Introduction.....	6
2.1.2 Empirical Method.....	6
2.1.3 Response Surface Methodologies (RSM).....	10
2.1.4 Neural Networks .....	11
2.1.5 Machining Theory / Mechanistic Model.....	14
<b>2.2 Existing Databases .....</b>	<b>18</b>
<b>2.3 Tapping .....</b>	<b>30</b>
2.3.1 Overview of Tapping .....	30
2.3.2 Tap Wear.....	35
2.3.3 Torque & Thrust.....	38
2.3.4 Deep Hole Tapping .....	44
2.3.5 Tapping Attachment and Feed Methods .....	45
<b>Chapter 3 Database Establishment .....</b>	<b>51</b>
<b>3.1 Database Structure .....</b>	<b>51</b>
<b>3.2 Work Materials Database.....</b>	<b>53</b>
<b>3.3 Tapping Module .....</b>	<b>55</b>
3.3.1 Introduction.....	55
3.3.2 Tap Surface Treatment.....	56
3.3.3 Tapping Attachment.....	56
3.3.4 Hole Depth .....	57
3.3.5 Torsional Rigidity .....	57
<b>3.4 Sort Order Algorithms and Calculations.....</b>	<b>58</b>
<b>3.5 Filemaker Database Conversion to SQL Web Server .....</b>	<b>59</b>
<b>Chapter 4 Experimental Procedure .....</b>	<b>60</b>
<b>4.1 Work Material and Hole Preparation.....</b>	<b>60</b>
<b>4.2 Tapping Procedure .....</b>	<b>61</b>
4.2.1 Tap Design .....	61
4.2.2 Experimental Set-up.....	66
4.2.3 Statistical Methodology .....	69

<b>4.3 Performance Measures .....</b>	<b>70</b>
4.3.1 Torque and Thrust Measurement Technique .....	70
4.3.2 Wear Measurement .....	72
<b>Chapter 5 Experimental Results / Discussion.....</b>	<b>74</b>
<b>5.1 Analysis of the HAAS CNC Machining Centre.....</b>	<b>74</b>
<b>5.2 Analysis of Metal Machining Performance Data .....</b>	<b>75</b>
5.2.1 Comparison of PVD Coated and Uncoated taps.....	75
5.2.2 Comparison of Tapping Attachments .....	85
5.2.3 Analysis of Cutting Tool Wear .....	90
5.2.4 Tool Life .....	98
<b>5.3 Deep Hole Tapping.....</b>	<b>100</b>
<b>5.4 Tool Rigidity .....</b>	<b>104</b>
<b>5.5 Metal Machining Conclusions.....</b>	<b>108</b>
<b>Overall Discussion .....</b>	<b>110</b>
<b>Conclusions .....</b>	<b>113</b>
<b>Future Work.....</b>	<b>115</b>
<b>References.....</b>	<b>116</b>
<b>Appendices.....</b>	<b>123</b>

## Figures

---

Figure 1.1. Graph of the categories of stainless steels showing the different microstructural phases in terms of percentage weight composition of nickel and chromium. ....	3
Figure 2.1. Zhang and Chen cutting model for conventional tapping [38].....	17
Figure 2.2. Chart of cutting speed recommendations versus thread tapping depth of the various expert systems [8-12] for M10 PVD coated spiral flute ‘VA’ style thread taps. The chart shows the different approaches to cutting speed recommendations among cutting tool manufacturers.....	20
Figure 2.3. Recommended cutting speed versus surface treatment of the various expert systems [8-10,12] for M6 spiral flute thread taps, showing the different approaches to cutting speed recommendations among cutting tool manufacturers when tapping austenitic stainless steel at a depth of one diameter. ....	21
Figure 2.4. Predicted cutting torque with surface treatments of the various expert systems [8-10,12] for M6 spiral flute thread taps, showing the different approaches to torque predictions among cutting tool manufacturers when tapping austenitic stainless steel at a depth of one diameter. ....	22
Figure 2.5. Predicted number of holes with surface treatments of the various expert systems [8-10,12] for M6 spiral flute thread taps, showing the different approaches to cutting speed recommendations between cutting tool manufacturers for various coatings when tapping austenitic stainless steel.....	23
Figure 2.6. Recommended cutting speeds for two expert systems [10,12] for M6 diameter spiral flute taps, showing the different approaches to cutting speed recommendations between cutting tool manufacturers for synchronous (rigid) and non-synchronous (axial floating) attachments when tapping austenitic stainless steel.....	24
Figure 2.7. Predicted cutting torque for two expert systems [10,12] for M6 diameter spiral flute taps, showing the different approaches to torque predictions between cutting tool manufacturers for synchronous and non-synchronous attachments when tapping austenitic stainless steel.....	25

Figure 2.8. Predicted number of holes with different tap attachments for two expert systems [10,12] for an M6 spiral flute thread taps, showing the different approaches to cutting speed recommendation between cutting tool manufacturers for synchronous (rigid) and non-synchronous (axial floating) tapping attachments. ....	26
Figure 2.9. Chart of recommended cutting speed with the tap diameter for three expert systems [8,10,12] for TiN coated taps machining stainless steel, type 316.....	27
Figure 2.10. Photograph of a thread-forming tap showing the continuous thread.....	30
Figure 2.11. Thread forming by plastic deformation of the work material [21].....	31
Figure 2.12. Straight flute taps showing three common chamfer lengths, (a) bottoming tap, (b) plug tap and (c) taper tap [51].....	32
Figure 2.13. Thread cutting taps, (a) straight flute ( <i>hand</i> ), (b) spiral point ( <i>gun</i> ) and (c) spiral flute.....	33
Figure 2.14. Spiral point tap [51].....	33
Figure 2.15. Spiral flute tap [51].....	33
Figure 2.16. End view of one land of a fluted tap, showing (a) the thread relief types and (b) the types of hook and (c) rake angles used on taps [52].....	34
Figure 2.17. 'Go/no'-go plug gauge, showing a double-ended screw that consists of two thread sizes that represent the upper (a) and lower (b) thread limits [51].....	36
Figure 2.18. Schematic of the axial and tangential forces acting on the lead taper of taps [51]. ....	39
Figure 2.19. Schematic illustration of flank cutting, which can result from excessive loading of the flanks, which results in incorrect slope of the thread flanks [51]. ....	39
Figure 2.20. A typical torque pattern in spiral flute tapping [51]. ....	40
Figure 2.21. Mean torque versus cutting speed over the life of straight flute thread taps cutting in carbon steel, showing the hyperbolic nature of the curve [66]. ....	42
Figure 2.22. Maximum torque versus cutting speed for spiral flute thread taps cutting graphitic cast iron, showing the parabolic nature of the torque results. The maximum torque results were used to clearly demonstrate the effects of low and high-speed ranges [51].....	43



Figure 2.23. A through-hole thrust pattern when thread cutting in steel at 175 rpm [33]. .....	44
Figure 2.24. Photograph of an axially compensating tap attachment with quick release mounted in a CNC machine. ....	47
Figure 2.25. Image of an auto-reverse tap attachment for a CNC machine tool.....	48
Figure 3.1. This is a schematic of the prototype database and details the navigational relationships among the pages.....	51
Figure 3.2. This is the ER diagram of the prototype database, showing all the entities about which data needs to be stored in the prototype database and how they are related to each other. ....	53
Figure 3.3. Chart of the work material application groupings showing how material properties are arranged in coloured groups according to their percentage elongation and tensile strength in $N/mm^2$ . ....	54
Figure 3.4. This is a graph of the cutting speed factor versus the hole depth ratio (depth/diameter), showing the percentage reduction of cutting speed with increasing hole depth, established by the knowledge-engineered approach. ....	57
Figure 3.5. This is a graph of a torsional strength limit for the cutting speed, verses the tap diameter for spiral flute, spiral point and forming taps, showing the percentage factor to increase cutting speed with an increase in tap diameter between the limits of 1mm and 6mm for the spiral flute design. ....	58
Figure 4.1. A schematic representation of the 45 degree helix three flute spiral tap of DIN 371 standard for ISO 2 / 6H class and nut limit used in the experiment [21]......	62
Figure 4.2. A schematic of an metric ISO standard thread form use for the taps under investigation, showing the relationships between $P$ and $H$ , where $P$ is the pitch and $H$ the thread height [21]. ....	62
Figure 4.3. A schematic of the test equipment set-up showing the Kistler piezoelectric dynamometer [74] mounted on a plate.....	70
Figure 4.4. A photograph of the Kistler dynamometer set-up in the HAAS CNC machining centre, showing an M6 spiral flute tap mounted in a non-synchronous (floating) attachment with lubricant directed at the tap flutes. ....	71

Figure 4.5. Schematic diagram of a cross section of a tap, showing the method used to measure wear of the outside diameter relief along the thread crest for one pitch, i.e. A to B.....	72
Figure 4.6. Schematic diagrams of a tap cross section (a) and a typical printed profile by the Junker CMS for one land (b) showing the method used to measure wear of the outside diameter relief along the thread crest. Cutting edge wear will decrease the measured O.D. relief from 2 to 2' shown in (b). The presence of material transfer on the thread crest at the cutting edge may increase the measured relief. ....	73
Figure 5.1. Graphs as a function of torque and thrust with respect to the number of holes tapped, for the uncoated taps using a non-synchronous tapping attachment, refer to Table 11 for data. ....	77
Figure 5.2. Graphs as a function of torque and thrust with respect to the number of holes tapped, for the TiN taps using a non-synchronous tapping attachment, refer to Table 12 for data.....	78
Figure 5.3. Graphs as a function of torque and thrust with respect to the number of holes tapped, for the TiCN taps using a non-synchronous tapping attachment, refer to Table 13 for data.....	79
Figure 5.4. Graphs showing plots of statistically analysed torque and thrust values with respect to a number of tapped holes, generated by the TiN coated taps using a non-synchronous attachment, refer to Table 14 for data. ....	81
Figure 5.5. Graphs showing plots of statistically analysed torque and thrust values with respect to a number of tapped holes, generated by the TiCN coated taps using a non-synchronous attachment, refer to Table 15 for data. ....	83
Figure 5.6. Graphs showing plots of statistically analysed torque and thrust values with respect to a number of tapped holes, generated by the TiCN coated taps using a synchronous attachment, refer to Table 16 for data. ....	85
Figure 5.7. Graphs comparing torque and thrust values for (a) non-synchronous and (b) synchronous attachments for TiCN coated taps, standard deviation not shown for clarity.....	86
Figure 5.8. Torque comparison of TiCN and TiN coated taps for non-synchronous attachment. ....	88

Figure 5.9. Thrust comparison of TiCN and TiN coated taps for non-synchronous attachment. ....	88
Figure 5.10. O.D. relief measurements of an uncoated tap for a) new, b) one hole, c) twenty holes, and d) eighty holes, showing measured relief profiles for three lands on an uncoated tap for an axial floating holder. ....	91
Figure 5.11. SEM image of a TiCN coated spiral fluted tap, showing material transfer on the surface of the thread crest near the heel edge of the tap. The box shows XRM selected area. ....	93
Figure 5.12. Relative compositional analyses using X-ray mapping, of the thread crest in the selected area (as shown in Figure 5.11), showing stainless work material transfer (Cr and Ni) and loss of PVD coating at the cutting edges (Fe and Mo). ....	94
Figure 5.13. SEM image of a full form sizing tooth and thread flanks for a new TiCN tap with the leading thread flank to the left and the rake face hidden from view. ....	95
Figure 5.14. SEM image of a TiCN tap after 450 holes using a non-synchronous attachment, showing minimal wear to the full-form sizing tooth. Inset: Magn 2000x. ....	95
Figure 5.15. SEM image of the rake face for a full form tooth of an uncoated tap after eighty holes with an non-synchronous attachment, showing adhesive wear. Magnified 2000x. ....	96
Figure 5.16. SEM image of a TiCN tap after 450 holes tapped using the synchronous attachment, showing wear and material transfer to a full form sizing tooth. ....	97
Figure 5.17. Histogram showing a comparison of tool life as measured in terms of threaded hole accuracy and surface treatment of spiral flute taps. Non-synchronous and synchronous indicating the type of attachment used. ....	99
Figure 5.18. Typical charts recorded for the torque as a function of time for hole depths 2D and 3D respectively, showing the torque to increase as the tapping progresses to the bottom of the hole. ....	100
Figure 5.19. Arithmetic mean values of the mean forward torque and maximum forward torque over ten holes with the ratio of threaded hole depth over nominal tap diameter, showing an increase in torque for increased threaded hole depth. ....	101

Figure 5.20. Arithmetic mean values of the maximum forward thrust and average reverse thrust over ten holes with the ratio of threaded hole depth over nominal tap diameter, showing an increase in thrust for increased threaded hole depth..... 101

Figure 5.21. Charts the qualitative trend in forward torque as a function of reduced tapping speed versus the ratio of threaded hole depth over nominal tap diameter, showing that after a depth of two tap diameters, reducing the cutting speed does not prevent an increase in torque [80]...... 103

Figure 5.22. Chart of the maximum torque and cutting speed at thread failure of a range of tap sizes for a tapped depth of 2D, showing the trend of increased cutting speed capability of taps larger than 5mm..... 105

Figure 5.23. Chart of the pitch and core size versus tap diameter, showing divergence between the pitch and core at the 5.0 mm tap diameter. .... 106

Figure 5.24. Chart of the pitch core ratio versus tap diameter, showing divergence between the pitch and core at the 5.0 mm tap diameter. .... 107

## Tables

---

Table 1. General extended Taylor tool life equations for turning, drilling and milling operations [15], where $T$ is tool-life, $K$ an empirical constant, $D$ , $V$ , $f$ , $a$ and $z$ are independent variables with exponents of the form $1/n$ . .....	7
Table 2. Nominal work material composition and hardness as supplied by the manufacturer [14]. .....	60
Table 3. Nominal substrate composition [71]. .....	61
Table 4. Published values and tolerances of spiral flute tap geometries given by the tap supplier for various cutting tool manufacturers for; ‘VA’ applications (Emuge, Sutton, Garant, OSG) or general-purpose $N$ applications (Yamawa, Prototyp), where VA was unavailable. ....	63
Table 5. Comparison of measured values of the cutting geometry of spiral flute taps of various cutting tool manufacturers as measured by the cutting tool supplier. ....	64
Table 6. Measured outer diameter relief for four sets of taps tested, with 5 taps in each set, showing median values with upper and lower bounds. ....	65
Table 7. Summary of experimental machining plan for three surface treatments and two attachment types. ....	67
Table 8. Experimental set-up to compare the effect of tapped hole-depth on the measured torque and thrust for TiCN coated taps. ....	67
Table 9. Experimental set-up to compare the effect of reduced tap diameter on the measured torque and hole accuracy for TiCN coated taps. ....	68
Table 10. Statistical results comparing the differences in the torque ( $T_q$ ) and thrust ( $T_h$ ) generated by the uncoated and coated taps using a non-synchronous (floating) attachment, refer to Appendix 2, Table A, for detailed statistical data. ....	75
Table 11. Statistical results of the uncoated tap’s using a non-synchronous attachment, showing differences in the torque ( $T_q$ ) and thrust ( $T_h$ ), with respect to the number of tapped holes (refer to Appendix 2, Table B, for statistical criteria). ....	77

Table 12. Statistical results of the TiN coated taps using a non-synchronous attachment, showing differences in the torque ( $T_q$ ) and thrust ( $T_h$ ), with respect to the number of tapped holes (refer to Appendix 2, Table C, for data).....	78
Table 13. Statistical results of the TiCN coated taps using a non-synchronous attachment, showing differences in the torque ( $T_q$ ) and thrust ( $T_h$ ), with respect to the number of tapped holes (refer to Appendix 2, Table D, for data).....	79
Table 14. Statistical results showing differences in the torque ( $T_q$ ) and thrust ( $T_h$ ), with respect of a number of tapped holes, generated by the TiN coated taps using a non-synchronous attachment, refer to Appendix 2, Table A, for data. ....	81
Table 15. Statistical results showing differences in the torque ( $T_q$ ) and thrust ( $T_h$ ), with respect of a number of tapped holes, generated by the TiCN coated taps using a non-synchronous attachment, refer to Appendix 2, Table A, for data. ....	83
Table 16. Statistical results showing differences in the torque ( $T_q$ ) and thrust ( $T_h$ ), with respect of a number of tapped holes, generated by the TiCN coated taps using a synchronous attachment, refer to Appendix 2, Table B, for data.....	85
Table 17. Mean values in outer diameter (O.D.) relief averaged over 5 taps for each surface condition and the three lands for each tap. ....	92
Table 18. Relative elemental constituents of the selected area detected by the EDS. ....	93

# Chapter 1

## Introduction

---

Over the last half century, the cutting tool industry has undergone a significant evolution. There has been a shift to greater use of carbide tooling and powdered metal high-speed steel (PMHSS) from high-speed tool steel [1]. Cutting tool geometry has become increasingly more complex through the introduction of CNC grinding machines. Chemical vapour deposition (CVD) and physical vapour deposition (PVD) now provide a wide range of surface coatings designed to improve the performance of cutting tools.

Advances in the design of cutting tools have introduced more complexity into the type and range of tools suited to a particular machining task. Due to increased demands for improved economic performance, cutting tool manufacturers have used two approaches to meet this challenge. One approach has been to utilise modern surface coatings and tool substrate combinations to give a greater machinability range for a general-purpose cutting tool design. The other has been to utilise the coating/substrate combinations with application specific geometries for a higher performance tool but with a narrow machinability range. These changes combined with the improved manufacturing methods have led to real gains in performance in the quality of machined components and in tool life.

Application specific cutting tools are aimed at work materials whose properties make them difficult to machine, such as, stainless steels, titanium alloys and various other alloys that each require different tool designs to achieve optimal cutting efficiency. Due to the huge range of work materials for which cutting tools need to be designed, work materials are classified into groups of 'like' machining properties. Cutting tools designed for the most common work material within a group will have the right combination of features to perform for the whole. These specialist cutting tools can be designed for individual customer needs but at a premium cost. The application specific range of tools aims to reduce this premium by selling in higher volumes to a larger consumer base. Consequently, cutting tool manufacturers now produce a large and technically complex range of tools.

This increased complexity, brought about through improved design and advances in materials technology, has made it more difficult to convey to an end-user the best method of choosing the most cost effective tool for a particular application. To date, cutting tool manufacturers have used product catalogues containing charts and technical data, to allow a user to select the correct tool and calculate the performance advantage. Inevitably, these printed catalogues outdate rapidly and often are not user friendly. To overcome this problem, manufacturers have introduced catalogues with inbuilt relational databases to allow cutting tool selection while providing performance calculations and predictions, in addition to catalogue information. Some of these have also been translated to web based systems that give improved end-user access and an opportunity to keep product information up-to-date.

The tool performance databases use various methods of calculating and predicting performance. Parameters, such as, rigidity, cutting speed, feed, hole depth, coolant and others influence cutting tool performance. The cutting tool manufacturer also has a significant effect on cutting tool performance, even when producing nominally similar general-purpose cutting tools. This link between design and performance, was statistically demonstrated by Dowey [2] in a study of tool-life performance of a general-purpose twist drill produced by different manufacturers. It is the variation in design of nominally similar cutting tools that allows cutting tool manufacturers to compete within the market. Engineers have, for many years, used cutting tool tests to establish empirical performance equations. The first of such equations was established by F.W. Taylor in the 1900's [3]. This allowed engineers to predict cutting tool performance for limited operations. As the complexity of cutting tool geometries and applications increased with the growth of the metal cutting industry, the Taylor type equations have been developed further to establish constants for tool geometry (chip formation) and work materials. Establishing empirical equations for each of the parameters requires a great deal of testing, which is time consuming and can become economically prohibitive for tool manufacturers.

Alternative methodologies to reduce the testing required for establishing reliable relationships between the cutting tool and its performance have been sought. Such predictive tool performance methods can be broadly categorised into two types, as follows:-



- Real-time on-line prediction at the end-user, monitoring tool conditions for variation from normal behaviour to predict cutting tool performance [4-7].
- Prediction for selected conditions based on a database using various decision-tree processes linked with a performance predictive strategy. These can be supplier or end-user based software packages [8-13].

This thesis is primarily concerned with the second category for predicting tool performance. Importantly, it will focus on a particularly challenging machining problem identified in the internal threading of blind-holes in stainless steel.

The consumption of stainless steels worldwide grew at an average of 6.4% per annum over the decade 1981-1990 [14] and this growth has continued. Stainless steels are essentially iron-based alloys containing amongst other alloying elements, greater than 10wt% chromium. It is the presence of chromium that provides a protective oxide film giving the corrosion resistance. Stainless steels are categorised according to the nature of their metallurgical structure. The microstructure may be made up of different phases, such as, austenite, ferrite, a combination of these, martensite or a precipitation hardened structure.

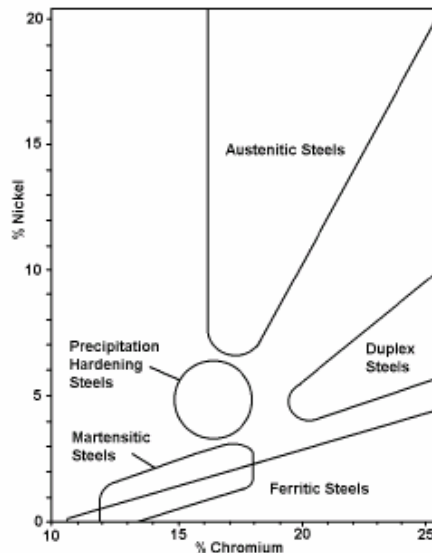


**Figure 1.1.** Graph of the categories of stainless steels showing the different microstructural phases in terms of percentage weight composition of nickel and chromium [14].

Figure 1.1 shows the relationship between the different microstructure phases in terms of percentage weight composition of nickel and chromium with the austenitic group containing at least 6wt% nickel and 16wt% chromium. Austenitic grade stainless steels are generally regarded as being difficult to machine, although alloying elements such as sulphur can be added to improve machinability at the expense of reduced corrosion resistance. In comparison to most plain carbon steels, austenitic stainless steels have a higher work hardening rate, ductility, elongation, strength and hardness. During metal cutting, the low thermal conductivity of stainless steels causes a large percentage of the heat generated by deformation and friction, to be concentrated in the immediate vicinity of the cutting edge thereby playing a significant role in reducing tool life [14]. This makes stainless steels more difficult to machine than plain carbon steels and, as such, place higher demands on the cutting tools.

Internal threading of holes, using multi-point cutting tools known as ‘taps’, requires a thorough understanding of the effects of tap design to the application. With a variety of design combinations suitable to an application, the need for a user-friendly method to both select the correct tap and to predict tap performance has become increasingly necessary. Tapping in stainless steels, has proven difficult, requiring specific taps to be developed that can offer benefits in the key areas of high speed and deep-hole tapping. Application specific taps designed for stainless steels aim to give thread accuracy with high performance over the general-purpose designs.

In industry, these application taps are commonly designated as “VA” or “Inox” application taps. “Inox” deriving from the French word “inoxydable” and 'VA' coming from German origin. To date there is no standard for producing taps for a particular group of materials or application, and consequently a range of tap designs are on the market suitable for threading stainless steel. In order to make performance predictions and selection of the taps, an understanding of how the design variations affect performance measures is required. As such, the craft oriented knowledge in this area will be challenged, in order to establish a working relational database for selection and performance recommendation of cutting tools supplied by a local manufacturer.

The structure of this thesis is as follows:

- A literature review of cutting tool, performance prediction methodologies.
- A review of databases provided by some cutting tool manufacturers and the data contained therein.
- A literature review of tapping processes with particular attention paid to application specific tapping tools for machining stainless steels.
- An experimental methodology section on the establishment of the database with attention to tapping in stainless steels.
- An experimental section studying the various performance measures in tapping of stainless steels to challenge the current knowledge and improve the database.
- A discussion section covering the results and their suitability for inclusion in a predictive database for tapping performance.
- Conclusions.

## Chapter 2

### Literature Review

---

#### 2.1 Metal Cutting Prediction Methods

##### 2.1.1 Introduction

To date a number of metal cutting theories and models have been developed with the goal of predicting cutting forces, power and tool life between the cutting tool and work material. Some of these models have been adapted to metal cutting, since initially being developed to solve predictive problems in areas other than the metal cutting industry. Section 2.1 is a discussion of these with regard to what variables have been considered, applicability to thread tapping processes and the suitability, at this time, for use within predictive cutting tool performance databases.

##### 2.1.2 Empirical Method

The accepted method for performance prediction of cutting tools is based on experimental testing. This method relies on the observation of the effect of independent variables, such as, cutting speed, feed, tool geometry etc. on machining outcomes. In this way, empirical equations can be set up from which the desired machining outcomes, such as, surface finish and tool-life can be predicted. As far back as 1907, F.W. Taylor conducted [15,16] extensive tool life tests based on tool wear-land measurement. He is credited as one of the first investigators to realise the importance of tool life prediction and the impact of economic performance models on manufacturing costs. The empirical tests performed by Taylor to establish the tool-life equation for turning operations, are commonly referred to as the Taylor tool-life tests. The basic Taylor tool-life equation is of the form:

$$T = C_1 / V^a \tag{1}$$

where  $T$ =tool life (sec)

$V$ =cutting speed

$C_1$  is an empirical constant of the form  $C_1 = C^{1/n}$

$a$  is a speed exponent of the form  $0 < (a=1/n) < 1$ .

Since the early work of Taylor, further equations have been established for drilling, milling, and turning. The equations developed are of a similar form to Equation (1), but extended to include more constants and exponents for different cutting tool geometry, tool/work material combinations and operation variables. The extended equations were necessary to keep up with the more complex cutting tools and the increasing range of work materials being used. From various manuals and handbooks, Armarego et al. [15] has tabulated the general form for these extended equations shown in Table 1, further collations of Taylor type equations can be obtained from sources in Russia, China and the United States [17-20].

**Table 1.** General extended Taylor tool life equations for turning, drilling and milling operations [15], where  $T$  is tool-life,  $K$  an empirical constant,  $D$ ,  $V$ ,  $f$ ,  $a$  and  $z$  are independent variables with exponents of the form  $1/n$ .

Turning	$T = \frac{K}{V^{\frac{1}{n}} f^{\frac{1}{m}} a_p^{\frac{1}{n_2}}} \quad (2)$
Drilling	$T = \frac{K_1 D^m}{V^{\frac{1}{n}} f^{\frac{1}{m}}} \quad (3)$
Peripheral, End - Milling	$T = \frac{K_2 D^m \delta^{\frac{1}{n_5}}}{V^{\frac{1}{n}} f_z^{\frac{1}{m_1}} a_a^{\frac{1}{n_2}} a_r^{\frac{1}{n_3}} z^{\frac{1}{n_4}}} \quad (4)$
Face Milling	$T = \frac{K_3 D^m}{V^{\frac{1}{n}} f_z^{\frac{1}{m_1}} a_a^{\frac{1}{n_2}} a_r^{\frac{1}{n_3}} z^{\frac{1}{n_4}}} \quad (5)$

The relative magnitudes of the exponents of Equations (2 – 5), listed in Table 1, reflect the relative influence of the operation variables on the tool life. The empirical constants ( $K$ ) from Table 1, represents the influence of cutting tool and work material combinations on tool life. Changes in the independent variables will change the exponents and constants requiring further tests to be run.

In a study by Armarego et al. [15], it was shown that the method of establishing the correction factors for these equations (see Equations 2-5) used a traditional international strategy for minimising testing, by allowing for the effects of variables not explicitly included in the empirical equations. Armarego et al. implied [15] that this strategy made assumptions that ignore interactions between the different variables and other work materials, and as these factors are multiplied in the equations, a small error in the correction factor can give a significant error in the result. Thus, for performance prediction with modern cutting tool geometries, surface treatments and the increasing range of work materials, the established empirical equations are no longer suitable.

Further, empirical tool life equations for thread cutting were not found in the engineering literature, although some of the databases reviewed, gave the impression that such data does exist. The latter may exist as proprietary in-house data. Cutting tool manufacturers have published torque and power equations [21,22] for thread tapping common work materials (see Equations 6 and 7 respectively). These equations have the form of the extended Taylor equations, but they differ from each other in the number of exponents used to establish cutting conditions.

$$M_D = \frac{k_c h^2 d_1}{8000} \quad (6)$$

where  $M_D$  is the tapping torque (Nm),  $k_c$  is specific cutting force value (N/mm<sup>2</sup>),  $h$  is the pitch (mm) and  $d_1$  nominal thread diameter (mm).

$$M_D = k_{c1.1} h_m^{(1-mc)} \cdot \frac{D.P.Z.Z_a}{40} \cdot T_d^{kt} \cdot T_a \cdot A_f \quad (7)$$

where:

$M_D$  = Torque in Ncm.

$k_{c1.1}$  = Specific cutting force (material constant) N/mm<sup>2</sup>.

$h_m$  =  $P/(2.Z.Z_a)$  in mm.

$mc$  = Exponent of chip thickness (material constant).

$D$  = Nominal thread diameter (mm).

$P$  = Pitch (mm).

$Z$  = Number of flutes.

$Z_a$  = Number of start threads.

$T$  = Depth of thread (mm).

$T_d$  = Factor depth of thread – Diameter.

$T_a$  = Factor depth of thread – Length of thread.

$kt$  = Factor.

$A_f$  = Bluntness factor.

It can be seen that Equation (7) takes into account more variables involved in the thread tapping process, however the publication did not make reference to a journal or study from which it was established. The inclusion of both specific cutting force and exponent of chip thickness may indicate origins from orthogonal metal cutting models (see Section 2.1.5) with factors and exponents developed from empirical tests. This researcher was unable to locate any such papers detailing the prediction of tapping torque using this particular group of variables. The two equations for torque prediction in tapping do not account for machine set-up, surface treatment or other machining variables. Therefore, they should only be considered for providing recommended torque values rather than ‘predicted’ for a cutting tool database.

It is evident that the lack of empirical equations and the large amount of machining variables involved in thread tapping, limit the use of empirically developed performance equations in a predictive database covering such a wide range of machining conditions and variables. The empirical equations for tool life and performance were enormously useful to engineers in production planning processes over the past century. However, the advances brought about through improved design, cutting tool materials technology and improved manufacturing techniques, has shown the extended Taylor equations to be reliant on a large investment in resources to maintain. This has caused many investigators to search for other methods of reducing the amount of empirical testing required.

### 2.1.3 Response Surface Methodologies (RSM)

The empirical method requires investigators to study the effects of cutting parameters on tool life by the one variable at a time approach. This requires a set of tests for each and every combination of cutting tool and work material, increasing the resources needed to conduct the experiments. When the simultaneous variation of speed, feed, and depth of cut are taken into account to predict a dependant variable (response), the approach is known as response surface methodology where the response of the dependant variable (tool-life) is viewed as a surface. For example, this allows the tool life to be plotted as a contour against cutting speed and feed, just as a land map may plot the rise and fall of the terrain with contour lines showing the height above sea level.

Wu [23] first applied response surface methodologies to tool cutting in 1964 and more recently by Choudhury and El-Baradie [24] in 1998. Choudhury and El-Baradie, applied RSM to turning operations, using empirical testing with factorial design of experiments, to reduce the relative (to one variable at a time) tests required. For later comparison, the forms of the RSM equations established by Choudhury and El-Baradie for turning are as follows:

$$T = C(V^l f^m d^n) \epsilon' \quad (8)$$

where  $T$  is the tool-life in minutes,  $V, f$  and  $d$  are the cutting speeds ( $\text{m.min}^{-1}$ ), feed rates ( $\text{mm.rev}^{-1}$ ) and depth of cut (mm) respectively.  $C, l, m, n$  are constants and  $\epsilon'$  is a random error.

Equation (8) can be written in the logarithmic form:

$$\ln T = \ln C + l \ln V + m \ln f + n \ln d + \ln \epsilon' \quad (9)$$

The linear form of Equation (9), expressed as an estimated response is:

$$\hat{y} = y - \epsilon = b_0 x_0 + b_1 x_1 + b_2 x_2 + b_3 x_3 \quad (10)$$

where  $y$  is the measured tool-life to a logarithmic scale,  $\epsilon = \ln \epsilon'$ ,  $x_1, x_2, x_3$  are  $\ln V, \ln f$  and  $\ln d$  respectively. First and second order equations can be established and statistically analysed, the parameters being estimated by the method of least squares.

RSM has to date, not been applied to the thread tapping process. If it were, the equations would require considerable modification, as the tool-life is dependant on more variables. Due to taps having a thread pitch or screw action, the feed  $F$  is fixed by the RPM and so with the cutting speed  $V$ . Depth of cut is also constant for a particular



tap design, as the depth of cut for successive teeth is determined by the lead angle of the tap (see Section 2.3.1). Therefore, other variables that influence tool-life in tapping need to be utilised potentially increasing the size of the 'factorial design' type experiments these RSM techniques are based upon. This increase in the quantity of variables to be measured introduces further complexity to the equations, possibly requiring third or fourth order equations. The RSM technique shows potential for determining optimal tool lives with reduced experimental testing in comparison to pure empirical methods, however, the resource intensive testing of the tapping operation in combination with the machining conditions and work materials still remains.

#### 2.1.4 Neural Networks

Software that mimic the structure of interconnected nerve cells within the brain are generally termed neural networks (N-N) but can have various definitions depending on subtle changes in operation. The type of networks various researchers use are made up of individual nodes, analogous to brain cells, arranged in layers. The user feeds data into an input layer, and the result emerges from an output layer. In between the two are one or more "hidden layers". Each node receives signals from nodes in the previous layer and adds them. If the total is big enough, then the node sends signals on to nodes in the next layer. The network takes information as an array of "off" or "on" states in the input layer, processes it, and generates a result as a series of off or on states. For any input, the programmer can change the result by adjusting the strength of signals sent out by a single node to others further on. At the same time, the network comes to associate certain combinations of characteristics with particular tools. And it learns these concepts without having to be fed an exhaustive set of "if-then" rules. In this same manner, the network can characterise the cutting parameters and conditions of a machining operation.

In response to the growing tests required, various neural networks that attempt to mimic higher biological functions have been employed as predictive models for various machining processes [25-27]. This means that for an individual tool manufacturer the N-N will adapt and predict for their product or used as a more general system, predict for different cutting tool manufacturers. The N-N research [25-27] has been directed towards on-line monitoring of cutting tool performance, in order to provide increased performance prediction and indicate potential tool failure. The performance of neural

network systems in this case has shown them to be dependant on an optimal training strategy for their applicability to realistic machining situations [27].

For offline systems however, training data sets will differ from an end-users working conditions and not represent the results of the end user, unless a training component is available and continually updated. Work materials from the same supplier can also vary, altering the results significantly. This is because of the reliance on training the database to establish internal coefficients or network architecture for the software to work. The result is that the database has been trained under certain conditions that may be unsuitable for another user. The variety of cutting conditions unrelated to the cutting geometries is large and presents a hurdle for researchers to overcome. Tap cutting N-N models would have to incorporate geometrical differences of tap designs into the network to distinguish results from other designs. Because of this, the main use for neural networks has been in the area of on-line prediction of cutting tool performance using sensors fitted to the machine tool. This specialisation by training of the network architecture to specific applications suggests they are not suitable for a general cutting tool database for prior predictive performance because these systems are data driven in order to refine their predictive ability.

### Polynomial Networks

The advantage of the polynomial networks over neural networks and empirical methods is they require a much smaller set of training data to develop relationships between the parameters and evolve specific to the data entered. Unlike RSM and neural networks, the technique is able to self establish or synthesize the optimal network architecture where the aforementioned methods require the network architecture in advance. A major advantage of this technique is the ability for the approach to be interpolated for different machining conditions and processes, Lee et al. [28] suggested the inability of other developed mathematical models to be readily applied in these circumstances has limited their use. The generalised polynomial equation used in a polynomial functional node is of the Ivakhnenko [29] form:

$$y_0 = w_0 + \sum_{i=1}^m w_i x_i + \sum_{i=1}^m \sum_{j=1}^m w_{ij} x_i x_j + \sum_{i=1}^m \sum_{j=1}^m \sum_{k=1}^m w_{ijk} x_i x_j x_k + \Lambda \quad (11)$$

The functional node can be expressed specifically into various types of nodes to provide different functions. These nodes are known as: normaliser, unitizer, single node, double node, triple node, and white node. These nodes are then used to construct a polynomial network. This form of network architecture has been applied to Drilling [13] and Turning [28] processes with promising results. An example of these functional nodes is as follows,

A white node 
$$y_1 = w_0 + w_1x_1 + w_2x_2 + w_3x_3 + \Lambda + w_nx_n \quad (12)$$

Interestingly, these equations are similar to the turning operation equations (see Equation 10) from the RSM technique. The difference between empirical and RSM techniques to neural and polynomial networks is that, the latter two, will evolve the network architecture which can be considered equivalent to evolving the exponents used in the empirical equations. However, neural networks, RSM and polynomial methods all require a form of empirical testing to establish and train the models. The advantage ascribed to them is the reduced testing required to establish the relationships between the individual variables and the desired output such as tool life. This is because they are able to consider multiple variables rather than the ‘one at a time’ approach used to establish the traditional empirical forms of testing.

Ultimately, the relationships established by all methods for tool life, should converge as their accuracy is improved resulting in a mathematical relation considering all possible variables. It is obvious that all prediction methods will require significant resources to develop accurate relationships. Wiklund [30] reported that the large variation in tool life reflects a complex picture of affecting sources, which indicates the difficulties in revealing simple relationships that can adequately predict tool life.

### 2.1.5 Machining Theory / Mechanistic Model

Alternative metal cutting models have been developed to either eliminate or reduce the reliance on empirical testing. To eliminate empirical testing, the use of a 'mechanics of cutting' approach was initiated to understand the metal cutting process. The models were then tested against empirical data for validation. The mechanics of cutting approach was established by various research groups to work towards optimised prediction models by using first principles in the study of machining operations [31,32]. These studies used the classical orthogonal and oblique cutting force trends.

Further, a great deal of research was published on the mechanistic modelling approach to predict cutting forces in various machining operations [4,31-34]. The mechanistic model approach uses both analytical elements to describe mechanisms at work in the cutting process and an empirical component to establish relationships [33]. A mechanistic model would have the advantage of determining ideal cutting geometries for new and different work materials once complete equations are established, leading to improved cutting tool design. Inclusion of torque, forces, power and tool life parameters into the models may allow more accurate forecasts for optimum economic cutting conditions.

With mechanistic models, there is some overlap with closed-form analytical models based on the minimum energy principle. Three closed form models have been developed to study the effects of rake angle and friction. The Merchant model predicts the shear plane angle from the rake and friction angles and requires an empirically derived coefficient of friction. The Oxley model considers the forces acting on the shear plane and the Rowe-Spick model includes temperature considerations. The latter two models both use empirical constants to calculate the final value of the shear plane angle. The difference between the analytical and mechanistic models, are that the latter were based on the assumption that the cutting forces are proportional to the uncut chip area [1,7] for which the constants are evaluated.

Mechanistic models reviewed by this researcher [4,7,33,35-38] were applied to specific problems within a machining operation. As more analysis is undertaken, the scope and accuracy of these models increases. The mechanistic model is one of the few methods that have been applied to the tapping process [4,7,33,35-38] and warrants discussion. DeVor et al. [4,7] have established models for fault detection in tapping including tap runout, axis misalignment and tooth breakage by analysing the radial force components

of the cutting torque. This is suited to online process monitoring of the cutting tool condition and would be difficult to interpret into a prior tool-life prediction model.

Cao et al. [33] has established a mechanistic model for torque and thrust prediction on straight flute tapping of 1018 steel, building on the work of Armarego [35] and Henderer [36], in which, a triangular groove cutting model was used to predict the magnitude of torque during thread tapping. The work of Cao et al. [33] allowed for different coolant types, spindle speeds and tap chamfer angles by predicting torque and thrust using a combination of an orthogonal cutting approach or chip formation model, and a friction/lubrication model. The torque and thrust models established are represented by Equations (13) and (14) as follows,

$$T = T_c + T_f \quad (13)$$

$$F_a = F_{ac} + F_{af} \quad (14)$$

where  $T_c$  and  $F_{ac}$  are the torque and thrust for the chip formation model respectively, and  $T_f$  and  $F_{af}$  are the torque and thrust for the friction/lubrication model respectively.

The general form of Equations (13) and (14) are as follows,

$$T = \sum_{i=1}^n \sum_{j=1}^{N_i} T_{ij} \quad (15)$$

$$F_a = \sum_{i=1}^n \sum_{j=1}^{N_i} F_{aij} \quad (16)$$

This research raised an interesting point on the prediction of tapping loads, showing that although a base tapping load was well predicted, random chip packing loads could be many times greater than the base load. In fact, these loads can lead to tap breakage when the chip becomes clogged in the tap flutes, the random nature of such loads cannot be predicted [33].

Neither does it account for an axial force component due to the cutting edge inclination associated with the helix angle (see Section 2.3.1) as reported by Gane [37] for straight and spiral fluted taps. The Equations (13 – 16) were established with axial spindle

synchronisation to the tap lead, limiting their use to this feed method. As many engineering shops also use the non-synchronous (floating) feed method, the equations would require alteration to account for the axial forces generated.

Cao et al. [33] acknowledge that higher torque at increased hole depths is not accounted for by this mechanistic model, proposing that, at higher hole depths there is increased chip compaction and therefore an increase in measured loads above the predicted base load for straight flute taps. Further, reduced coolant access in a deep hole has the potential to cause work hardening of the chip at the tool/chip interface in some materials [39,40] thus affecting the torque. Cao et al. provided an excellent model to expand upon, but again the suitability for use in a predictive system was limited for this present investigation.

Zhang and Chen [38] also utilised a simplified orthogonal cutting model for tapping, to predict the ratio of thread cutting torque with radial assisted vibration cutting torque and found they could reduce thread tapping torque in Titanium work materials. Their model, shown in Figure 2.1 simplifies the analyses by modeling one cutting tooth only of a tap showing the side view of a tap tooth with the contact area between tool and work material. The rake face performs the cutting action and the tool nose comprises the tool edge radius which contacts the work material at point  $D$ , and the tool relief face of length  $l_0$  and width  $b$ . Zhang and Chen proposed the theoretical frictional torque  $M_{fc}$  which is composed of relief face frictions in conventional tapping as determined by;

$$M_{fc} = R . b l_0 . \tau_s \quad (17)$$

where  $R$  is the tap radius and  $\tau_s$  is the shear strength of the work material.

These predictions were similar to those obtained from works of Armarego [35], Henderer [36] and Gane [37], but in this instance the triangular cutting area was not considered. The problem was simplified to a two-dimensional problem from the side view and was reported to have good agreement with the experimental results. Like the other models reviewed, it was limited in its practical application.

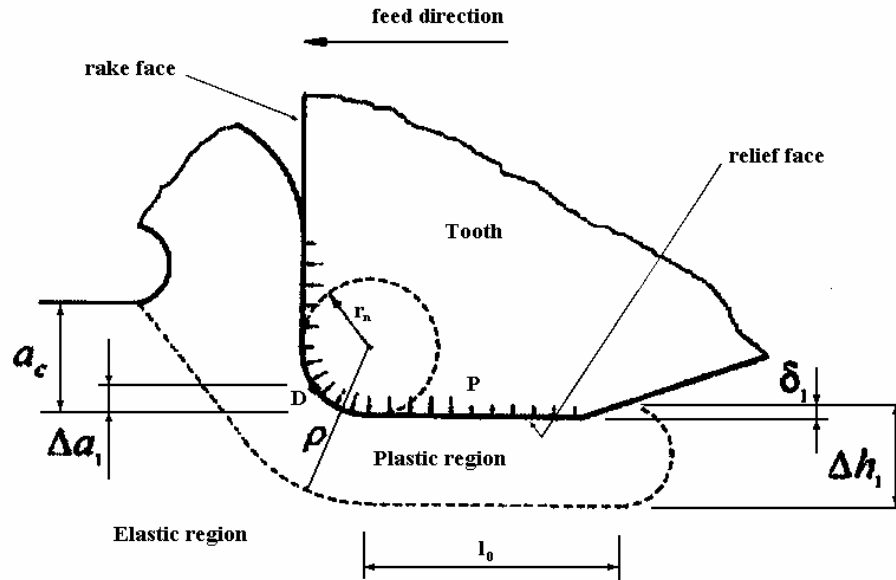


**Figure 2.1.** Zhang and Chen cutting model for conventional tapping [38].

It is evident from the above review of the mechanistic models developed, that the goal of having complete metal cutting model, particularly in tapping, will require significant investigation. The current models available for application tapping do not comprehensively consider the effects of all the tapping process conditions, PVD surface coatings, and associated effects on tool life. Many of the models also introduce new parameters, which need to be determined through extensive experimentation and thus, as with other metal machining models, the ideal goal of being totally predictive for tool life has remained unrealised [41].

With respect to metal machining, Armarego et al. [15] suggests this is still a long-term approach, before results can be utilised for the increasingly huge range of materials and cutting conditions. Therefore, the use of such models in a comprehensive cutting tool database is limited to a very narrow application range and prevents their use in the present investigation for a practical application.

## 2.2 Existing Databases

Cutting tool manufacturers now provide electronic databases, also referred to as electronic tool selection catalogues or *expert systems* [8-12], to simplify the traditional method of cutting tool selection via printed technical catalogues. Available on CD-ROM or on-line through the Internet, the expert systems contain modules for different machining processes such as Milling, Drilling, Tapping and Turning. The programs used to drive the expert systems appear to be established by *knowledge engineering*, in which, computer scientists interview skilled craftspeople and codify rules that express the craft-oriented knowledge [1].

The expert systems thus contain a series of detailed *If / then* rules that the program uses to interrogate an inbuilt relational database of cutting tool data. The rules are based on conditional statements, for example, IF; *a set of conditions is satisfied*, THEN; *a set of consequences can be inferred*. The rules combined with a form of prediction model, can give end-users the ability to obtain a recommended cutting speed, feed, and estimated tool life of the cutting tool, under predefined cutting conditions [8-12].

Researchers have also applied *fuzzy-logic* [42-44] systems to the knowledge engineering method. Fuzzy logic is described as a mathematical theory of inexact reasoning that allows one to model the reasoning process of humans in linguistic terms [42] and is formulated with if/then conditional statements to form an algorithm. The algorithm refers to fuzzy data sets of input and output variables that are discretised between a minimum and maximum value designated to control the system. A weighted response or membership function, e.g. a value residing between 0 and 1, where 0 is minimum and 1 maximum, are used to describe how the fuzzy sets overlap one another.

To date, fuzzy logic methods applied to metal machining [42-44] have been based on the knowledge and data contained within the Machining Data Handbook [45] and are therefore limited in their predictive accuracy by the experimental data used to establish the fuzzy sets of data. These knowledge-engineered approaches can be considered a sub-field of an artificial intelligence (AI) based model of metal cutting processes [1]. It is important to note that within the larger field of AI modeling, a combination of metal cutting models may be utilised [1].

Expert systems built on the knowledge of experienced engineers and manufacturers handbooks, have databases to coordinate the various cutting tools available, with the parameters and variables controlling the cutting tool performance. The cutting tool

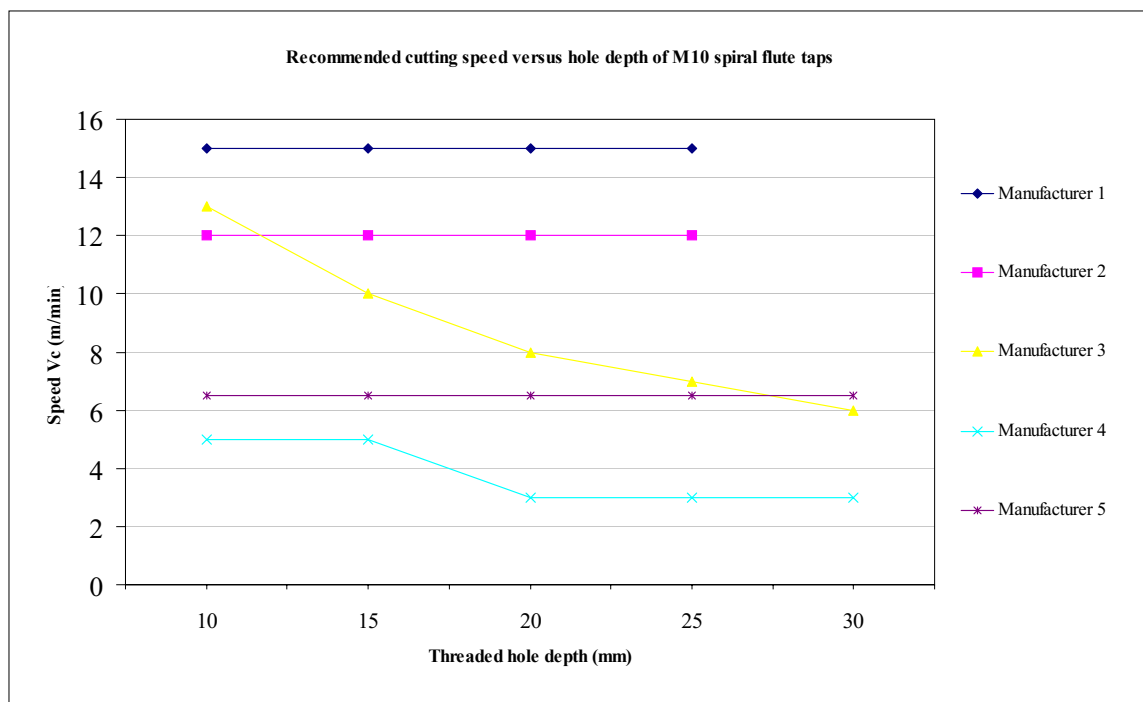


performance recommendations tend to be conservative for safe and productive machining, as with the Machining Data Handbook recommendations [45]. An expert system can, by altering the performance measures of the tool according to the decisions made by a user, demonstrate the various machining relationships in metal cutting. General machining rules incorporated into such databases, provide an underlying structure for further testing and improvement in cutting tool performance recommendation. In addition to these forms of expert systems, some cutting tool and machine tool manufacturers have offered proprietary expert software for production engineers to select speeds, feeds and predict cutting tool life embedded in machine test software and/or CAD/CAM software. These systems may be based on various metal cutting models combined with 'fuzzy-logic' to form an expert system.

Testing of cutting tool manufacturers expert systems by the present investigator and Armarego et al. [15,46,47], revealed that the predictions generally qualitatively follow accepted empirical machining rules and relationships, however quantitatively the predicted results given can be considered circumspect. An expert system utilising empirical equations, is limited in its ability to make predictions for a range of work materials, because of the lack of empirical data for modern cutting tools. Armarego et al. [15,46,47] reported that two drilling databases (expert systems) tested for torque, thrust and tool life predictions, appear not to have been backed up by an exhaustive experimental testing process, to properly establish the coefficients of the empirical equations for the tool-work combinations tested. In their studies, Armarego et al. proposed that the coefficients of the equations appeared to be assumed for different cutting conditions. These coefficients modify the behaviour of the empirical equations for various metal cutting parameters. This suggests an attempt to reduce the amount of testing required when establishing the predictive equations.

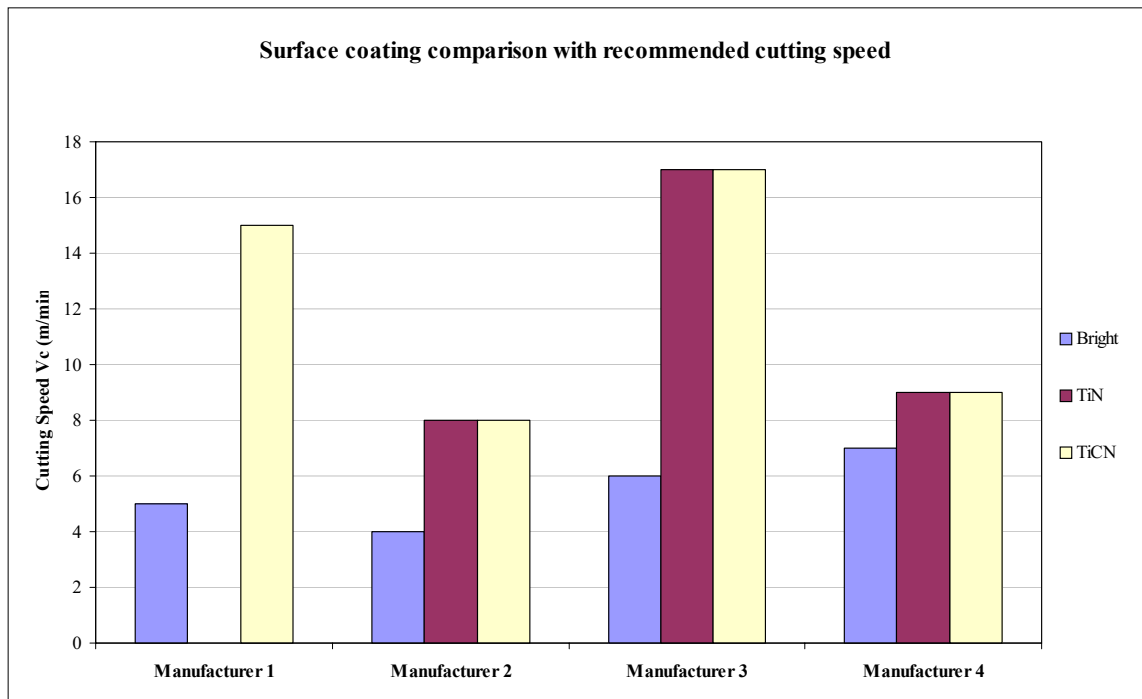
Any form of cutting tool expert system should have the capability to recommend for different types of cutting tool geometry. In thread tapping for example: straight flute, gun, and spiral flute designs of varying cutting geometries, various work materials, tool materials and lubricant types will require consideration. Some of the expert systems tested [8-10] were found to be in disagreement with competing expert systems [11,12], for example, threaded hole depth with variation of recommended cutting speed in tapping.

Figure 2.2 charts the cutting speed recommendations versus threaded hole depth, of various expert systems for diameter M10 spiral flute ‘VA’ style thread taps. This shows the different approaches to cutting speed recommendations among cutting tool manufacturers. Manufacturers 3 and 4 recommend reduced cutting speeds for tapping holes deeper than two diameters depth, the other databases show no change in recommended cutting speed for changes in thread depth. Of the two that do vary cutting speed with threaded depth, Manufacturer 3 appears to have used mathematical relationships to reduce cutting speed. A study of tap styles at each depth for Manufacturer 3, showed a series of empirical relationships were used to alter cutting speed with depth for each tap style. Manufacturer 4 shows a drop in recommended cutting speed at a depth  $\geq 1.5$  diameters, in the style of an *If / Then* rule to reduce cutting speed.



**Figure 2.2.** Chart of cutting speed recommendations versus thread tapping depth of the various expert systems [8-12] for M10 PVD coated spiral flute ‘VA’ style thread taps. The chart shows the different approaches to cutting speed recommendations among cutting tool manufacturers.

A comparison of recommended PVD coated and uncoated taps with recommended cutting speed, torque and tool life for various cutting tool manufacturers expert systems can be seen in Figure 2.3, Figure 2.4 and Figure 2.5 respectively. In each comparison, thread cutting taps were chosen for machining stainless steel grade 316, taps of similar geometry and for similar set-up conditions. From Figure 2.3, it can be seen that four of the five manufacturers offer taps in TiCN coated and bright finish. Manufacturer 1 recommended no TiN coated taps under the selected conditions.



**Figure 2.3.** Recommended cutting speed versus surface treatment of the various expert systems [8-10,12] for M6 spiral flute thread taps, showing the different approaches to cutting speed recommendations among cutting tool manufacturers when tapping austenitic stainless steel at a depth of one diameter.

Manufacturer 5 recommended only a steam treated tap in which, no comparison was shown here. It is clear that there is no distinction made between TiN and TiCN coatings for cutting speed recommendations for all the expert systems tested, where both these coatings were offered. However, the recommended cutting speeds of the PVD coated taps, were either 30%, 100% or 300% greater than the uncoated (bright finish) taps.

Figure 2.4 is a chart showing the predicted cutting torque versus the surface treatment for four of the expert systems when tapping with M6 spiral flute taps. The different approaches among cutting tool manufacturers are shown when tapping austenitic stainless steel at a depth of one diameter. Manufacturers 1 and 2, recommend no change in cutting torque for different surface finish for M6 taps. Manufacturers 3 and 4, show a slight drop in cutting torque for PVD coated taps compared to bright finish taps.

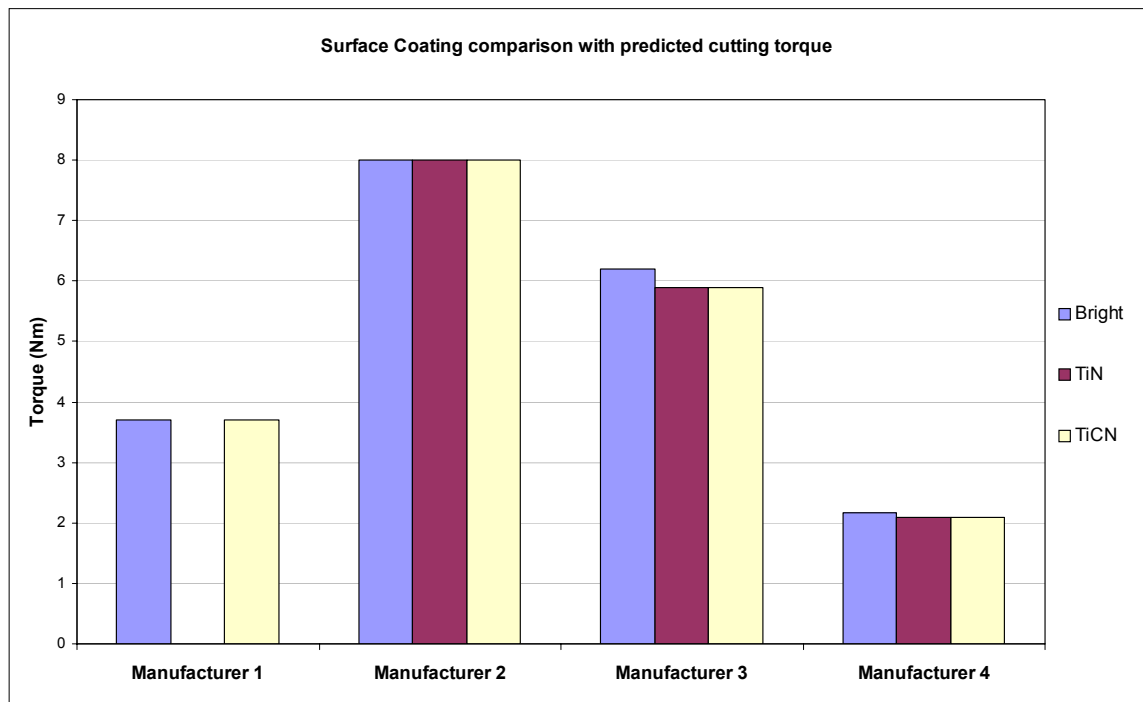
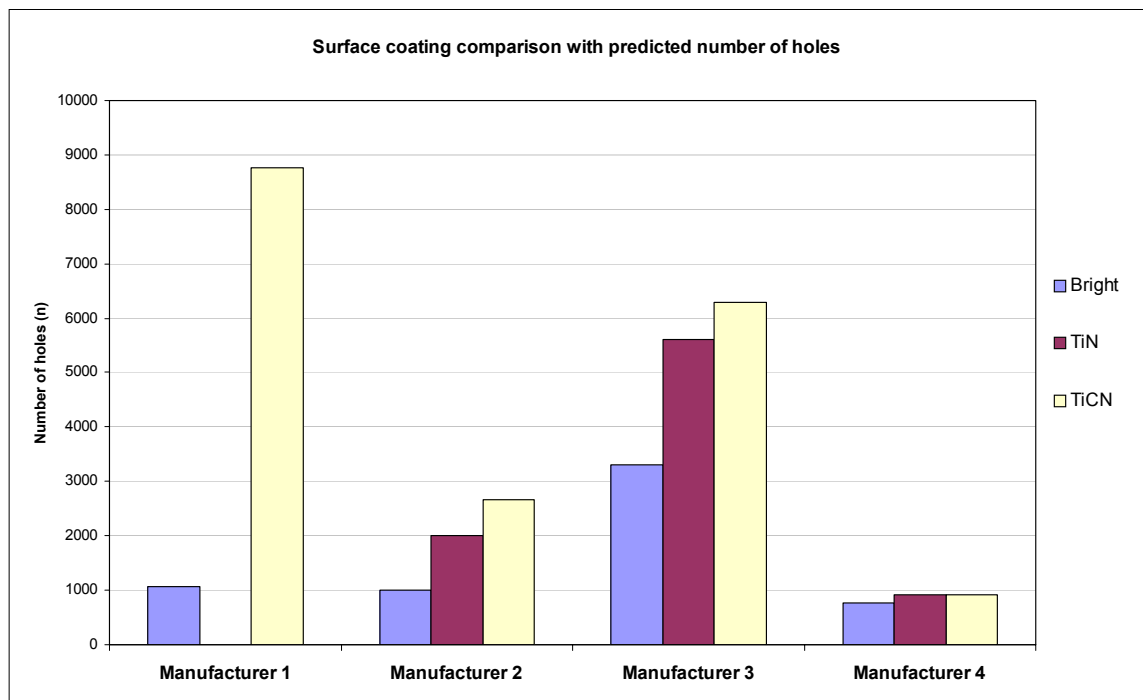


**Figure 2.4.** Predicted cutting torque with surface treatments of the various expert systems [8-10,12] for M6 spiral flute thread taps, showing the different approaches to torque predictions among cutting tool manufacturers when tapping austenitic stainless steel at a depth of one diameter.

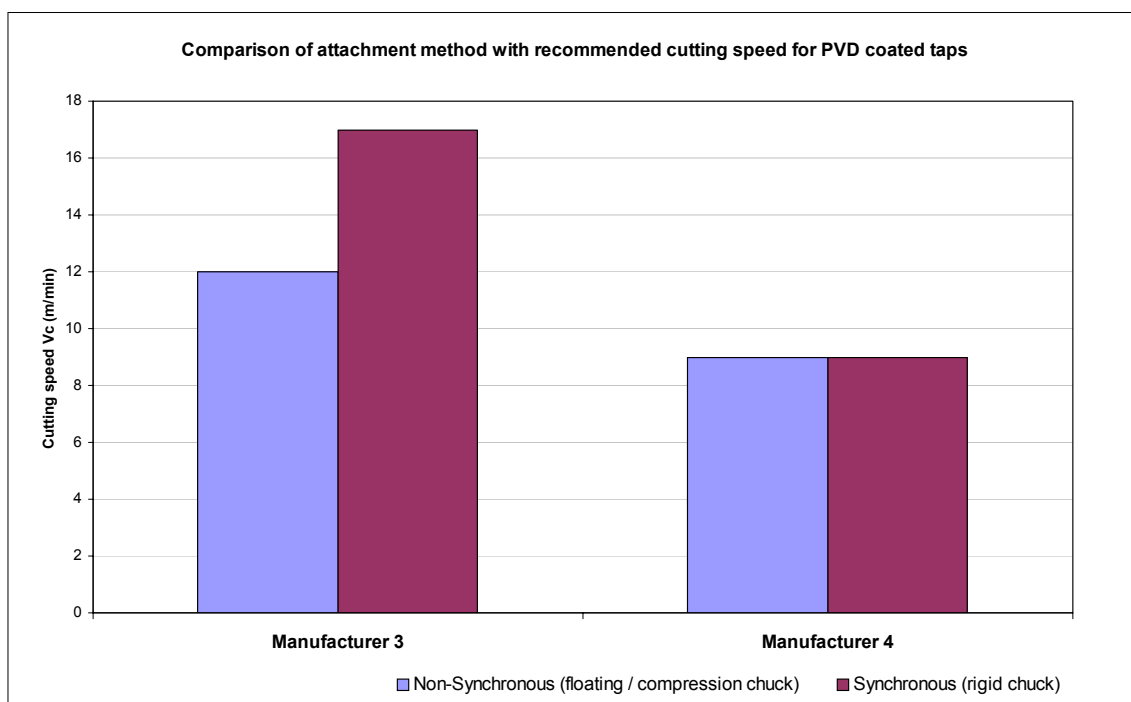
Figure 2.5 charts the predicted number of holes with uncoated (bright), TiN and TiCN surface treatments of the various expert systems for M6 spiral flute taps, showing each expert system to predict a higher value of tool life (number of holes) for the PVD coated taps. Manufacturer (4) predicts the same tool life for both TiN and TiCN coatings and only marginally higher than for the bright tap. Interestingly this set also has the smallest increase in cutting speed over the bright taps. Manufacturer (1) had the largest predicted increase in the number of holes tapped for a PVD tap compared to a bright tap

and this set had the largest difference (300%) in cutting speed between the TiN and bright tap.

Thread taps can be attached and fed into the prepared hole via a variety of tap holding attachments. There are two basic feed types, *synchronous* and *non-synchronous*, with variations of tap fixing methods to the machine spindle for each. A detailed description of the different tap attachment methods is presented in Section 2.3.5 and a discussion on the effects they have on tap performance. Only two of the expert systems have the option of selecting the tap attachment method between the tap and the machine spindle, while the other systems showed no indication of why or for what attachment method the taps were recommended.

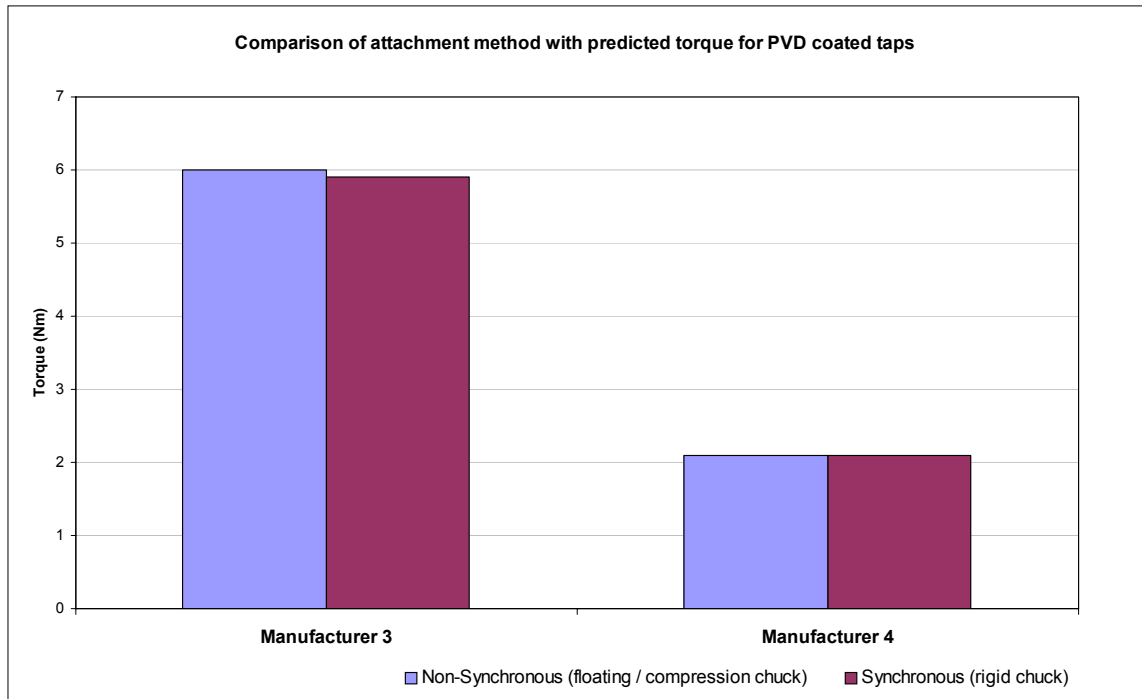


**Figure 2.5.** Predicted number of holes with surface treatments of the various expert systems [8-10,12] for M6 spiral flute thread taps, showing the different approaches to cutting speed recommendations between cutting tool manufacturers for various coatings when tapping austenitic stainless steel.



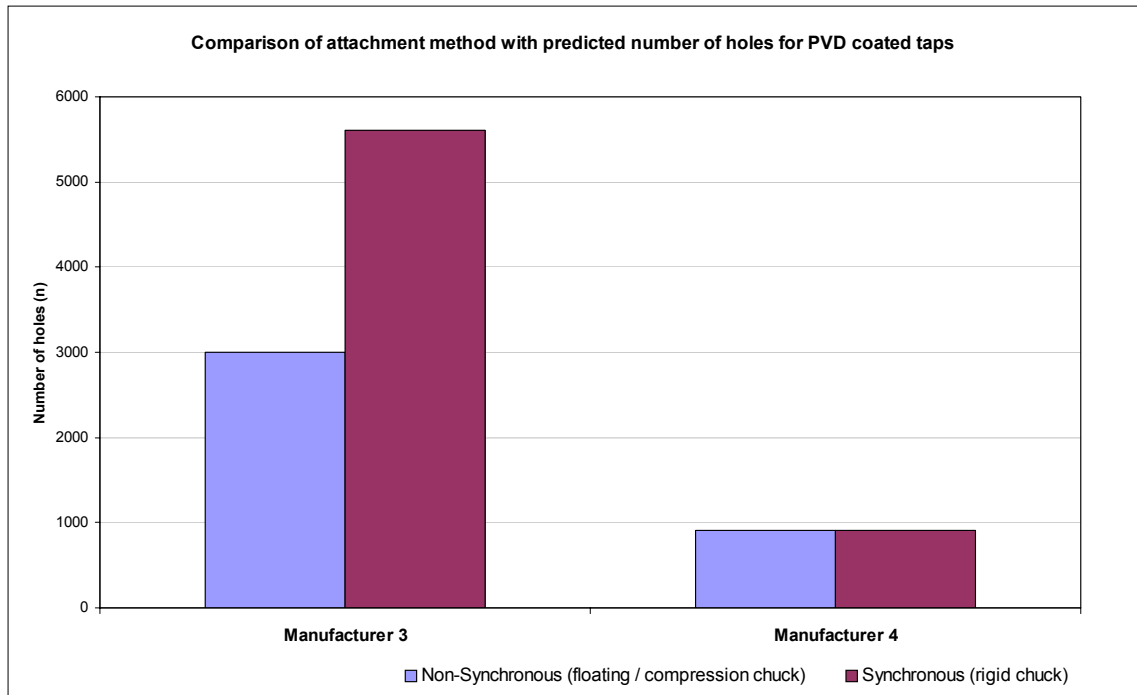
**Figure 2.6.** Recommended cutting speeds for two expert systems [10,12] for M6 diameter spiral flute taps, showing the different approaches to cutting speed recommendations between cutting tool manufacturers for synchronous (rigid) and non-synchronous (axial floating) attachments when tapping austenitic stainless steel.

Figure 2.6, Figure 2.7 and Figure 2.8 show two different approaches to the performance differences between non-synchronous (axial floating) and synchronous (rigid) tapping attachments between manufacturers (3 and 4). Manufacturer (4) recommends no change to the tap performance measures for either attachment. The selection in this case may only limit the tap designs recommended, when synchronous tapping is selected. Manufacturer (3) recommends higher cutting speed for synchronous tapping, slightly lower torque and almost double the number of tapped holes.



**Figure 2.7.** Predicted cutting torque for two expert systems [10,12] for M6 diameter spiral flute taps, showing the different approaches to torque predictions between cutting tool manufacturers for synchronous and non-synchronous attachments when tapping austenitic stainless steel.

It is generally known [48] that small taps, particularly below 6.0 mm in size, have a tendency to fail more frequently in tapping. As a consequence, cutting tool engineers often recommend reduced surface cutting speeds to compensate the frequent failure. Patil et al. [48], suggested several factors such as, incorrect tap geometry, chip jamming, and poor lubrication to be the cause and reported that many researchers have tackled the problem from different approaches such as; tap geometry, safety tap attachments and the introduction of controlled radial vibrations. The latter approach was used to analyse the optimal frequencies for introduced torsional vibrations to reduce chip jamming and built up edge (BUE).



**Figure 2.8.** Predicted number of holes with different tap attachments for two expert systems [10,12] for an M6 spiral flute thread taps, showing the different approaches to cutting speed recommendation between cutting tool manufacturers for synchronous (rigid) and non-synchronous (axial floating) tapping attachments.

Zhang and Chen [38] provide an excellent study on the effects of reducing torque by introduced torsional vibrations indicating that reduced relief face friction is achieved by repeated cutting of the machined surface in elastic materials. This was an interesting finding as it related to machining single-phase work materials (Titanium alloys) that do not form BUE [49]. Another important factor is that smaller diameter tools have a reduced torsional strength in comparison to a larger diameter tap and torsional deformation can cause an increase in effective diameter of a tapped thread [50]. So a cutting speed suitable for a 6.0 mm diameter tap, may cause thread distortion or failure for a tap of 2.0 mm diameter, requiring a reduced cutting speed to account for this. Matveev [50] established a method to calculate the effective diameter increase according to the torque applied to the shank and working section of the tap for high speed tool steel and plain carbon steel work materials.

Analysis of the manufacturers expert systems has shown only one manufacturer to adjust recommended cutting speeds for reducing tap diameter. Figure 2.9 is a chart of the recommended cutting speed with the tap diameter for three of the cutting tool



manufacturers expert systems for TiN coated taps machining stainless steel type 316. Only one manufacturer recommended reduced surface cutting speeds for taps below 6.0 mm in diameter. Taps of 6.0 mm diameter and larger did not increase in cutting speed for the design or expert systems examined.

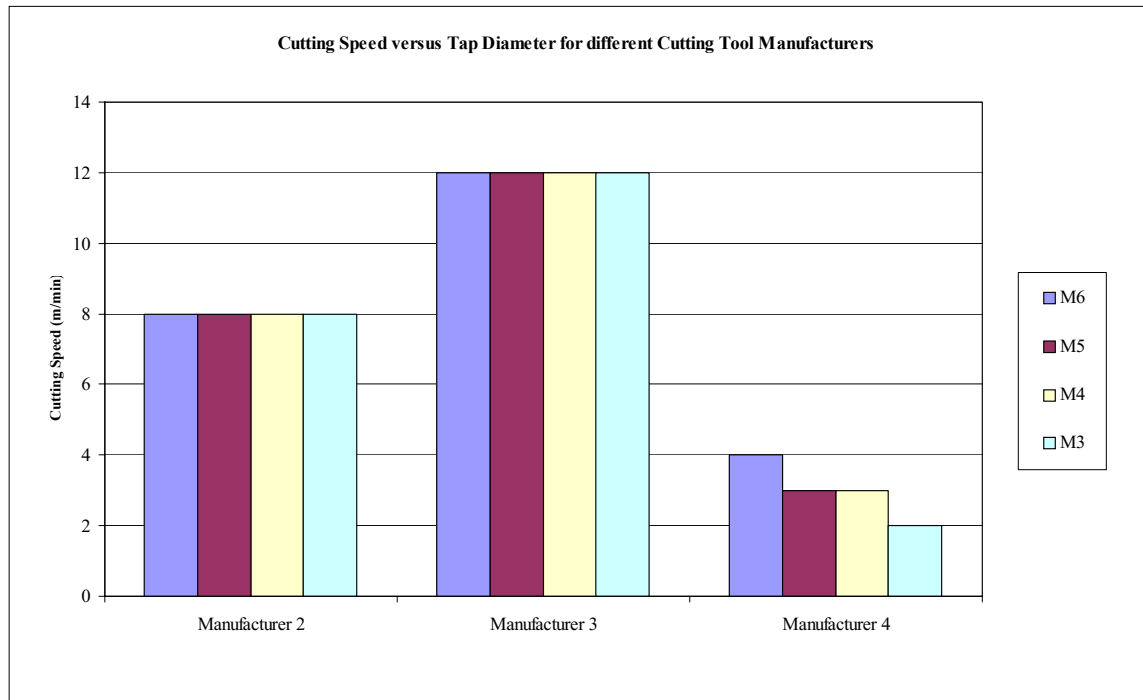


**Figure 2.9.** Chart of recommended cutting speed with the tap diameter for three expert systems [8,10,12] for TiN coated taps machining stainless steel, type 316.

In practice, tap life tests conducted in-house by Sutton of competitors taps, has not shown a great divide in cutting tool performance, consequently, variations between cutting tool manufacturers performance predictions should be small. However, the tool life predictions, cutting speed and torque recommendations from the expert systems showed large variations. This may be the result of some expert systems being established with conservative recommendations on cutting tool performance. Alternatively, if the recommendations have been established from controlled laboratory test results, the recommendations can be high and the cutting tool performance may not be realised by end-users in the field.

It has been suggested in the literature [15,30,46], that expert systems providing conservative recommendations can have significant penalties in production efficiency, because the tools may be capable of much higher cutting speeds while tool life remains acceptable. Indeed, from the current analyses of these expert systems, the large differences in performance prediction between manufacturers would raise serious doubts on production gains envisaged from the use of the expert systems in light of the comparative tests.

The difficulty for a developer of an expert system is to predict for all tool set-up possibilities, as the actual in-service tool conditions can vary greatly from the ideal set-up conditions. For this reason, the performance recommendations given in the Machining Data Handbook [45] are for a starting point only, in which the tested expert systems may be based on. From the tool manufacturer's point of view, they can only provide a conservative recommendation rather than an accurate prediction, due the large number of variables to be considered. This leaves the cutting tool manufacturer little choice of providing data that does not fall within the conservative capabilities of the cutting tool. Some of the expert systems [10,11] attempt to overcome this deficiency by providing efficiency calculators that can adjust cutting speeds, feed rate and tool life for optimised economic efficiency, taking into account tool change frequency and cutting tool cost. Information within these databases make statements to the effect, "the performance data provided within this database is a recommendation only", in which case it could be argued, that the efficiency calculators are not working with 'optimised' speeds and feeds.

An alternative approach to quantitative prediction in metal cutting is that of qualitative prediction proposed by Lo et al. [41]. This approach looks at the ideal geometry of the general-purpose cutting tool, specifically drills, that will maximise tool life for a given set of cutting conditions within a practical range by a reduction in cutting forces. Combined with rule-based selection criteria, it could also be developed for the application style of cutting tools. The use of such a system would require cutting tool manufacturers to forgo the attraction of presenting cutting tools with high tool lives as a marketing tool. However, until a reliable tool life prediction model is available, predictive tool life claims can be considered dubious [15,46] in terms of its applicability to an end-users specific cutting conditions.

Although to date the method of Lo et al. [41] does not appear to have been included within a proprietary software package, and its application to other machining processes, such as tapping and milling would require further research, it has the potential of being a helpful tool to production engineers for the selection of optimum cutting tools. With this in mind, the knowledge-engineered approach would appear to be the most consistent method of cutting tool performance recommendation for a large family of cutting tools designed for different machining processes and work materials.

## 2.3 Tapping

### 2.3.1 Overview of Tapping

Internal screw threading of holes is a critical machining process in that most other machining processes have been completed by this stage, and failure of the screw threading tool can lead to a highly value added component being scrapped. The process by which internal screw threads are produced is known as thread tapping, and the cutting tools used are called taps [51]. The thread tapping process generates internal threads by one of two methods; the formation of threaded grooves by cutting, while the second forms threaded grooves by plastic deformation. The latter method uses forming taps that are designed to form the thread instead of cutting it, therefore eliminating any chips.



**Figure 2.10.** Photograph of a thread-forming tap showing the continuous thread.

Figure 2.10 shows a thread-forming tap with a continuous thread that features lobes at three or four points around the tap circumference separated by regions of relief. Figure 2.11 is a cross-section of a thread-forming tap in a suitable work material, showing unbroken lines of grain microstructure formed around the threads. This gives stronger threads than that of thread cutting but requires additional torque of up to 50% [21]. Forming taps are particularly well suited for thread tapping ductile materials such as aluminium, brass, copper, zinc, and stainless steel.

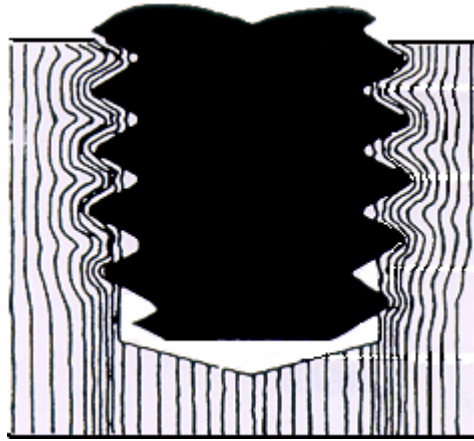


**Figure 2.11.** Thread forming by plastic deformation of the work material [21].

Thread-cutting taps are basically a screw that has longitudinal channels (flutes) formed to create cutting surfaces, providing a multiple cutting edge tool. The flutes also provide a path for the chip transportation and coolant/lubricant access (see Figure 2.12). At the leading end of the tap, a radially relieved chamfer is generated that forms the active cutting edges. The length of this chamfer dictates the number of active cutting teeth, the chip load per tooth and the limit to the depth of thread in blind holes. Furthermore, the number of active cutting teeth in the chamfered section defines the type of chamfer as either; taper (7 to 10 pitches), plug (3 to 5 pitches), semi-bottom (2 to 3 pitches) or bottoming (1 to 2 pitches) [52], as shown in Figure 2.12.

The taper chamfer is well suited to tapping difficult-to-machine metals because it distributes the cutting load over a large number of cutting edges, however, when tapping blind holes a large part of the hole is left untapped. Bottoming taps are specifically designed to alleviate this, but the cutting loads are distributed over a smaller number of teeth and consequently larger and coarser chips are produced. A trade off between these two taps is the semi-bottom tap, which uses an intermediate chamfer length so that the load is distributed over 2 to 3 teeth with minimal untapped hole remaining.

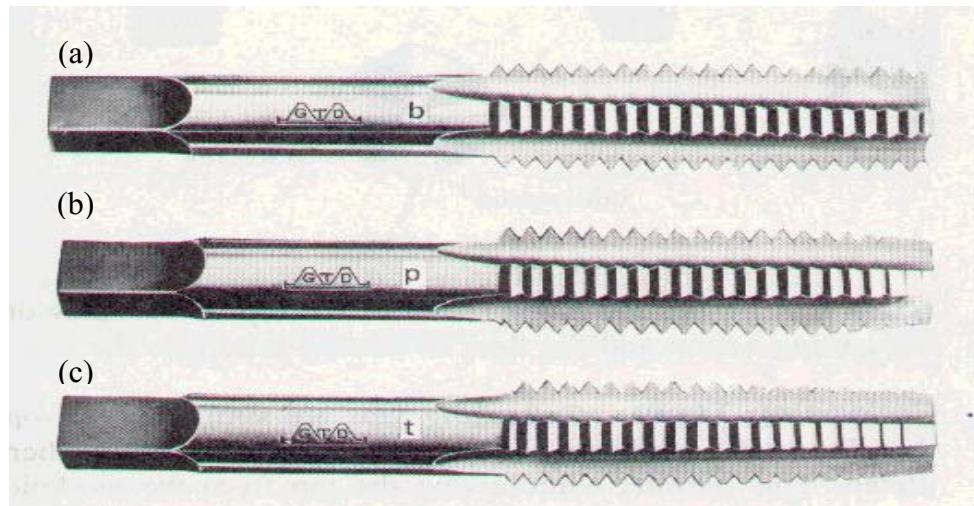


**Figure 2.12.** Straight flute taps showing three common chamfer lengths, (a) bottoming tap, (b) plug tap and (c) taper tap [51].

It is important that chips be removed from the flutes of taps during the tapping process in order to avoid tap breakage and thread damage when the tap is reversed and removed from the hole. Straight flute taps are limited in cutting speed and threaded hole depth in blind holes when used in long chipping materials, due to chip clogging in the flutes. Figure 2.13 shows three thread-cutting tap styles, (a) straight flute, (b) spiral point and (c) spiral flute, i.e. the tap style refers to the flute construction of the tap. To aid chip removal, designs (b and c) utilise the forces controlling chip transportation by an angling of the active cutting edges. This either forces the chips out in front of the tap during tapping (i.e. spiral-point taps, Figure 2.14), or draws the chips up the flutes (i.e. spiral-flute taps, Figure 2.15). This method of drawing out of chips with the spiral flute design also has the effect of driving the tap further into the hole in addition to the effect of the thread helix.



**Figure 2.13.** Thread cutting taps, (a) straight flute (*hand*), (b) spiral point (*gun*) and (c) spiral flute.

The spiral-point taps are well suited for tapping through holes, or blind holes that have sufficient room to accommodate chips in the drilled hole, as the chips are forced out in front of the tap. When chips are required to be removed from the hole and transported away from the cutting edge, the spiral fluted tap is recommended.

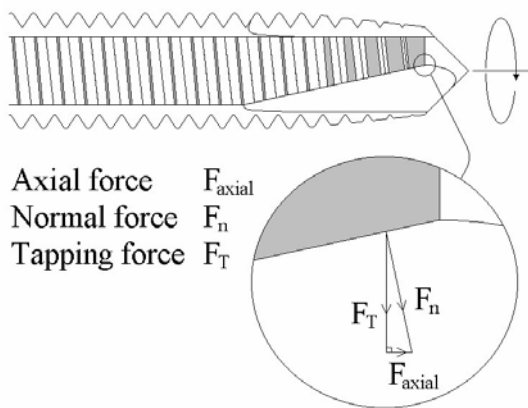


**Figure 2.14.** Spiral point tap [51].

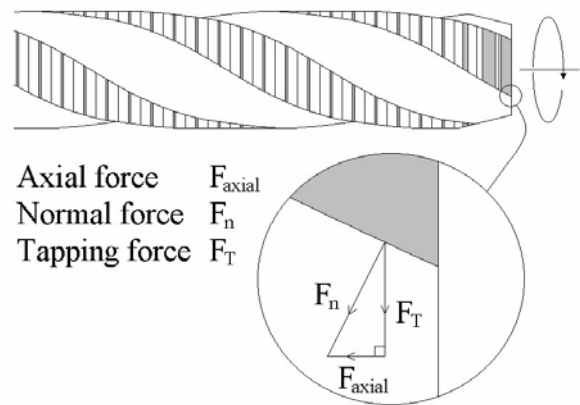


**Figure 2.15.** Spiral flute tap [51].

The *thread relief*, *rake* and *hook* of the cutting edges are also important factors in the cutting efficiency of taps. The cross section width of the non-fluted portion of a tap is called the *land* of which the leading edge is the cutting face and the trailing edge is the heel. Figure 2.16 shows schematic diagrams of one land of a fluted tap, showing (a) the thread relief types and (b) the range of hook and rake angles used on taps. The quantity of relief, rake and hook, is not subject to a national or international standard and is determined by the cutting tool manufacturer for the application.

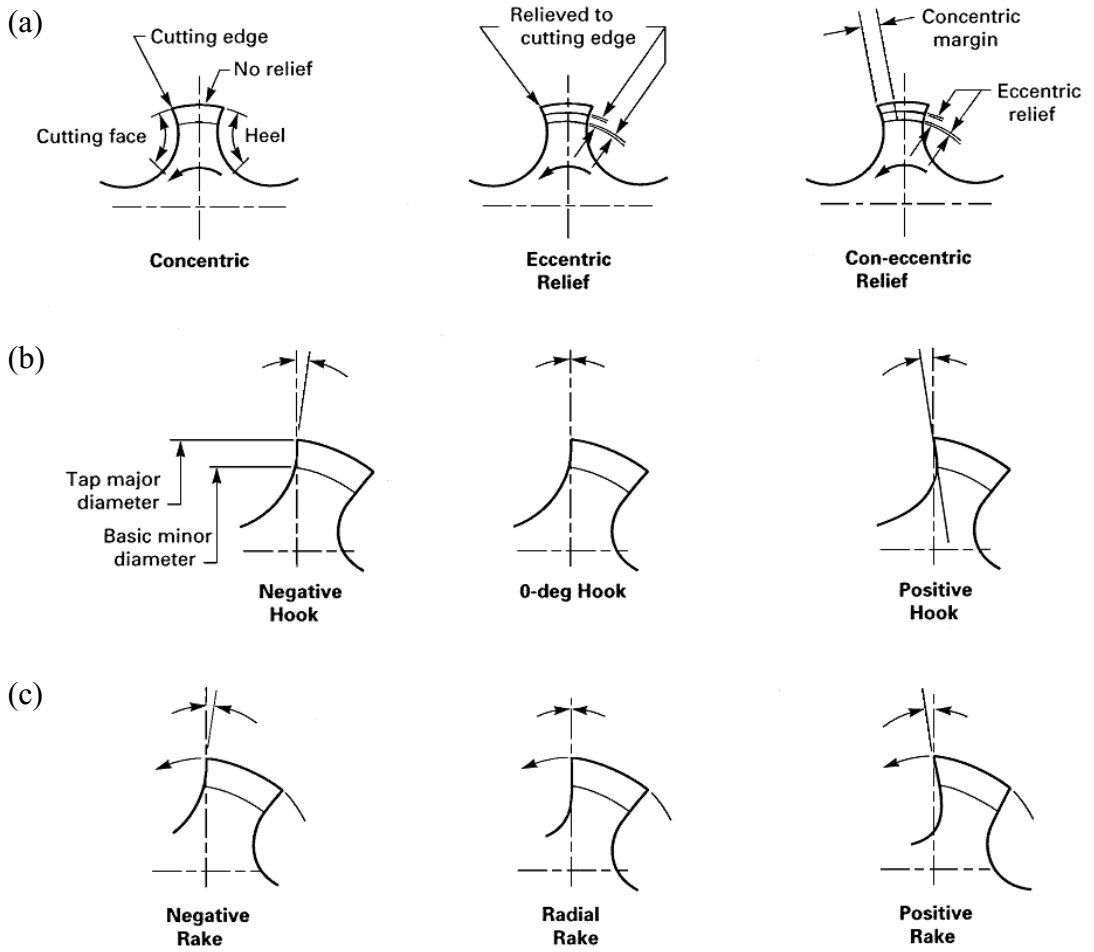


**Figure 2.16.** End view of one land of a fluted tap, showing (a) the thread relief types and (b) the types of hook and (c) rake angles used on taps [52].



### 2.3.2 Tap Wear

Large amounts of research can be found on turning and drilling, however published papers on thread tapping are less in comparison. The majority of literature on thread tapping in metals has focussed on the straight-flute style of tap designs [36,37,50,60,61,63-67], with a dearth of information on the spiral-flute tap style. It is evident from non peer reviewed engineering literature [39,40,53-58], that in the last ten years, increased research on spiral tap designs for improved performance has taken place. This is also evident by the products released by major tap manufactures and promotional claims [53] of the improved performance in tapping various work materials. These claims made in the industry magazines, are not referenced to research publications, and usually allude to in-house testing without peer-reviewed publication allowing repeatability. If referenced to scientific studies [54], those studies have not been readily available through journal publication. This is most likely due to a concern in maintaining product advantage in the market place. Tapping has been largely overlooked in terms of published research papers of standardised wear models in regard to empirical equations for tool-life, especially with the advent of modern surface coating and the associated increase in tap life. The jury is still out on the best method of measuring and gauging internal thread accuracy [59] and therefore tap life.

It appears tool life tests for taps are still not standardised as reported earlier by Turkovich et al. [60], due to the variety of options available for the selection of tool-life failure criterion and the complexity of the tap features influencing technological performance. Alternatively, the life of taps in industry, have been commonly determined by measuring the tapped hole for which standards have been established. The most widely used method for gauging internal threads is by using go/no-go plug gauges (as shown in Figure 2.17) on the threaded hole produced by the tap [59]. These gauges are effectively a double-ended screw consisting of two thread sizes that represent the upper and lower thread limits.

The gauges simultaneously check the maximum size of the pitch diameter, together with the thread form, pitch, straightness and roundness, and also ensure that the root radius does not encroach on the thread flanks based on AS-1014 standards. If the larger of the screw gauges can be screwed into the tapped hole then the internal thread is deemed oversize. This is typically experienced when new taps are supplied oversize, rather than when changes in tap geometry occur throughout the life of the tap. If excessive axial

thrust occurs there is potential for the first few threads to be oversize, known as *bell mouching* in some soft materials.

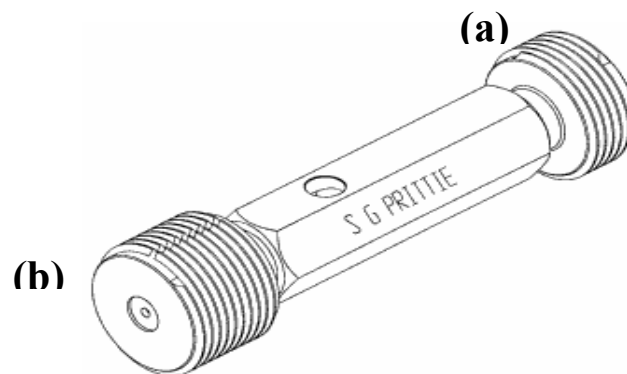


**Figure 2.17.** 'Go/no'-go plug gauge, showing a double-ended screw that consists of two thread sizes that represent the upper (a) and lower (b) thread limits [51].

The more common scenario for gauging the life of taps is by measuring tapped holes with the smaller end of the screw gauge. The latter detects incomplete tapping, which occurs as the thread profile is eroded due to wear at the cutting edge. Notwithstanding the formation of wear lands at the chamfered cutting teeth, which occurs early in the life of taps, the ultimate performance of taps is determined by the extent of wear at the full form teeth which size the final thread profile. It has been argued that failure of a threaded joint can also be attributed to loosening - placing greater emphasis on tapped thread form as the measure of tap life – and whether fixed plug gauges are sensitive enough to determine a fault [59]. With the advent of modern computerised measuring machines (CMM), the ability to measure various thread dimensions allows control charts, capability studies and tool life studies to be undertaken. Small internal threads may still present a problem, however dedicated CMM devices are available for measuring external threads and taps.

Wear inflicted on a thread tap can occur in a number places on the tap and by a variety of tribological processes. As stated previously, it is common for the chamfer cutting teeth to experience wear early in the tap life. The form of this wear depends on the number of holes tapped, properties of the tap substrate, surface coating and work material among others. It was found in previous research [60]; that in high chromium steel, cutting edge damage began with micro-chipping on incomplete threads of the chamfered section of the tap; and in softer materials gradual wear occurs with

occasional chipping being promoted by micro-fracture. The nature of this wear has been investigated by Doyle et al. [61] and confirmed by Turkovich et al. [60], in that two modes of fracture appear to occur on the cutting teeth: cleavage (brittle) fracture at the bottom of the rake face, and ductile fracture at the thread crests.

The chamfer teeth make the initial depth of cut, followed by the full form teeth for the finishing cut to size the thread. Wear progresses along succeeding chamfer teeth until the first full thread and then as that suffers wear the next full thread will size the tap. As the load applied to these full threads increases, the thread crest will start to wear and affect the maximum diameter cut by the tap. Wear on the finishing teeth will lead to the plug gauge failing the *go* limit (minimum tapped size). Gane [37] has shown by grinding the tooth corner and crest individually, that corner wear of the tooth has a greater effect on torque than wear on only the tooth crest with a rougher thread being produced along with a wider cut. In practice, both the corners, crest of the tooth, flanks, rake face and relief lands would experience wear.

Research [62] on the effect of PVD surface coatings on cutting tools, has shown that large increases in wear life can be found and importantly thrust forces can be reduced in drilling at high speeds in comparison to uncoated drills. Recent research [51] with PVD coatings on thread cutting taps has also shown wear life to increase, however it was also suggested the lower frictional properties of the PVD coatings (often cited for reduced torque and thrust) have a negligible effect on tapping torque during thread cutting.

### Tap wear and Stainless Steels

Smart and Williams [49] have shown that for two-phase materials, BUE was observed from the commencement of cutting and remained for cutting speeds below 100 f.p.m. (30m/min). In contrast, machining single-phase materials were not observed to develop built up edge (BUE) at the tool chip interface. However, only small amounts of a second phase impurity can cause BUE to form [49]. The austenitic stainless steel (18/8/1) tested by Smart and Williams, was considered a two phase metal in that the carbon content was high, giving rise to a high carbide content with a high proportion of ferrite observed.

Given that the typical percentage composition of austenitic stainless steel reported by steel suppliers [14], is at least 16wt% chromium and 6wt% nickel with less than

0.08wt% carbon, austenitic stainless steels are considered single-phase materials, and should not contain ferritic grain structure. Therefore, it could be assumed that minimal or no BUE should form at the cutting tool edge. However, at the tool-chip interface, rubbing contact between cutting tool material and work material during metal cutting may allow work material transfer to the cutting tool surface at low cutting speeds [1], irrespective of BUE formation.

### 2.3.3 Torque & Thrust

The forces generated during tapping are strongly dependent on a number of factors, not the least of which is the complex geometry of these multi-point cutting tools. The forces can be considered as either radial cutting forces or axial feed forces. The latter is influenced by the feed mechanism adopted and the tap geometry. As a result of the inclined angle of the lead taper (see Figure 2.18), an axial component of force is generated against the direction of tapping. Consequently, taps require an initial external axial force that acts in the feed direction to engage the foremost chamfered cutting teeth with the workpiece. Once this engagement has commenced and the first few threads are partly machined, the axial feed force is borne by the flanks of the active cutting teeth and the external axial force is no longer required to drive the tap into the hole. Notwithstanding this self-driven axial feed, it is not uncommon in industrial practice for taps to be mechanically advanced at a feed rate of one revolution per pitch. The latter improves hole accuracy by avoiding excessive loading of the flanks that can result in flank cutting, which leads to incorrect slope of the thread flanks (see Figure 2.19).

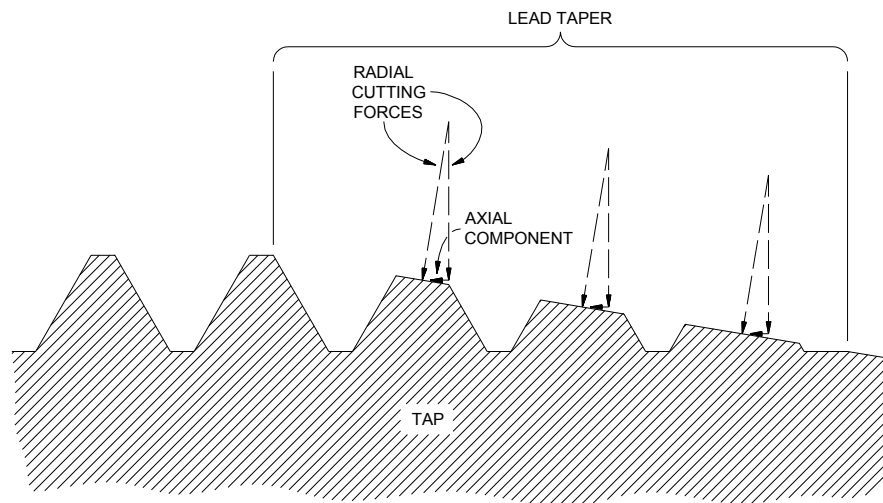


**Figure 2.18.** Schematic of the axial and tangential forces acting on the lead taper of taps [51].

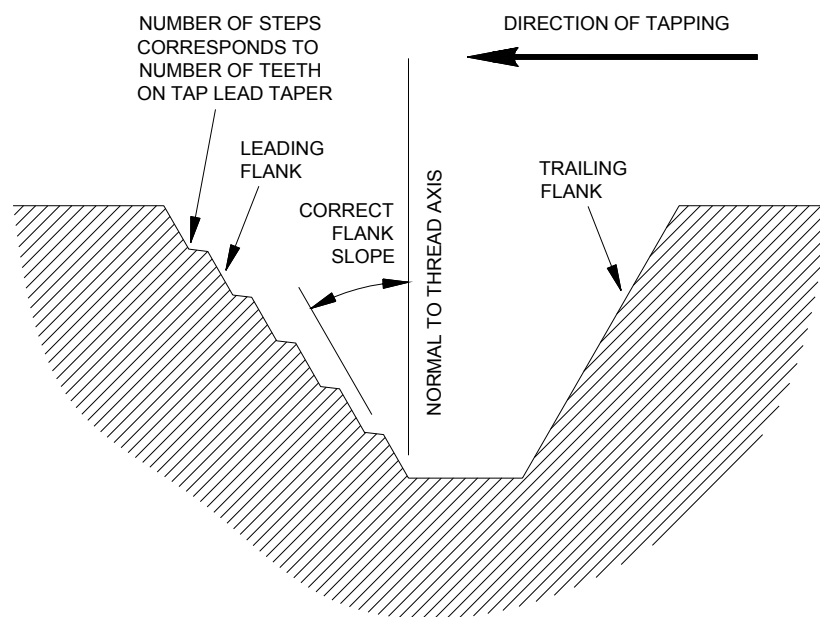


**Figure 2.19.** Schematic illustration of flank cutting, which can result from excessive loading of the flanks, which results in incorrect slope of the thread flanks [51].

The above considerations do not take into account the cutting edge angle relative to the flutes, namely the oblique cutting actions of spiral-point and spiral-flute taps. The oblique cutting action of the spiral point creates a shearing action at the cutting edge that generates an additional axial component of force that opposes the feed direction (see Figure 2.14). In contrast, the oblique cutting action of spiral flute taps generates an axial component of force that acts in the feed direction and forces chips up the flutes

(see Figure 2.15). These additional components of axial force can amplify the loads on the flanks and exaggerate the extent of metal cutting that occurs in these regions. Axial thrust forces have been studied in some detail for the forward cutting portion of tapping on straight flute taps in various work materials. From the literature, these studies have observed the effects of; torque, flank cutting, pitch diameter, lubricant, cutting speed, chamfer and thread relief on the measured axial thrust [33,37,63].

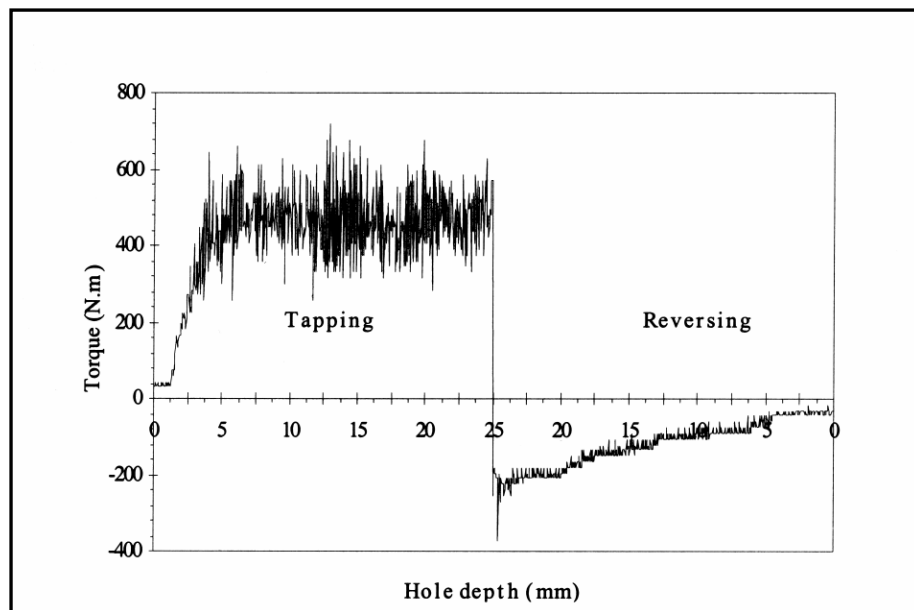


**Figure 2.20.** A typical torque pattern in spiral flute tapping [51].

The torque pattern shown in Figure 2.20, is one in which, torque increases initially as the chamfered cutting teeth engage with the work material until all the active cutting teeth are engaged. At this point, the torque reaches a plateau for the length of the hole. On reversal, the torque reaches a maximum negative value and reduces to zero as the tap exits the hole. A thrust pattern appears similar to the torque pattern however inverted. The thrust is inverted due to negative thrust acting on the dynamometer. This indicates the self feed action of the tap as it pulls on the dynamometer. A small positive thrust is commonly seen on tap entry into the prepared hole before the cutting teeth engage and self drive the tap.

Research on the effects of tap-holding and feed methods has shown significant influence on axial thrust [63, 64, 65] during thread cutting with straight flute taps. However, it is evident that a great deal of confusion exists about the usage and benefits of the different

tap holding methods in terms of axial forces produced and the effects on technological performance measures outside of the scientific literature. In fact, the cited research [63,64] on tapping attachments, investigate axial thrust effects on manual and semi automatic machine tools. Articles published in the last decade in metal cutting and process engineering magazines, relates to current discussion on the advances in CNC operated machine tooling and the tapping attachments developed for such machines.

These attachments appear to be further developments of the tap holders designed for non-CNC machines with only vague references to research showing improvements on technological performance measures. Product advertisements by manufacturers of tapping attachments cite end-user results as evidence for improved performance [64]. With increased use of spiral fluted taps tapping difficult materials such as stainless steel on CNC machinery, the effects of axial thrust on technological performance measures and the benefits of the holding and feed method of the tap are required. A discussion on the various tapping attachments follows in Section 2.3.5 .

Valuable research has been conducted on the cutting torque (radial forces) in thread tapping with regard to the various geometric features and cutting conditions. Grudov [66] studied the effect of cutting speed on torque for various types of steels with 3-flute machine taps of M12 size measuring tooth flank wear. It was found that in the initial period of work before wear, no noticeable increase in torque was observed. With further increases in wear, torque increased, interestingly a greater rate of wear was observed at low cutting speeds, i.e.  $\sim 2$  m/min compared with  $\sim 20$  m/min. The influence of measured flank wear was approximately doubled over that of the latter cutting speed with the life of the taps at 2 m/min and 20 m/min, being  $\sim 600$  holes and 2000+ holes respectively. It showed that the influence of cutting speed on the mean torque over the life of the tap was significant and is illustrated in Figure 2.21, with the recommendation of increased cutting speeds when tapping these types of steels.

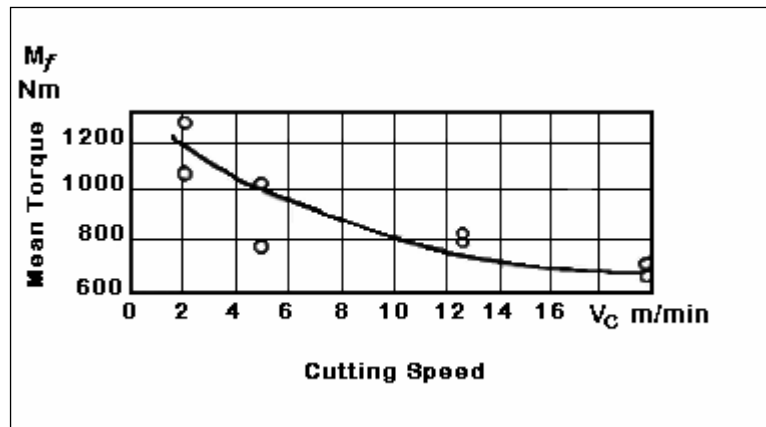


**Figure 2.21.** Mean torque versus cutting speed over the life of straight flute thread taps cutting in carbon steel, showing the hyperbolic nature of the curve [66].

Grudov [66] also suggested that when tapping steels of increased ductility at higher speeds, the torque might increase rather than decrease due to less favourable chip formation and removal conditions. Other researchers [37,67] have reported that tapping torque is usually a quadratic function of the log of the cutting speed and contrasts to Grudov's findings of a hyperbolic speed effect on torque. Moreover, the quadratic function does not follow the general relationship found for other machining processes in metal cutting theory [67] as discussed in the preceding sections. Lorenz [67] explains this hyperbolic behaviour seen by Grudov [37], as part of a parabola, which reaches its minimum at the speed limit of the experiments for the tap geometry in his investigation.

Harris [51] reported a similar quadratic function of torque to Lorenz on the effects of cutting speed with measured tapping torque in tapping cast iron using various PVD coated spiral fluted taps. Figure 2.22 shows the increased torque at low cutting speeds (Harris proposes this to be an effect of increased BUE formation known to occur for low speed machining in some cast irons) continuing in a parabolic trend through a minimum to a maximum torque. However when comparing spiral fluted taps with spiral point (gun) taps under the same conditions, the latter did not show increased torque in the lower range of cutting speeds tested. This may be explained by the differences in cutting geometry and chip disposal. Therefore, the point at which torque increases for reduced cutting speeds may not be seen at the same speeds as for spiral flute taps.



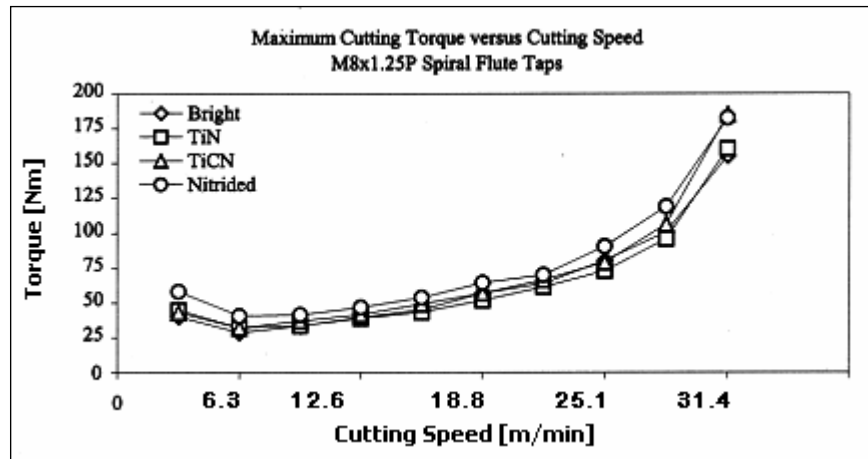


**Figure 2.22.** Maximum torque versus cutting speed for spiral flute thread taps cutting graphitic cast iron, showing the parabolic nature of the torque results. The maximum torque results were used to clearly demonstrate the effects of low and high-speed ranges [51].

Lorenz [67] has found the interactions between the cutting speed and chamfer relief to be a major influence on tapping torque when tapping CS1114 free-cutting steel and that increased thread relief combined with chamfer relief  $>3^\circ$  can reduce tapping torque. Thread relief was found to have less of an influence on tapping torque for chamfer angles between 2 and 3 degrees, and insensitive to effects of cutting speed on torque within this range. The effect of rake angle on dimensional tolerances was also studied, conclusions on its effect with torque by statistical analysis found that deviation of the rake angle from an ideal will increase tapping torque.

The lubricant used for a tapping operation can have significant results on torque and wear, as shown by tests completed at CSIRO [37, 67]. This research has shown that cutting fluids in straight flute tapping can have different effects on torque at different cutting speeds, and the effect of coolant should be studied at a minimum of three different cutting speeds due to the quadratic relationship observed between torque and cutting speed.

In fact, researchers have found with a change in cutting speed, a different coolant may be necessary [67,68] as tool life can be increased at a higher cutting speed because of improved coolant performance under specified cutting conditions. Extreme-pressure additives to cutting fluids will have an ideal performance range and may well be the reason for such effects.

Cao et al. [33] included coolant effects in the reported model by examining the change in frictional coefficient between the cutting tool and work material under simulated conditions. An important finding of this test was that the sliding speed was significant for all lubricating conditions including ‘dry’ sliding on the measured frictional coefficient. Interestingly, the cutting tool manufacturer’s expert systems show recommended surface cutting speed to be independent of coolant type used [8-12]. Thus, from the research conducted, expert systems that use models to predict tap performance measures e.g. torque, must also consider lubricant type and attachment method for various work materials.

The literature shows thrust [33] and torque [63] patterns when tapping in steels for only the forward motion of thread cutting. The thrust pattern in Figure 2.23 shows a spike in the pattern attributed to chip packing [33] toward the bottom of the hole. Taps are known to break on reversal in blind hole tapping of tough materials such as stainless steels [69], however from the literature, the withdrawal component of the torque pattern has only been found for tapping in cast iron (see Figure 2.20). The literature [37,48,63,64,67] suggests that these patterns for thrust and torque may be different with various tap attachments for the forward tapping component.

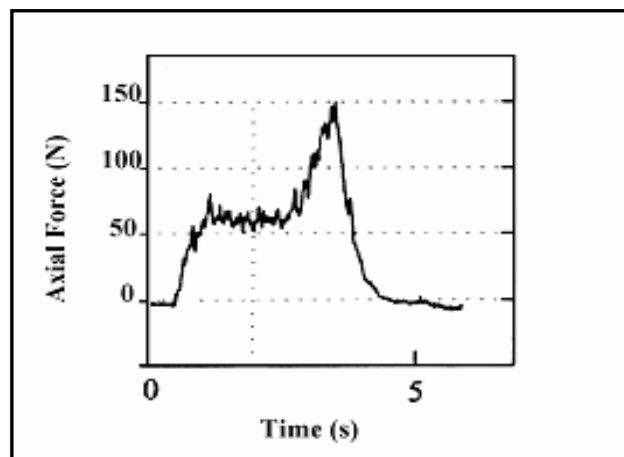


**Figure 2.23.** A through-hole thrust pattern when thread cutting in steel at 175 rpm [33].

#### 2.3.4 Deep Hole Tapping

Deep-hole tapping is commonly considered to be any hole tapped at 1.5 times the nominal diameter of the tap, or deeper [39,40]. And all the factors causing taps to wear under normal conditions are exaggerated for deep hole tapping because of; increased

dulling, chipping and abrasion of the cutting edges, and restricted coolant flow with more heat generated. It has been suggested, that with increased heat at the cutting edges in deep-hole tapping, galling occurs [39] and this has been observed to cause seizure of the tap and breakage [38]. The primary factors listed by Zhang et al. [38] as the cause for the galling, were large relief-face friction between the tool and work material at the newly machined surface, and low conductivity causing a concentration of heat at the cutting edge of the tap. Increased thread relief will reduce this contact pressure between tap and work material.

For work materials with elastic memory, such as stainless steels and titanium, increased back taper along the axial length of the tap is often introduced. Back taper is a decreasing tool radius from the tip to shank of the tap, to reduce friction and torque beyond the thread sizing teeth as the work material springs back after machining [39,40,53]. Cao et al. [33] has shown for straight flute taps, at hole depths of 1 to 1.5 diameters, the torque consists of a base load due to friction and chip formation with an additional chip compaction load of random magnitude and occurrence [33]. It was suggested that as tapping hole depth was increased, the chip-packing load becomes more dominant as the chips are confined for a longer period. Spiral flute tap designs in comparison, have much more complex frictional surfaces for chip transportation and cutting edge geometry and are more susceptible to torsional failure from chip compaction loads.

### 2.3.5 Tapping Attachment and Feed Methods

#### Introduction

Important unknowns in machining operations from a predictive point of view are the method of holding the tool, the type of machine tool being used and the rigidity of the workpiece and its alignment with the spindle axis. This is a major problem for cutting

tool engineers when recommending a suitable tool or pre-empting causes of tool failure. The tap attachment method between the tap and machine spindle has been reported in various periodicals [54-57,63,64] to have an effect on various performance measures such as gauging, torque, thrust and wear. Attachment manufacturers have published [64] end-user reports of improved tool life and efficiency in tapping for various forms of tapping attachments, however, methods to predict the effect on tap performance for the different attachments were not given.

### Non-synchronous Attachments

The axial compensating types of attachment come in a number of varieties; the two most widely used are an automatic self-reversing unit and a non-reversing type shown in Figure 2.24 and Figure 2.25 respectively. Both of these holder types have spring-loaded axial movement to allow the tap to float up and down during the axial feed of the machine tap combination. The axial compensating feed method can also be referred to as a floating tap attachment and requires the machine to feed the tap between ninety-five to ninety-eight percent of the recommended feed so that the cutting action is not affected by thrust from the machine z-axis. The only thrust acting on the tap should be the self-feed of the tap against the internal spring of the attachment.

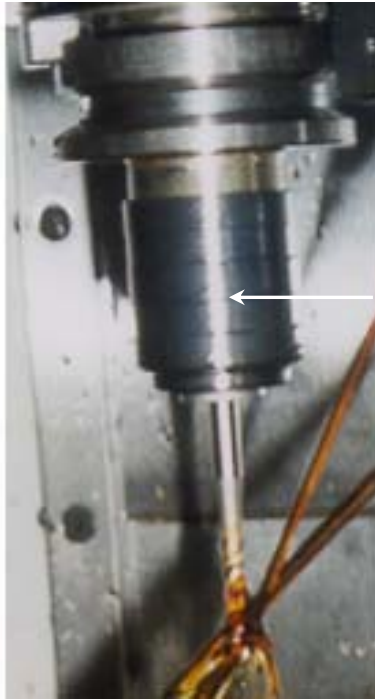


**Figure 2.24.** Photograph of an axially compensating tap attachment with quick release mounted in a CNC machine.

The tap advances at its fixed lead rate using only rotational speed to guide it so that the tap feeds by its own cutting action and the attachment compensates for differences in the acceleration and deceleration of the spindle versus the feed of the z-axis. When the tap reaches the bottom of the hole, the z-axis feed stops at a pre-programmed depth and the spindle reverses. They also have a small amount of radial movement that compensates for small amounts of misalignment. Length compensating holders have been predominately used with machines lacking synchronisation between feed axis and spindle rotation available with CNC machine tools.

### Non-synchronous Auto-reverse Attachment

This type of unit has a bevel gear system that allows the machine spindle to continue in the same rotating direction but reverses the tap as soon as the z-axis of the spindle changes direction to pull the tap out of the hole. This has the advantage of providing high production rates and reducing wear to the drive system of the machine because the spindle does not need to accelerate and decelerate at high rates when using high speed taps. The attachment itself does the reversing at very high speed, thus reducing the amount the cutting edges of the tap slow and increase in speeds for each phase. This in turn reduces tool wear from changing the cutting speed during the cut [54,55,57]. Length compensation is employed to allow for mismatches in synchronisation and programmed feed is recommended at 100% of the recommended feed of the tap for modern versions in CNC machine tools.



**Figure 2.25.** Image of an auto-reverse tap attachment for a CNC machine tool.

Very high RPM can be obtained to make this method very productive, however there is tendency with the floating style of holder to side-cut at higher speeds in soft materials such as aluminium causing oversize threads. Reducing the RPM or using a rigid attachment can eliminate side cutting.

## Synchronous Tap Attachment

For this style, the tap is mounted in a conventional drill collet holder and feeds at 100% of the recommended feed value. The z-axis feed of the spindle is synchronised with the spindle RPM by the servo controlled motors of modern CNC machine centres. The synchronous (rigid) method requires the machine to reverse for tap withdrawal, there is no axial or radial movement allowed by the holder, allowing threads to be re-tapped if required. The disadvantage is that the smaller the diameter of the tap, the higher the RPM needed and the power to accelerate and decelerate the tap. Depending on the size and mass of the machine spindle and the machine design, this can limit the effectiveness of rigid tapping as a high-speed solution. It is still faster than conventional non-synchronous floating holders for the same accuracy of thread produced. The literature reports an elimination of side forces generated on the flanks of the threads allowing tighter thread tolerances for high-speed rigid tapping and reduced wear [56-59, 63,64]. It has been reported that at high tapping speeds with rigid holders accentuates any mismatch between the synchronous feed and the tap pitch due in part to electrical, hydraulic and mechanical movement error in some CNC machine tools. Also machine wear, backlash and lack of calibration can contribute to errors in synchronising spindle feed, speed and spindle reversal [54,58]. Mismatch on reversal can cause the tap to rub against the flanks of the threads leading to cold pressure welding and poor thread quality [54].

The literature suggests that there is an advantage in using “soft synchro” or “synchro-flex” tapping attachments for rigid tapping for increased tool life. These semi-rigid synchro attachments have small axial and/or radial movements to compensate for programmed and actual machine movements where there are discrepancies in machine accuracy due to speed/lead match and spindle wear. The soft-synchro attachments have been shown to reduce thrust forces in rigid tapping [54,64].

In summary, the current metal cutting prediction methods do not provide for all the variables encountered in metal machining at the present time and this places constraints on their usage. The survey of existing databases shows the knowledge-engineered approach to be the most favoured method of conveying empirical and craft oriented knowledge to the end user. However, these databases provide conflicting information with regard to the performance of thread taps under the conditions presented. Similarly, the literature on tapping theory is incomplete and requires investigation, specifically, in the area of spiral flute tapping. Finally, the effects of advanced surface coatings, tapping attachments, deep hole thread tapping and tap rigidity in tough materials such as stainless steel is required.



## Chapter 3

### Database Establishment

---

#### 3.1 Database Structure

A prototype database was established using a licensed software program specifically designed for database development called Filemaker Pro Developer [70]. This software package allowed knowledge engineered *scripts* to be written that use “If / Then / Else” style rules and mathematical relationships within a relational architecture. Figure 3.1 is a Schematic of the prototype database and details the navigational relationships among the pages or screens.

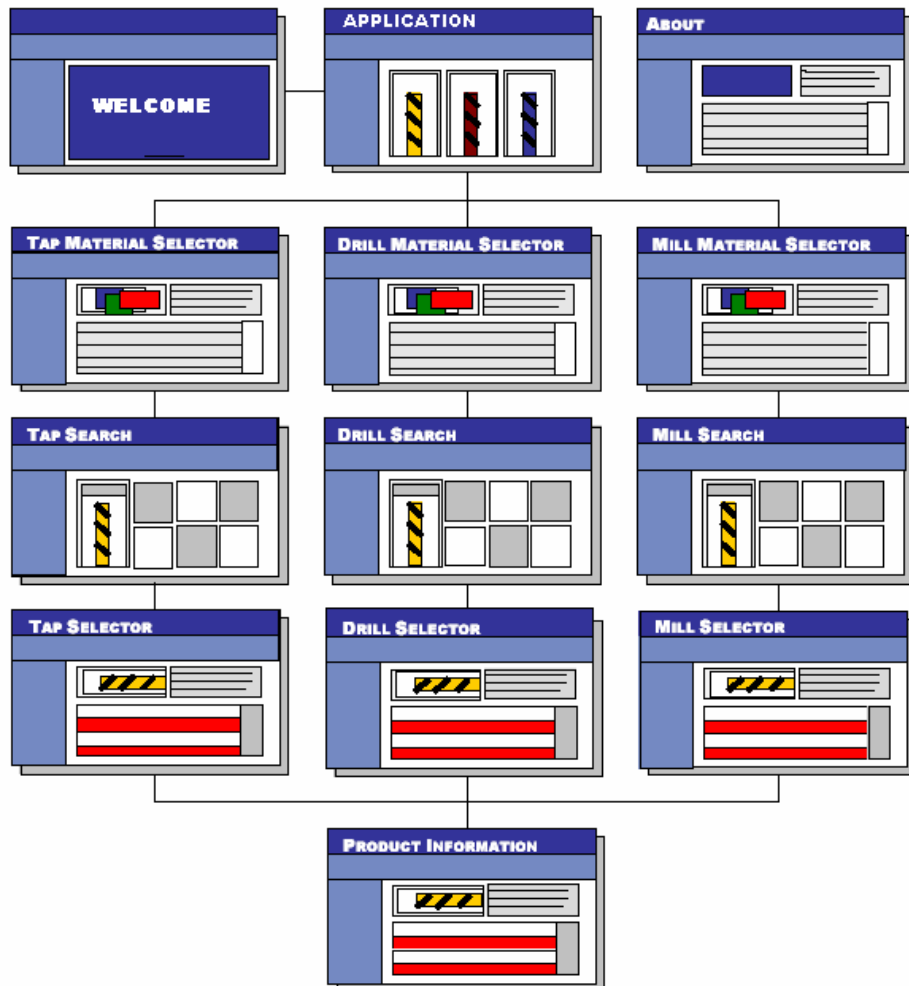


**Figure 3.1.** This is a schematic of the prototype database and details the navigational relationships among the pages.

The machining application module of Tapping, Drilling or Milling is chosen from the top row, then the second row presents a list of work materials for an end-user to select from. The selected cutting tool search module is then displayed for further interrogation of the end-user and the final two rows list product information and performance data according to an end-users search conditions.

The schematic of the prototype database was then used to form the Entity Relationship (ER) diagram that allows determination of what files of data are required. The entities are the files of data or 'tables' that make up the basic building blocks of the database. Figure 3.2 is the ER diagram of the prototype database, showing all the entities about which data needs to be stored in the prototype database and how they are related to each other. The separate entities (tables) of data were first established, compiled from product catalogues, electronic inventory databases and empirical cutting tool tests. An interview process was then used to codify the rules governing the relationships among the data within these tables.

These tables were as follows,

1. Application.
2. Work Materials.
3. Tap.
4. Drill.
5. Mill.
6. Select.

The work material table was divided into three sub-tables of materials for each of the Tap, Drill and Mill applications to allow work material and coolant options to be tailored for each. The Taps table required an extra sub-table for selection from the large array of thread types and sizes available with taps.

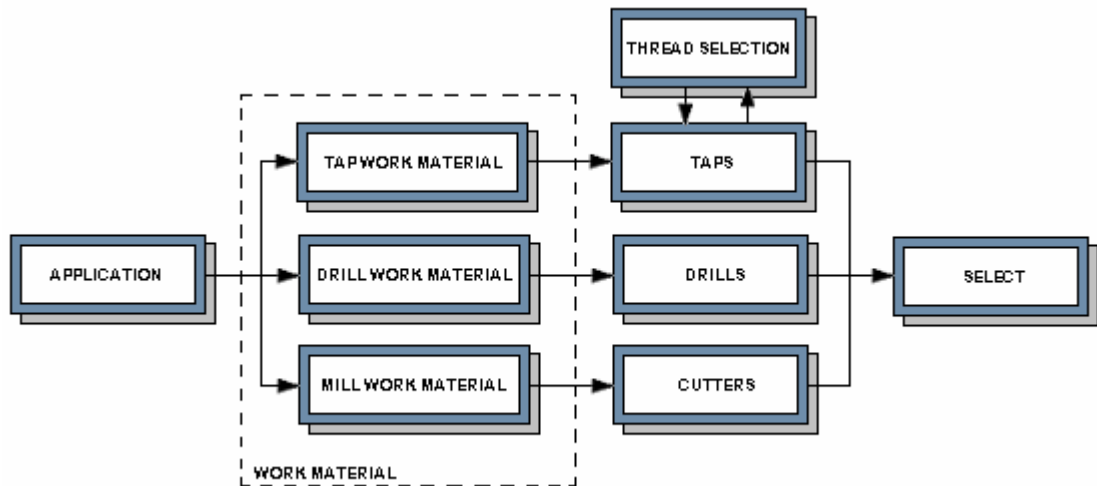


**Figure 3.2.** This is the ER diagram of the prototype database, showing all the entities about which data needs to be stored in the prototype database and how they are related to each other.

### 3.2 Work Materials Database

Investigation of published databases [8,21,22] and cutting tool manufacturer's printed product catalogues showed a common trend of arranging work materials into small groupings for which cutting tools are recommended. The small groupings actually include a large range of materials as typically represented in the Machining Data Handbook [], however, many material subgroups are combined into the same group for simplicity.

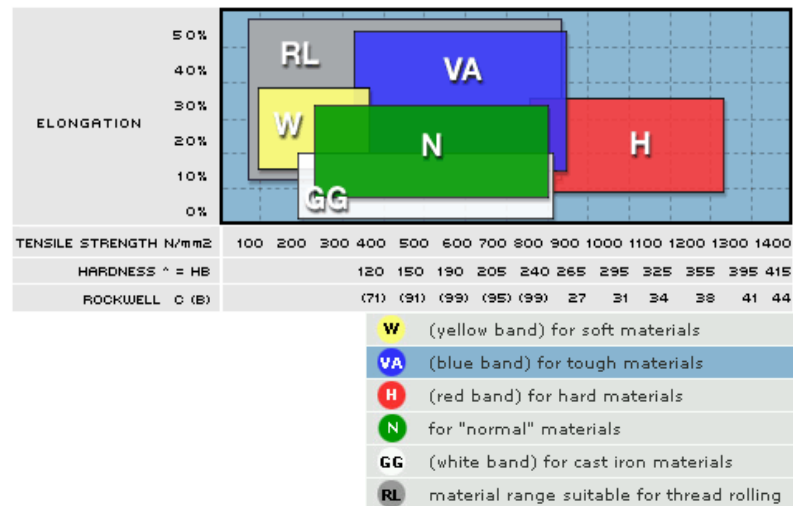


**Figure 3.3.** Chart of the work material application groupings showing how material properties are arranged in coloured groups according to their percentage elongation and tensile strength in N/mm<sup>2</sup>.

Figure 3.3 is a chart of work-material application groupings showing how each coloured box represents a group of materials exhibiting similar mechanical properties. From the above chart, it can be seen that the 'VA' group has an elongation range of approximately 12% - 50% and a tensile strength range of approximately 300 – 900 N/mm<sup>2</sup>. This range includes stainless steels, titanium alloys, high alloy steels, copper, nickel alloys and aluminium alloys. The data for each work material group was taken from a published catalogue [21], which in turn was based on the Machining Data Handbook [45].

### 3.3 Tapping Module

#### 3.3.1 Introduction

The database was established to be sufficiently flexible to accommodate changes in thread cutting knowledge gained from continued research in the field. A consultation process with skilled craftspeople from within the company was undertaken to establish the rules required to manage the stored data for the different tap features and how this data and the application conditions related to tap performance and suitability. This consultation process began by mapping out the decision process for choosing the correct tap for a particular application. This process was repeated until all the variations that are normally considered in choosing a tap were codified into *If / Then* statements and formulae. These were then contained in scripts used by the database software as a control link between the viewing screens and raw data of the database. An example of the consultation process for selecting a tap is as follows,

1. Select Work Material, e.g. Stainless steel
2. Hole Type, e.g. Blind Hole
3. Operation Type, e.g. Thread Cutting
4. Lead Type, e.g. Bottoming
5. Tapping Parameters, e.g. Type / Size / Pitch / Tolerance / Threaded Hole Depth
6. Direction of Cut, e.g. Right Hand
7. Tap Standard, e.g. DIN
8. Coolant Type, e.g. Oil
9. Pitch Control, e.g. non-synchronous
10. Display all Taps matching selection criteria.

At each step, a series of choices were available that had an effect on the type of tap design suitable. A series of *If / Then* rules contained within scripts were used to control the remaining choices available at each step and consider any skilled craft-oriented knowledge relationships where required.

### 3.3.2 Tap Surface Treatment

From the literature review (see Chapter 2, Section 2.2 , Figure 2.3 and Figure 2.4), it was found that cutting tool manufacturers have used different approaches for recommendations of cutting speed and torque values according to the surface treatment of a tap. Cutting tool manufacturers recommended higher cutting speeds for PVD coated taps than non-surface treated taps, this was also the view of the skilled crafts people and design engineers of the company. However, torque values were recommended to be either the same or slightly lower for PVD coated taps. Therefore, allowance was given for the use of different types of surface treatments e.g. PVD coatings, nitriding, so that calculations could be carried out to obtain values of torque and cutting speed (for individual taps for each material group classification). In the database, the default was for a non-surface treated tap.

### 3.3.3 Tapping Attachment

An investigation into the effects of tapping attachments within the expert systems (see Chapter 2, Section 2.2 , Figure 2.7 and Figure 2.8) showed that, only one system recommended increased cutting speed and reduced torque when using the synchronous attachment, the others did not provide differentiation between the two attachments.

Two choices were provided for the tapping attachment, namely synchronous and non-synchronous (floating) feed methods, relating to two forms of suitable tap designs. The synchronous attachment allows taps to be designed to cut with greater surface speeds by reducing the amount of full form thread in contact with the work material. This can be achieved because the tap is rigidly held in the attachment. Allowance was made to distinguish between these types of tap within the database and experiments were undertaken to compare the attachments for torque, thrust and tool-life differences with taps suitable for the non-synchronous attachments. It should be noted that these taps are also used with synchronous attachments. Further development may require additional selections for each type, such as for auto-reverse attachments and soft-synchro attachments.

### 3.3.4 Hole Depth

An initial hole-depth graph was established based on skilled craft-oriented knowledge contained within the company. This graph (see Figure 3.4) shows the percentage reduction of cutting speeds for increased tapped hole depths. It was anticipated that this research would provide further information in relation to this graph for its applicability to work material group stainless steel and different tap styles.

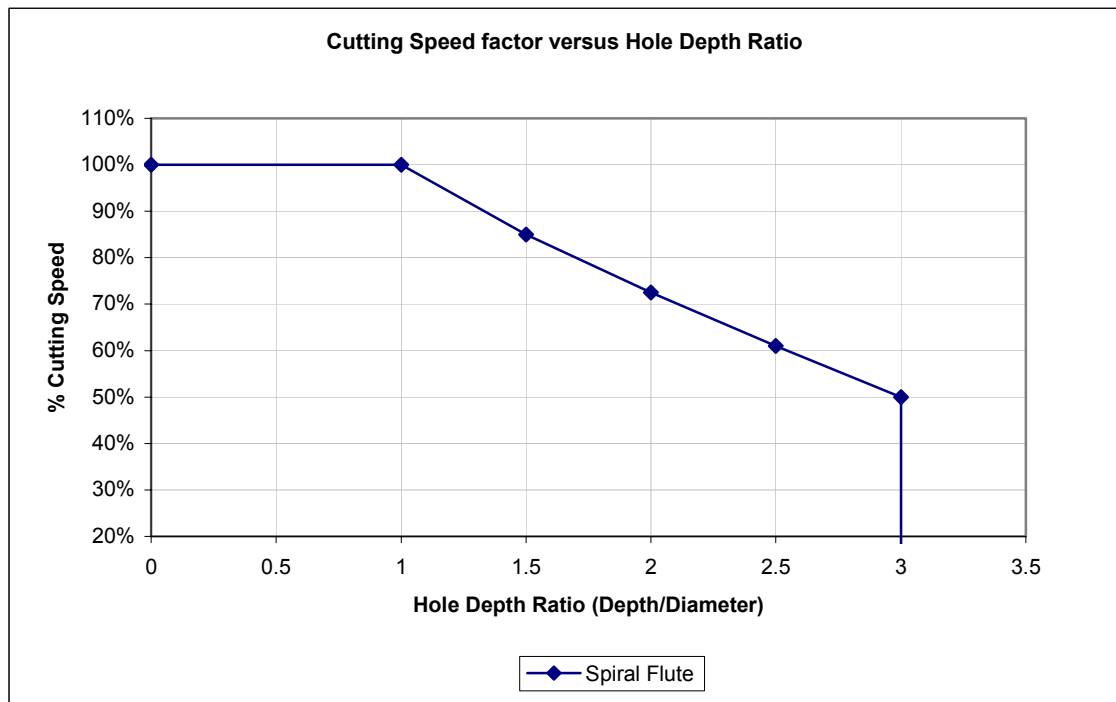


**Figure 3.4.** This is a graph of the cutting speed factor versus the hole depth ratio (depth / diameter), showing the percentage reduction of cutting speed with increasing hole depth, established by the knowledge-engineered approach.

### 3.3.5 Torsional Rigidity

When taps are subject to torque during thread cutting, elastic deformations of the tap lead to an increase in the effective diameter of the thread [50] and one would expect that the elastic deformation of the tap would be work material specific. For increased cutting speeds, the elastic deformation will increase, altering the geometry of the cutting edges leading to an increase in torque until the point of tap failure. Examination of the cutting tool manufacturers expert systems showed only one system to reduce cutting speed with a reduction in tap diameter below 6 mm (see Chapter 2, Section 2.2 , Figure 2.9).

Consequently, a torsional strength factor has been established, based on skilled craft-oriented knowledge within the company, for reducing cutting speeds for small diameter taps of less than 6 mm. Figure 3.5 is a graph of the torsional strength limit factor for the cutting speed, verses the tap diameter for spiral flute, spiral point and forming taps, showing the factor to increase cutting speed with an increase in tap diameter between the limits of 1 mm and 6 mm for the spiral flute design. Research into this area will provide further improvements to this graph and its applicability to different material groups. The factor will be based on the limit at which a tapped thread no longer passes the ‘go’ gauge test or by catastrophic tap failure, whichever comes first.

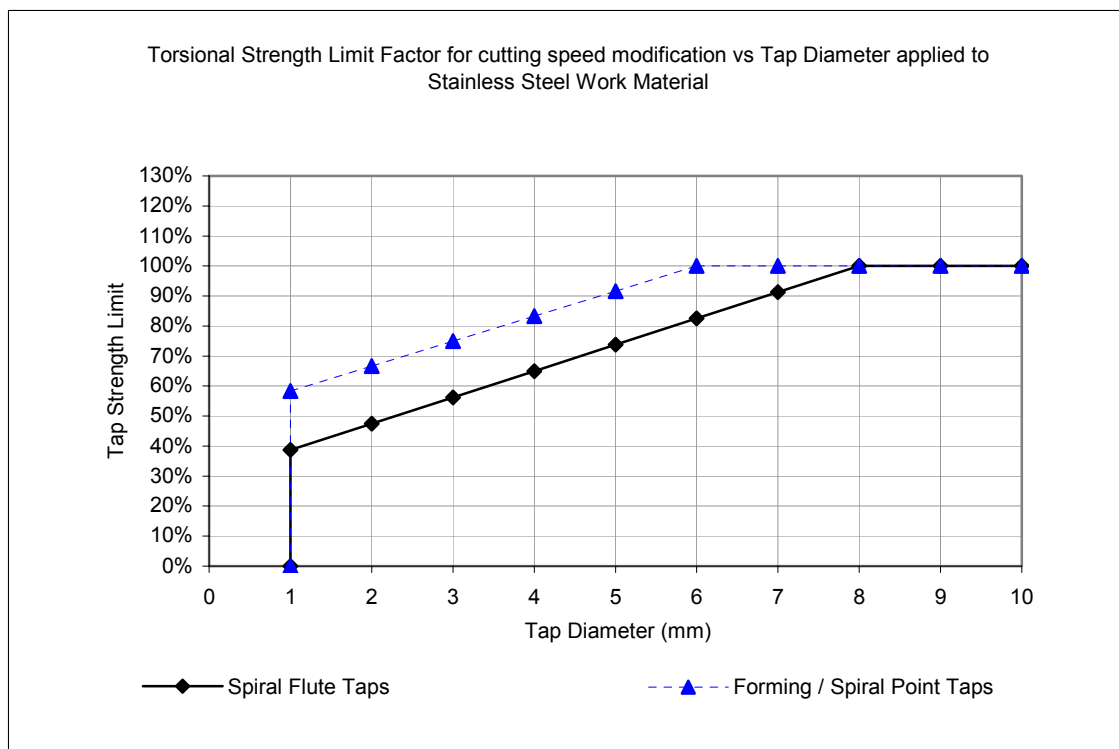


**Figure 3.5.** This is a graph of a torsional strength limit for the cutting speed, verses the tap diameter for spiral flute, spiral point and forming taps, showing the percentage factor to increase cutting speed with an increase in tap diameter between the limits of 1 mm and 6 mm for the spiral flute design.

### 3.4 Sort Order Algorithms and Calculations

After the application conditions have been selected by an end-user of the database, the search performed then provides a list of suitable cutting tools. In the tap database, as many as ten different taps may be suggested for use under the specified cutting conditions, however, some will be more suitable than others depending on the



individual design features of the taps. Therefore a sort order was established to provide the end-user with the listed cutting tools in order of most to least suitable as defined by the taps performance capability and the marketing criteria of the company (where no performance difference is ascribed). The sort order is written by way of an algorithm using *If / Then* and *True / False* statements against the data stored for individual taps within the database.

Calculations are performed upon completion of a database search to provide technical performance data to an end-user for the selected taps. Two main formulae are used for modification of surface cutting speed and recommended cutting torque. The surface cutting speed uses an initial recommended value set by the cutting tool engineer for each of the work material groups per tap design. This value is then modified by the formula depending on the individual surface treatment of the tap and the application conditions selected by an end-user. The recommended torque is calculated from the equation described in the literature review (see equation 7) for taps in new condition. Refer to Appendix 1 for further specification detail of the tap database sorting algorithms and technical performance calculations.

### 3.5 Filemaker Database Conversion to SQL Web Server

Structured Query Language (SQL) is an ANSI standard computer language for accessing and manipulating databases. Conversion to SQL Internet software language for web hosting was implemented when a decision was made to host the database over the Internet rather than via distribution on CD ROM. The advantage of this conversion was to allow faster operation of the website and future expansion of the database without losing process speed, which was anticipated with Filemaker.

It should be noted that the original database written (in Filemaker) for the current investigation, was used as the prototype for a web design contractor to convert into SQL. Consequently, the present investigator controlled all functional design and the contractor using their proprietary SQL language scripts performed the changes. One computer and server is required to host the database and website, and should allow future additions to the system, of neural network architecture or prediction software programs to interface with the SQL front-end giving flexibility to the database.

## Chapter 4

### Experimental Procedure

---

#### 4.1 Work Material and Hole Preparation

The work material investigated in this study was 316 austenitic stainless steel in the form of 25.0 mm thick rolled plate (refer to Table 2 for the nominal composition). From this, disks 203 mm in diameter were laser cut to fit the holding fixture on a HAAS CNC machining centre. Once the disks were secured in the fixture, 18.0 mm deep holes were drilled with 5.0 mm TiAlN coated Co-HSS (M35) 4-facet split point twist drill with a 120-degree point angle and 40-degree flute helix. The holes were drilled at a speed of 830 rpm and feed of 42 mm/min. A second operation chamfered the holes to a depth of 1.0 mm equal to one tap pitch for an M6 size tap. The chamfer tool used was a 90-degree point angle, three-flute countersinking tool. For all machining operations a non-water soluble tap cutting oil was used.

**Table 2.** Nominal work material composition and hardness as supplied by the manufacturer [14].

---

Austenitic Stainless steel 316 (annealed rolled plate), Nominal Hardness: 95 HRB										
Element	C	Si	Mn	P	S	Cr	Mo	Ni	N	Fe
wt.%	0.08	0.75	2.0	0.045	0.03	16.0 – 18.0	2.0 – 3.0	10.0 – 14.0	0.10	bal.

---

## 4.2 Tapping Procedure

### 4.2.1 Tap Design

Torque and thrust measurements for both forward (cutting) and withdrawal of the tap are to be recorded for analyses. Measurement of the forward component of the torque and thrust will allow limited comparison with the published literature for other tap styles. The problem of tap breakage during tap reversal has been identified and therefore a study of the reversal torque and thrust will be undertaken as described in the preliminary investigation. Tap manufacturers recommend various tap designs and tap treatment processes for tapping austenitic stainless steel. The treatment processes may be of a type that improves substrate microstructure or by PVD surface coatings. It is commonly claimed in industry that PVD coatings reduce torque in the tapping process, however research in tapping [51] has shown that this may not be true.

The taps tested were of a geometry designed for blind hole threading in stainless steel work materials. Their commercial classification was R45 VA DIN371 spiral flute taps with a bottoming taper lead of 2.5 threads. They were made from M9V steel (refer to Table 3 for the nominal composition). The taps were manufactured to the standard DIN 371 for the tap blank and ISO 2 - 6H for the thread form (see Figure 4.1, Figure 4.2 and Table 4 respectively).

**Table 3.** Nominal substrate composition [71].

---

HSSEV substrate (M9V): Typical Hardness: 850 – 900 HVN

---

Element	C	Cr	Mo	V	W	Co
wt.%	1.2	4.2	8.5	2.7	3.5	-

---

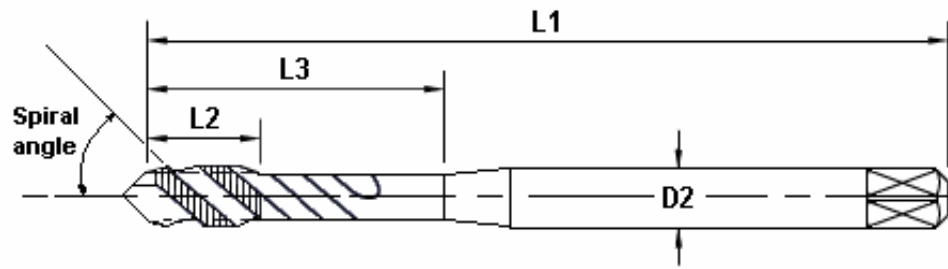


**Figure 4.1.** A schematic representation of the 45 degree helix three flute spiral tap of DIN 371 standard for ISO 2 / 6H class and nut limit used in the experiment [21].

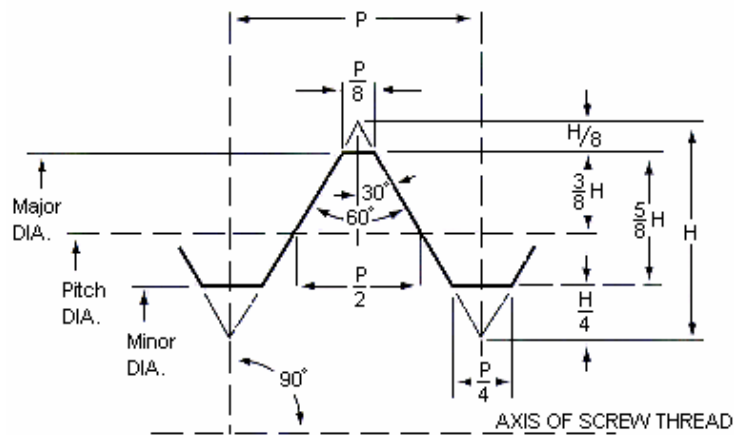


**Figure 4.2.** A schematic of an metric ISO standard thread form use for the taps under investigation, showing the relationships between  $P$  and  $H$ , where  $P$  is the pitch and  $H$  the thread height [21].

A comparison of the taps under investigation with competitor's taps is listed in Table 4 showing the typical values for spiral flute taps suitable for tapping in stainless steel published by cutting tool manufacturers. The chamfer form is commonly given in a qualitative manner in terms of the pitch range before full thread is reached. The terminology of which varies between national standards for the pitch range included. From Table 4, the chamfer form  $C$  denotes a pitch range of two to three threads. Interestingly, researchers [33,37,67] have shown that the chamfer geometry (lead angle, rake and relief) can have significant effects on tap wear due to load distribution across the cutting teeth and chip formation. However, cutting tool manufacturers generally do not specify if *form c* thread taps are; two or a three length pitch chamfer, or the value of the chamfer rake and relief. This is surprising given its effect on tap performance and life.

**Table 4.** Published values and tolerances of spiral flute tap geometries given by the tap supplier for various cutting tool manufacturers for; ‘VA’ applications (Emuge\*, Sutton, Garant, OSG) or general-purpose *N* applications (Yamawa\*\*, Prototyp), where VA was unavailable.

Thread limit / Nut tolerance	Thread Form	Major diameter minimum (mm)	Pitch diameter (mm)	Minor diameter (mm)	Pitch (mm)	Rake angle	Hook Angle	Chamfer Form
ISO2 / 6H	M	6.0	5.35 – 5.50	4.917 – 5.153	1.0	x	x	C (2-3 pitch)
Chamfer lead angle	Chamfer Rake	Chamfer relief	Thread relief	Flute Helix (degree)	No. of Flutes	L1 (mm)	L2 (mm)	L3 (mm)
x	x	x	x	35*, 40**, 45	3	80 ±0.5	10 ±0.5	30 ±0.5

Note: x – data not supplied

It is also evident that the thread relief values of the full form teeth are not supplied by the cutting tool manufacturers. Research has shown thread relief to be an important factor in tap performance in terms of torque and life [37,38,67,69]. Grudov [69] has also shown thread relief to have an import effect in the reduction of tooth fracture arising from the unscrewing motion of the tap. From the survey in Table 4, it is evident that a variety of flute helix angles are recommended, however no tolerance range is specified. It is known that flute helix angles, core diameter and core taper, alter chip transportation and tool rigidity.

Table 5 lists a further comparison of tap features from the taps shown in Table 4 measured by a local tap supplier, for various parameters of cutting geometry that are known to affect tool performance. The features of; thread limit, nut tolerance, thread form, major diameter, pitch diameter, minor diameter, pitch, L1, L2 and L3 are given as recommended by the *metric ISO coarse pitch* standard [21] for screw threads. The land width, thread relief, flank relief, flute length, core diameter and core taper are all shown to vary between tap manufacturers. These parameters are generally known to affect the cutting forces tap strength or rigidity and chip transportation, not withstanding the effect of helix angle on chip disposal. The ‘back taper’, (measured as the drop (mm) normal to the axis per 10 mm axial travel) is not quantitatively specified for all taps shown, however, it has been reported to reduce torque in deep-hole tapping [39,40,53].

**Table 5.** Comparison of measured values of the cutting geometry of spiral flute taps from various cutting tool manufacturers as measured by the cutting tool supplier.

Reference	Major diameter min. (mm)	Pitch diameter (mm)	Pitch (mm)	Rake angle (degree)	Chamfer Form	Chamfer lead angle (degree)	Chamfer Rake (degree)	Chamfer relief
Emuge	x	x	1.0	x	C	x	x	x
Sutton	6.059 +0.025	5.38 – 5.41	1.0	12 - 14	C	15 ± 1	2.5 ± 1	0.6 ± 0.1
Yamawa	x	x	1.0	8	C	x	x	x
Prototyp	x	x	1.0	x	C	x	x	x
Garant	x	x	1.0	x	C	x	x	x
OSG	x	x	1.0	x	C	x	x	x

Reference	Land width (mm)	Thread relief (mm)	Flank relief (mm)	Flute Helix (degree)	No. of Flutes	Flute Length (mm)	Core diam. at full thread (mm)	Core Taper (mm) / 10mm	Back Taper (mm) / 10mm
Emuge	1.85	0.030	0.024	x	3	x	2.41	0.24	x
Sutton	1.76 – 1.83	0.018	0.018	43	3	27	2.35	0.1	0.006 – 0.012
Yamawa	1.97	0	0.001	x	3	31	2.28	0.1	0.008
Prototyp	1.83	0.002	0.007	x	3	26	x	0.1	x
Garant	x	x	x	x	3	29	x	x	x
OSG	1.65	0.001	x	x	3	30	2.6	0.08	x

Note: x – data not supplied.

The taps supplied for this investigation are shown to be placed conservatively, in terms of tap features, among the competing cutting tool manufacturer's taps.

The O.D. relief measured from the taps under the current investigation were all within the manufacturing tolerance range of 13  $\mu\text{m}$ . Cylindrical runout of the CNC grinding machine between centres of the tap when producing the thread form and thread lands is nominally 5  $\mu\text{m}$ , with contamination of mating surfaces between centres potentially increasing this to 13  $\mu\text{m}$ . Table 6 lists the measured outer diameter relief range for the four sets of taps used in this study before testing.

**Table 6.** Measured outer diameter relief for four sets of taps tested, averaged over 5 taps for each set, showing median values with upper and lower bounds.

Surface Treatment	Bright	TiN	TiCN (I)	TiCN (II)
O.D. relief range ( $\mu\text{m}$ )	$19.80 \pm 2.10$	$21.30 \pm 4.20$	$18.20 \pm 5.50$	$18.90 \pm 5.30$

#### 4.2.2 Experimental Set-up

The PVD coatings of TiN and TiCN were chosen because cutting tool manufacturers recommend these coatings for improved performance when tapping stainless steels [8-12]. The experimental plan shown in Table 7 was designed to compare the performance of commercially available uncoated, TiN and TiCN coated taps with respect to tapping torque, thrust, outer relief dimensional changes and tapped hole accuracy. The uncoated, TiN and TiCN coated taps were all obtained from the one source. The chosen measurement intervals were 1, 20 and 80 holes for the uncoated taps and 1, 20, 80, 200, 300 and 450 for the coated taps at which the measured quantities were assessed. The measurement intervals were set by intermittently inspecting the progress of wear on the uncoated taps and then repeating measurements at the chosen intervals for all taps to allow comparison.

A double-ended plug gauge was used to test tapped hole accuracy for all experiments. Non-conformance was judged as a failure of the *go* end, effective pitch diameter 5.362 mm to enter the hole or more than 1.5 turns of the *no-go* end, effective pitch diameter 5.505 mm. The recommended tolerance range for the pitch diameter of the supplied taps was 5.35 to 5.50 mm for a nominal diameter of 6.0 mm [21]. The maximum and average values of torque and thrust were recorded for the forward tap motion and the withdrawal tap motions. In total, 15 taps were tested. Also, two different types of tap attachment were employed, namely conventional non-synchronous (floating) and synchronous (rigid).

Preliminary tapping tests using uncoated taps, tapping to a depth of 1.5 tap diameters, showed tap breakage to occur at speeds above 3.0 m/min. Therefore, a cutting speed of 3.0 m/min requiring a feed rate of 0.159 m/min was chosen for all taps. After many hours of testing it was found that the set of taps used to set the cutting speed for the experiments were manufactured with the wrong thread and outer diameter relief. This effectively caused the taps to wedge into the hole and at cutting speeds above 3.0 m/min, resulting in catastrophic failure. Due to time constraints, the cutting speed was continued at 3.0 m/min, requiring only the faulty set of taps to be replaced and tested with the correctly manufactured relief. It was assumed that wear of the taps would be reflected in the measured quantities.



**Table 7.** Summary of experimental machining plan for three surface treatments and two attachment types.

No. of taps	Tool surface conditions	Measured Quantities				Chosen measurement intervals (No. of holes)	Tap Holder
		Torque	Thrust	Outer relief wear	Hole accuracy		
5	Uncoated					1, 20, 80	Conventional floating
5	TiN coated	Torque	Thrust	Outer relief wear	Hole accuracy	1, 20, 80, 200, 300, 450	Conventional floating
5	TiCN coated					1, 20, 80, 200, 300, 450	Conventional floating and rigid

A further experiment, shown in Table 8, was carried out to study the effect of threaded hole-depth on torque and thrust when using the same type of taps to machine 316 stainless steel work material. The maximum threaded hole-depth capability of a tap is generally identified in the literature by the ratio of hole-depth to tap diameter, reported in 0.5 increments at  $\geq 1D$ , where  $D$  represents the tap diameter. In blind-hole tapping, cutting tool manufacturers generally recommend  $3D$  as a maximum. A total of five taps from the same batch were tested. The effect of hole-depth ratios  $1D$ ,  $1.5D$ ,  $2D$ ,  $2.5D$  and  $3D$  (i.e. 6, 9, 12, 15 and 18 mm depths respectively for an M6 tap) on torque, thrust and hole accuracy were investigated. As previously, the cutting operation was set out with the same speeds and feeds and the plug gauge was used to check hole accuracy. Ten holes were tapped by each tap and measurements recorded for each.

**Table 8.** Experimental set-up to compare the effect of tapped hole-depth on the measured torque and thrust for TiCN coated taps.

No. of taps	Thread depth (mm)	Measured Quantities			Chosen measurement intervals (No. of holes)
1	6				10
1	9				
1	12	Torque	Thrust	Hole accuracy	
1	15				
1	18				

It was anticipated that the increase in hole depth will lead to an increase in measured quantities of torque and wear as reported in the literature for straight flute taps [33,39]. However, recommendations from the cutting tool manufacturer's expert systems [8-10] provide conflicting advice, therefore further investigation is required.

The experimental plan listed in Table 9 was a preliminary study, to investigate if the physical limitations of tap size would have a bearing on the maximum surface cutting speed and torque obtainable before thread failure. The results of which, could be used to modify the hole-depth to tap diameter ratio recommendations within the database. The study was conducted under cutting conditions to simulate torsional distortion of the tap and the tap teeth under load. Hole accuracy was tested by plug gauge and limited by possible catastrophic (by fracture) tap failure. A total of four taps were tested, one each of M3, M4, M5 and M6 diameters. An auto-reversing non-synchronous attachment was used to allow the CNC machine to reach the required operating rpm for a maximum depth of tap engagement.

**Table 9.** Experimental set-up to compare the effect of reduced tap diameter on the measured torque and hole accuracy for TiCN coated taps.

No. of taps	Tap size	Measured Quantities			Chosen Measurement Intervals (speed m/min)
1	M6	Torque	Hole accuracy	Failure / Screech	Increments of 1.0 m/min
1	M5				
1	M4				
1	M3				

It is anticipated that reduced torsional rigidity and the reduction in the core diameter of the smaller taps will be reflected in the measured quantities.

### 4.2.3 Statistical Methodology

A number of statistical tests were selected and employed to analyze the experimental results from the tap tests. The Bartlett test (recommended for comparing variances of three or more samples) and the Fisher test (recommended for comparing variances of two samples) were chosen to test the homogeneity of variances. If the tests passed at the selected confidence level (95%), the homogeneity of variances was confirmed, and the analysis of variance test (ANOVA) or *Student t-test* was used to determine whether or not the mean values of three or more samples, or of two samples, respectively, could be considered statistically equal at the selected confidence level. If the variances were not homogeneous according to the Bartlett or Fisher test, the Welch test was used instead of the ANOVA or t-test, to compare the mean values of samples of three or more, or two samples, respectively [72].

The approach for design and analysis of the experiments was that the measured quantities, analytical assumptions, statistical methods and expected results were considered in terms of the number of holes tapped. It was anticipated that no or negligible tool wear would take place when tapping the first hole. Hence, the measured quantities would be those for new taps and be influenced only by the geometrical variability, if any, between the taps. For the data taken when tapping the twentieth and eightieth holes it was anticipated that different wear would take place for the uncoated and coated taps *i.e.* wear would be greater for the uncoated taps than for the PVD coated taps. Thus, for geometrically similar taps the recorded thrust and torque would be statistically different. Moreover, the torque and thrust should increase with the number of tapped holes because of tool wear. The expected pattern for the uncoated taps would be greater outer relief wear than the coated taps. It was expected that geometrical differences arising from the manufacture of the taps would affect the thrust and torque intercepts as a function of the first hole tapped.

## 4.3 Performance Measures

### 4.3.1 Torque and Thrust Measurement Technique

It has been recognised that technological performance measures, such as chip formation, cutting forces, power and tool life, are indicators of economic performance as assessed in terms of cost per component, time per component and other similar measures [73]. Measurements of torque and thrust were made during tapping of the first hole in the stainless work material and then at various times during the life of the tap. The device used for measuring the torque and thrust was a Kistler piezoelectric dynamometer [74] linked to a laptop computer via an analogue to digital converter and support software. Figure 4.3 is a schematic of the equipment set-up showing the dynamometer mounted on a plate. This plate was then mounted in the HAAS CNC machining centre as shown in Figure 4.4.

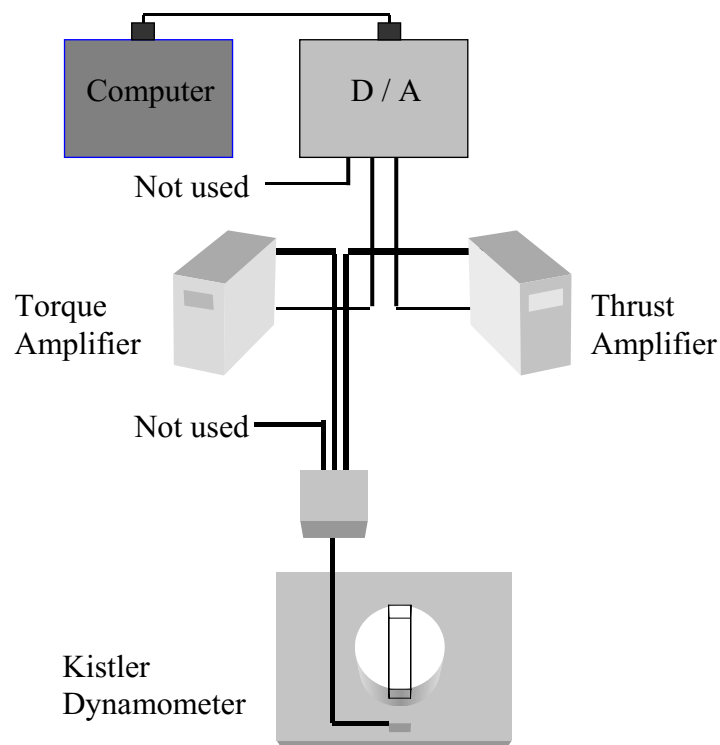


**Figure 4.3.** A schematic of the test equipment set-up showing the Kistler piezoelectric dynamometer [74] mounted on a plate.

Note that the thread tapping operations were carried out on the stainless steel disks in situ with the measurements on the Kistler dynamometer. Therefore for the holes tapped

between the chosen measurement intervals, no data was recorded for torque and thrust values.



**Figure 4.4.** A photograph of the Kistler dynamometer set-up in the HAAS CNC machining centre, showing an M6 spiral flute tap mounted in a non-synchronous (floating) attachment with lubricant directed at the tap flutes.

The software was set to collect 120000 data points at a frequency of 500 points per second. Charge amplifiers were set at a scale of 500 measurement units, so that data for both torque and thrust required multiplication by 500 to give torque in Ncm and thrust in N. The dynamometer was reset and manually triggered before the tapping cycle of each test and manually triggered again after the cycle was completed. This gave approximately 1 to 2 seconds of data (500 – 1000 data points) before the tap engaged the work piece and after disengaging the work piece. Each drill, chamfer and tapping operation took approximately four minutes, which equated to approximately 600 hours of testing, performed between production jobs on the machine.

### 4.3.2 Wear Measurement

Tap wear occurs on the thread crest, flanks and outer relief on both the chamfer and full form teeth. Difficulty arises in measuring this wear, however, an effective method to measure wear on the thread crest of the full form teeth was gauged by measuring the outer diameter (*O.D.*) relief using a CNC controlled computerised measuring system (*CMS*) or machine (*CMM*). Figure 4.5 shows the *O.D.* relief measurement on the *CMS* using a stylus that traces the outside diameter of the first full-thread crest for one complete revolution of the tap, i.e. one pitch. The *O.D.* relief was measured from the trailing edge of the crest to the leading edge of the crest, i.e. from the heel to the cutting edge along the thread land. The amount of relief measured on a new tap is set by the tap design.

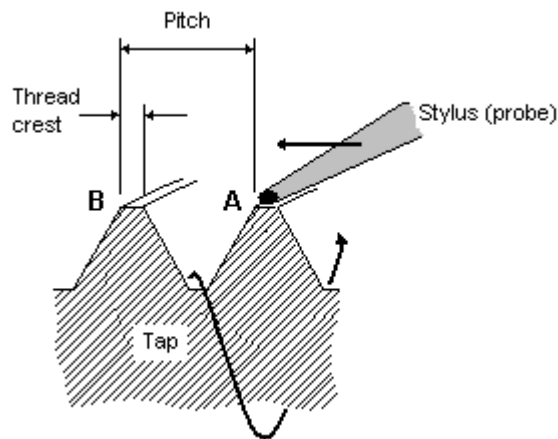


**Figure 4.5.** Schematic diagram of a cross section of a tap, showing the method used to measure wear of the outside diameter relief along the thread crest for one pitch, i.e. A to B.

As the tap wears, the relief values change over time as the leading cutting edge wears down and trailing (heel) edge is worn by its chip shearing action on the reversal of the tap from the threaded hole. During thread cutting, the cutting edges makes the longest contact with the work material producing chips and the heel edges shear through the chips on tap reversal, therefore it is anticipated that the heel-edge wear will be negligible. Figure 4.6 (a) is a schematic of a tap cross section in the plane of the full form thread helix and Figure 4.6 (b) is the typical profile produced by the *CMS* for one crest of a three flute tap. The profile from points 1 to 2 represents a new tap and 1' to 2'

a worn tap. It is evident that cutting edge wear decreases the measured O.D. relief from 2 to 2'.

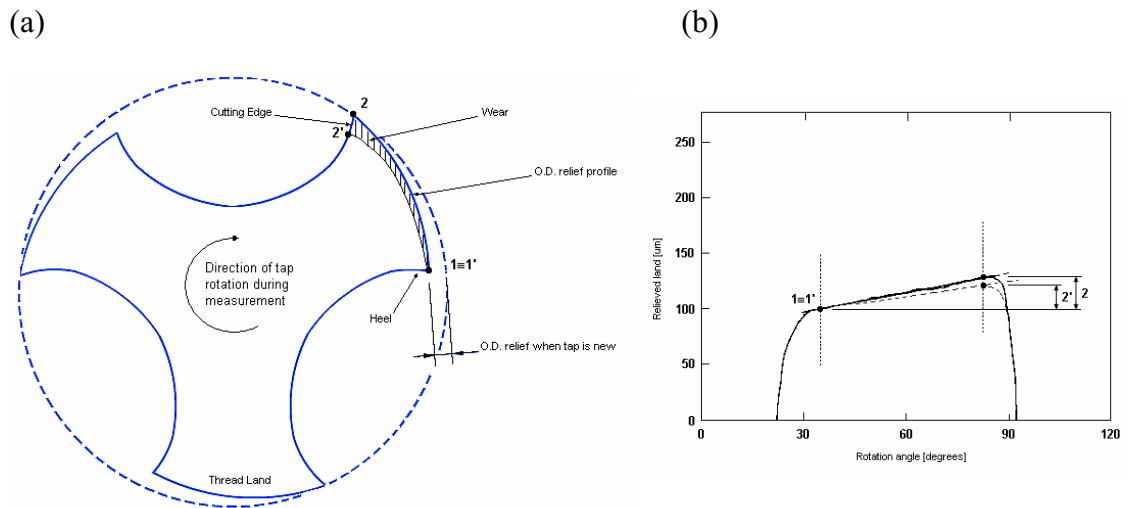


**Figure 4.6.** Schematic diagrams of a tap cross section (a) and a typical printed profile by the Junker CMS for one land (b) showing the method used to measure wear of the outside diameter relief along the thread crest. Cutting edge wear will decrease the measured O.D. relief from 2 to 2' shown in (b). The presence of material transfer on the thread crest at the cutting edge may increase the measured relief.

At each stage of wear measurement, a threaded plug gauge of the go/no-go type was used to check the threaded hole accuracy. The go/no-go gauge is generally used in production to determine the life of the tap. A threaded hole that allows the “no-go” end, or fails the “go” end of the gauge will require a component to be scrapped or reworked in the production environment. Therefore, this gauge was used as the deciding factor on tool life in this research.

## Chapter 5

### Experimental Results / Discussion

---

#### 5.1 Analysis of the HAAS CNC Machining Centre

The HAAS CNC machining centre contained an actuated X-Y table and vertical spindle (Z-axis), with a speed capability of 6000 RPM. Before tapping tests were undertaken, the dynamics of the machine were investigated in order to minimise possible effects of the machining centre on the results. The machine tool axis movement and spindle axis rigidity were found to be within tolerances and considered negligible when compared with the movement within the tap attachments. A fixture was used to secure the work-piece rigidly to the dynamometer. It was found that the programmed spindle speed did not match the measured spindle speed and was between 1% and 5% greater than the programmed RPM at speeds between 3 m/min and 10 m/min respectively. A correction was carried out so that the measured speed was suitably matched to the set feed. The set feed matched the measured feed during all tests.

Cyclic variations were observed in the torque and thrust values measured in the preliminary tap tests. The frequency of these variations in torque and thrust values was 0.5 Hz, which was attributed to the variation in measured spindle speed of 0.5 Hz. Researchers [4,67] have investigated cyclic variations in tapping operations and proposed frequency modulation of the spindle to be the cause. Interestingly, Meezentsev et al. [4] found that tap runout and axis misalignment can manifest in the form of cyclic modulation of the torque. However, radial force components of the torque were used to come to this conclusion and it has been shown previously [7], that the effects of the faults, on torque and thrust values, are not sensitive enough to consistently detect them in the presence of normal process variations.



## 5.2 Analysis of Metal Machining Performance Data

### 5.2.1 Comparison of PVD Coated and Uncoated taps

Table 10 shows the torque and thrust values generated by the uncoated and coated taps, using a non-synchronous (floating) attachment. Values are given for both forward and reverse tap motions after tapping one, twenty and eighty holes.

**Table 10.** Results of torque ( $T_q$ ) and thrust ( $T_h$ ) generated by the uncoated and coated taps using a non-synchronous attachment, refer to Appendix 2, Table A, for detailed statistical data.

Number of holes tapped	one				twenty				eighty			
	Forward		Reverse		Forward		Reverse		Forward		Reverse	
Torque [Ncm]	Mean	st.dev.	Mean	st.dev.	Mean	st.dev.	Mean	st.dev.	Mean	st.dev.	Mean	st.dev.
Uncoated Taps	301	24.9	266	58.3	369.5	25.7	315.4	37.4	380.8	39.6	272.7	31.7
TiN coated Taps	348	24.9	304	58.3	369.5	25.7	315.4	37.4	380.8	39.6	272.7	31.7
TiCN coated Taps	383	24.9	374	58.3	369.5	25.7	315.4	37.4	380.8	39.6	272.7	31.7
Thrust [N]	Forward		Reverse		Forward		Reverse		Forward		Reverse	
	Mean	st.dev.	Mean	st.dev.	Mean	st.dev.	Mean	st.dev.	Mean	st.dev.	Mean	st.dev.
Uncoated Taps	50.9	7.4	30.8	4.2	57.2	8.9	29	2.8	53.3	10.5	29	2.4
TiN coated Taps	50.9	7.4	30.8	4.2	57.2	8.9	29.6	2.8	53.3	2.7	25	2.4
TiCN coated Taps	50.9	7.4	30.8	4.2	57.2	8.9	36.2	2.8	53.3	4.5	24	2.4

Table 10 is a summary of the torque and thrust values for the uncoated and PVD coated taps after tapping one, twenty and eighty holes. It is evident from Table 10 that, after tapping one hole, the uncoated taps produced lower torque and thrust values than the TiN coated taps which, in turn, were lower than the TiCN coated taps.

At first sight, this result may be surprising given that a commercial selling feature of PVD coatings is their reduced friction in metal cutting. However, in the process of tapping this can initiate against the free cutting action of a tap. For example, the severe rubbing contact on an uncoated tap can lead to material transfer and build-up on the rake and clearance faces of the tap. This can lead to the tap cutting slightly oversize but within tolerance. This means that the real area of rubbing contact is reduced. Whereas, a PVD coated tap arguably will have less material transfer and build-up due to its lower friction. Thus, the coated taps real area of rubbing contact will be greater and the tap

will cut much closer to size. This is reflected in the higher torque and thrust values observed for the PVD coated taps.

The fact that TiCN coated taps initially cut with a higher torque and thrust than TiN coated taps, can be accredited to an extension of the above argument. It should be recognised that TiCN is largely a TiCN coating which towards the end of the PVD coating process has the nitrogen flow rate reduced significantly and hydrocarbon gas introduced e.g. CH<sub>4</sub> or C<sub>2</sub>H<sub>2</sub>. This means that TiCN contains high stoichiometric levels of carbon at the surface which, in the sp<sup>2</sup> form [75-77], could lead to lower friction and therefore even closer cutting to size and hence high values of torque and thrust. Support for this argument is presented later in the results in Section 5.2.2, Figure 5.8.

After twenty and eighty tapped holes, it was found that the forward and reverse torque values were the same over the measured range of tapped holes. In order to provide a more detailed analysis of the results, the torque and thrust values for each of the uncoated and PVD coatings are shown in Table 11 and Figure 5.1 for uncoated taps, Table 12 and Figure 5.2 for the TiN coated taps and Table 13 and Figure 5.3 for the TiCN coated taps.

**Table 11.** Results of torque ( $T_q$ ) and thrust ( $T_h$ ) generated by the uncoated taps using a non-synchronous attachment, with respect to the number of tapped holes (refer to Appendix 2, Table B, for statistical criteria).

Measured Quantities	Torque [Ncm]				Thrust [N]			
	Forward		Reverse		Forward		Reverse	
	Mean	st. dev.	Mean	st. dev.	Mean	st. dev.	Mean	st. dev.
one	301	39.21	278.1	45.4	53.7	9.46	29.6	1.1
twenty	360	39.21	278.1	45.4	53.7	9.46	29.6	1
eighty	418	39.21	278.1	45.4	53.7	9.46	29.6	3.5

Table 11 and Figure 5.1, show that, for uncoated taps used in a non-synchronous tapping attachment, the forward torque increases with the number of holes tapped.

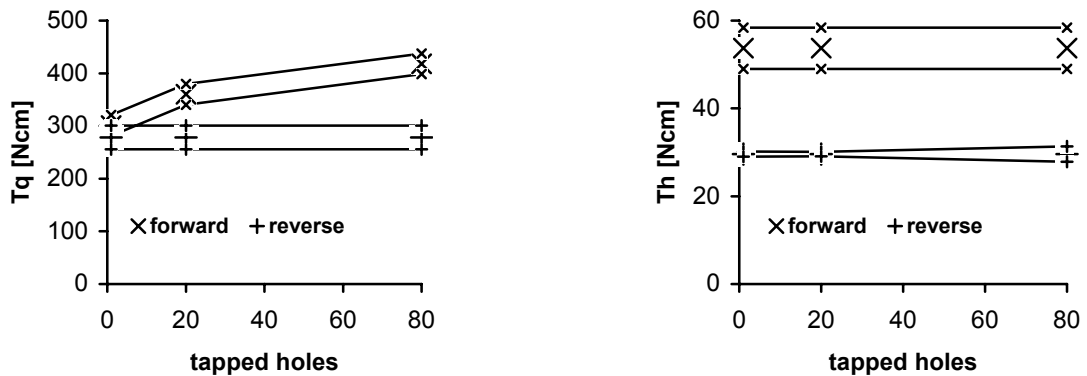


**Figure 5.1.** Graphs as a function of torque and thrust with respect to the number of holes tapped, for the uncoated taps using a non-synchronous tapping attachment, refer to Table 11 for data.

However, the reverse mean torque values remain the same, this is consistent with there being little or no wear on the heel of the tap. For forward thrust, the mean values are equivalent at one, twenty and eighty holes as are the reverse mean values, however at eighty holes, there is an increase in scatter.

**Table 12.** Results of torque ( $T_q$ ) and thrust ( $T_h$ ) generated by the TiN coated taps using a non-synchronous attachment, with respect to the number of tapped holes (refer to Appendix 2, Table C, for data).

Measured Quantities	Torque [Ncm]				Thrust [N]			
	Forward		Reverse		Forward		Reverse	
	Mean	st. dev.	Mean	st. dev.	Mean	st. dev.	Mean	st. dev.
one	357	23.67	299.6	25.68	52.7	4.29	33.6	3.89
twenty	357	23.67	299.6	25.68	52.7	4.29	29.6	3.89
eighty	357	23.67	299.6	25.68	52.7	4.29	25.6	3.89

From Table 12 and Figure 5.2, the TiN coated taps show the torque to be in a steady state for both forward and reverse motions. The forward torque of a TiN coated tap is similar in magnitude to uncoated taps at eighty holes. The forward thrust is shown to be in a steady state, however, the mean values of the reverse thrust, showing a reduction occurring at or before twenty tapped holes.

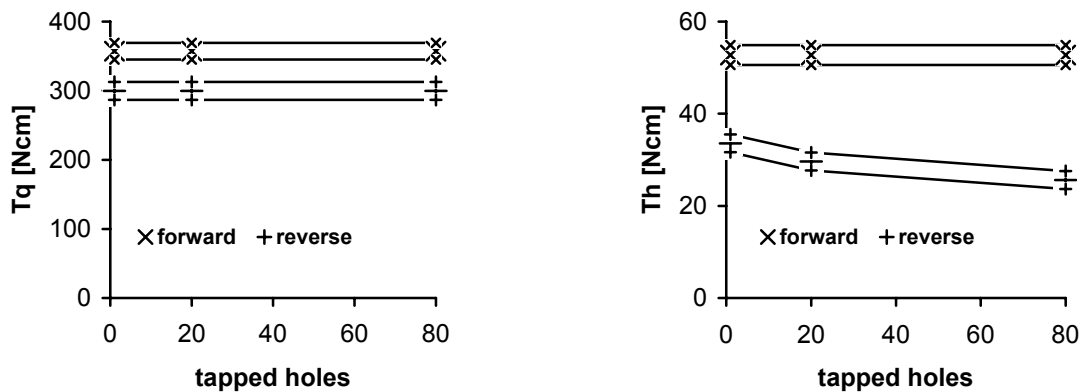


**Figure 5.2.** Graphs as a function of torque and thrust with respect to the number of holes tapped, for the TiN taps using a non-synchronous tapping attachment, refer to Table 12 for data.

**Table 13.** Results of torque ( $T_q$ ) and thrust ( $T_h$ ) generated by the TiCN coated taps using a non-synchronous attachment, with respect to the number of tapped holes (refer to Appendix 2, Table D, for data).

Measured Quantities	Torque [Ncm]				Thrust [N]			
	Forward		Reverse		Forward		Reverse	
	Mean	st. dev.	Mean	st. dev.	Mean	st. dev.	Mean	st. dev.
one	376.8	27.4	374	55.5	54.3	8.44	35	3.36
twenty	376.8	27.4	339	55.5	54.3	8.44	36	3.36
eighty	376.8	27.4	263	55.5	54.3	8.44	24	3.36

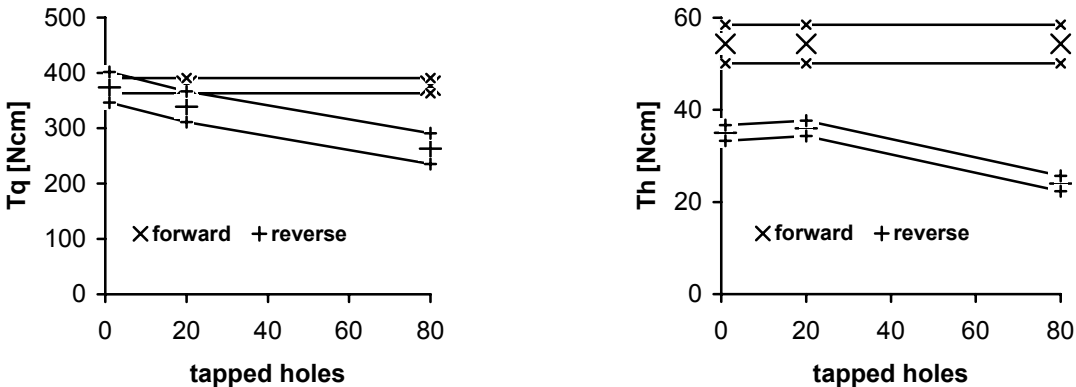


**Figure 5.3.** Graphs as a function of torque and thrust with respect to the number of holes tapped, for the TiCN taps using a non-synchronous tapping attachment, refer to Table 13 for data.

From Table 13 and Figure 5.3, the mean values of the forward torque for the TiCN taps with the non-synchronous attachment show qualitatively similar trends to the TiN coated taps. However, the mean value is slightly higher than the TiN tap. Harris [51] reported a similar trend when tapping cast iron with TiCN and TiN spiral flute taps, with the TiCN taps displaying consistently higher torque values (20 to 40% higher) than uncoated and TiN coated taps. Table 13 shows the reverse torque and thrust mean values to decrease with holes tapped, the thrust reducing significantly after twenty holes had been tapped. The forward thrust was higher than for TiN coated taps with a larger scatter for all measured holes tapped.

Failure of the 'go' end of the plug gauge for the uncoated taps after eighty holes and catastrophic failure of four of the uncoated taps, eliminated them from further comparison with the PVD coated taps, at the chosen measurement intervals. The TiN and TiCN coated taps were tested to four hundred and fifty holes with the incidence of tap breakage increasing for the TiN coated taps. All five of the TiCN coated taps survived to four hundred and fifty holes, however the incidence of randomly occurring plug gauge failures increased.

**Table 14.** Results of torque ( $T_q$ ) and thrust ( $T_h$ ) generated by the TiN coated taps using a non-synchronous attachment, after four hundred and fifty holes tapped (refer to Appendix 2, Table A, for data).

Measured Quantities	Torque [Ncm]				Thrust [N]			
	Forward		Reverse		Forward		Reverse	
	Mean 95%C.L.	st. dev. 95%C.L.	Mean 95%C.L.	st. dev. 95%C.L.	Mean 95%C.L.	st. dev. 99%C.L.	Mean 95%C.L.	st. dev. 95%C.L.
Number of holes tapped with the TiN coated taps								
one	348	24.14	304.2	28.6	52.9	3.1	26.9	5.6
twenty	364	24.14	318.8	28.6	52.9	6.1	26.9	3.3
eighty	360.8	24.14	276	28.6	52.9	2.7	26.9	1.6
two hundred	336	24.14	244	28.6	52.9	5	26.9	1.5
three hundred	371	24.14	266	28.6	52.9	2	26.9	2.3
four hundred fifty	399	24.14	259	28.6	52.9	21	26.9	10.4

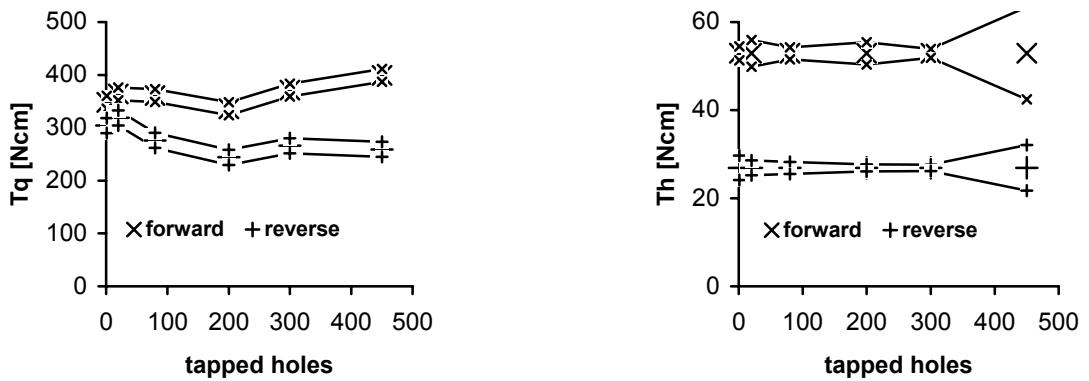


**Figure 5.4.** Graphs showing plots of statistically analysed torque and thrust values with respect to a number of tapped holes, generated by the TiN coated taps using a non-synchronous attachment, refer to Table 14 for data.

From the TiN coated taps in Figure 5.4, it is evident that the *forward* torque is initially on a downward trend until two hundred holes were tapped. From this point, the pattern shows a rise in the mean torque values suggesting a wear process is taking place, not evident with the forward torque of the TiCN taps. Similarly, this initial pattern of a reduction followed by a rise, was observed with the *reverse* torque for both TiN and the previous TiCN results. However, the mean values of the reverse torque for the TiN coated tap appear to have reached a plateau after two hundred holes. For thrust, the mean value is shown to be the same for all holes for forward thrust and the same for the reverse thrust. Interestingly, after three hundred holes, the scatter for both forward and reverse thrust increases significantly when measured at four hundred and fifty holes. It is suspected that this scatter is in part due to chip jamming in both forward and reverse tap motions.

Chip clogging or swarf jamming in the flutes is a random process that was observed to occur more frequently when the taps had tapped over three hundred holes. In the instance when this occurred, fine stringy chips (swarf) were observed to wrap tightly around the flute. These constrained chips would have affected the transportation of the larger swarf from the hole. It is interesting that swarf jamming has also been reported [33] as a random process when tapping below 1.5 tap diameters with straight flute taps. However, the swarf produced by straight flute taps behaves differently in that the chips are not transported from the flutes as they are with spiral flute taps, and such random swarf jamming of straight flute taps can be observed from the first hole tapped.



**Table 15.** Results of torque ( $T_q$ ) and thrust ( $T_h$ ) generated by the TiCN coated taps using a non-synchronous attachment, after four hundred and fifty holes tapped, refer to Appendix 2, Table A, for data.

Measured Quantities	Torque [Ncm]				Thrust [N]			
	Forward		Reverse		Forward		Reverse	
	Mean 95%C.L.	st. dev. 95%C.L.	Mean 95%C.L.	st. dev. 95%C.L.	Mean 97%C.L.	st. dev. 95%C.L.	Mean 95%C.L.	st. dev. 95%C.L.
one	372	22.52	374	58	54.5	7.1	35.4	3.68
twenty	372	22.52	339	58	54.5	7.1	36.2	3.68
eighty	372	22.52	262	58	54.5	7.1	24	3.68
two hundred	372	22.52	240	58	54.5	7.1	28.9	3.68
three hundred	372	22.52	244	58	54.5	7.1	27.9	3.68
four hundred fifty	372	22.52	251	58	54.5	7.1	25.4	3.68

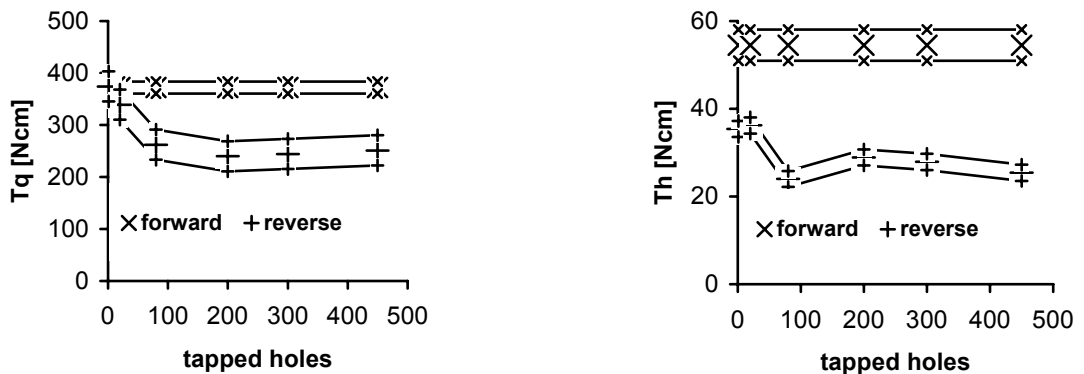


**Figure 5.5.** Graphs showing plots of statistically analysed torque and thrust values with respect to a number of tapped holes, generated by the TiCN coated taps using a non-synchronous attachment, refer to Table 15 for data.

The statistical results of the torque and thrust for a TiCN tap over four hundred and fifty holes, using a non-synchronous attachment, are shown in Table 15 and Figure 5.5. It is evident that the forward torque pattern shows the same mean value and standard deviation for all measurement intervals, slightly lower than the results in Table 13 for the same TiCN taps over eighty holes. The forward thrust results over four hundred and fifty holes show negligible change in comparison to the forward thrust results over eighty holes. Interestingly, the reverse torque and thrust results show a decrease in mean values from the initial starting values. The mean reverse torque is shown to be at a minimum value at two hundred holes at which point it starts to progressively increase. The reverse torque results may indicate increased relief wear after two hundred holes, causing increased friction and hence torque on reversal. The reverse thrust is shown to be at a minimum at eighty holes then to increase at two hundred holes, followed by a progressive decrease in mean values.

Increased wear promotes higher cutting temperatures and cutting forces, and removal of the PVD coating by wear processes, thus one would expect the high carbon content of the TiCN coatings to increase wear life. The TiCN coating is reported [77] to form a metal stabilised carbon structure with the carbon mostly in the form of  $sp^2$  bonding, as per the graphitic coating developed by Teer Coatings [75,76].

Agreement with recommendations of the expert systems for torque versus surface treatment for Manufacturer's 1 and 2 (see Chapter 2, Section 2.2, Figure 2.4) was found after eighty holes tapped, that is, no change in recommended torque for uncoated or PVD coated taps. In contrast Manufacturer's 3 and 4 from Figure 2.4 recommend reduced torque for PVD coated taps in comparison to uncoated taps, however it should be noted that the uncoated and PVD coated taps have recommended tool lives significantly greater than eighty holes when tapping 316 stainless steel (see Chapter 2, Section 2.2, Figure 2.5). The uncoated taps began failing after eighty holes tapped without torque and thrust values recorded, preventing further comparison with the PVD coated taps, which continued to perform.

### 5.2.2 Comparison of Tapping Attachments

As discussed in the literature review (see Chapter 2, Section 2.2, Figure 2.6, Figure 2.7 and Figure 2.8) there is a general recognition that different types of tapping attachments may affect the performance of taps. In the present study, it was decided to test this by using two different types of tapping attachments, namely, non-synchronous and synchronous when tapping stainless steel with TiCN coated taps. Results for forward and reverse components of torque and thrust obtained when using the synchronous tapping attachment are shown in Table 16 and Figure 5.6.

**Table 16.** Results of torque ( $T_q$ ) and thrust ( $T_h$ ) for TiCN coated taps after 450 holes tapped using a synchronous attachment, refer to Appendix 2, Table B, for data.

Measured Quantities	Torque [Ncm]				Thrust [N]			
	Forward		Reverse		Forward		Reverse	
	Mean 95%C.L.	st. dev. 95%C.L.	Mean 97%C.L.	st. dev. 97%C.L.	Mean 95%C.L.	st. dev. 95%C.L.	Mean 99%C.L.	st. dev. 95%C.L.
one	422.1	20.1	397.6	32.9	185.9	41.5	335.3	60.3
twenty	364	20.1	300.46	34.9	185.9	41.5	682	60.3
eighty	338.4	20.1	266	13.4	185.9	41.5	571	60.3
two hundred	375.7	20.1	308.5	120.3	185.9	41.5	391	60.3
three hundred	356.8	20.1	283.2	59.6	185.9	41.5	637	60.3
four hundred fifty	397.6	20.1	207.5	63.3	185.9	41.5	376	60.3

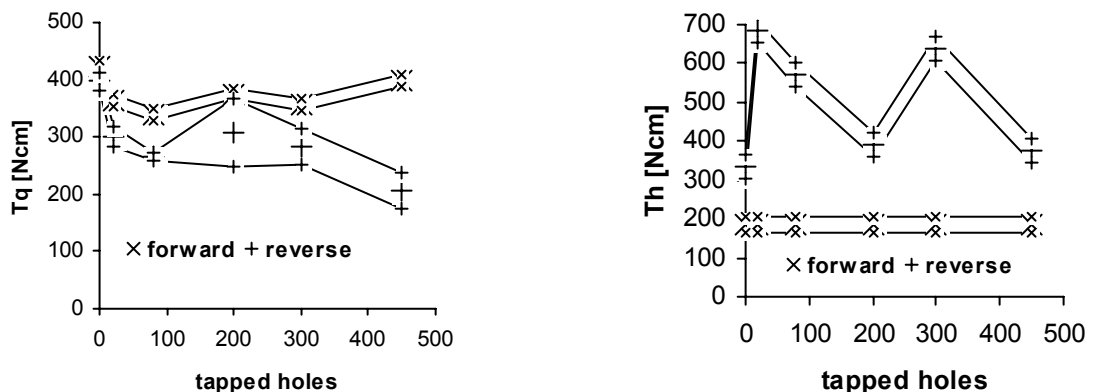


**Figure 5.6.** Graphs showing plots of statistically analysed torque and thrust values with respect to a number of tapped holes, generated by the TiCN coated taps using a synchronous attachment, refer to Table 16 for data.

It is evident that (refer to Table 16 and Figure 5.6) after the first hole there is a slight fall in the forward torque up to eighty holes tapped, after which, it increases with the number of holes tapped. Likewise, the reverse torque shows a decrease over the first twenty to eighty holes. However, at two hundred holes, the scatter has increased significantly and further investigation of the individual torque results revealed that two of the five taps experienced a significant rise in measured torque for both the forward and reverse components increasing the mean value and the upper bound of the scatter. It is evident from the torque graph in Figure 5.6 that the forward component has a trend of increasing torque with the number of holes tapped and the reverse component a trend of decreasing torque with the number of holes tapped.

The forward thrust is shown to be consistent in both mean values and scatter, however, the reverse torque shows erratic behaviour with significant variation in mean thrust values while the scatter remains similar in magnitude.

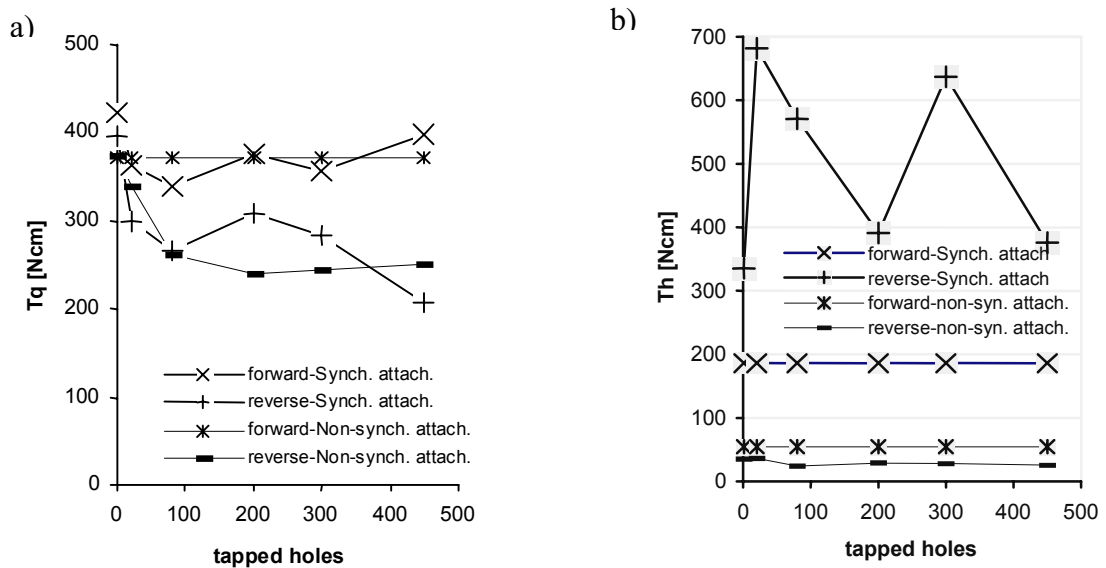


**Figure 5.7.** Graphs comparing torque and thrust values for (a) non-synchronous and (b) synchronous attachments for TiCN coated taps, standard deviation not shown for clarity.

In order to better compare the two attachments, an overlay of the graphs is presented in Figure 5.7, in which, it is evident from Figure 5.7 (a) that the forward and reverse torque values for both attachments are of a similar magnitude with the synchronous attachment showing a steady rise in forward torque after one hundred holes tapped. The scatter of the reverse torque for the synchronous attachment shown in Figure 5.6 is broad and can contain the mean values and scatter (see Figure 5.5) of the non-synchronous attachment within its boundaries.

From Figure 5.7 (b), the mean values of the forward thrust for the synchronous attachment are the same for all holes tapped, however, significantly larger (up to 14 times larger) than the mean values of all TiCN taps using the non-synchronous attachment. The scatter is also large in comparison to the taps using the non-synchronous attachment. The erratic behaviour of the mean values for reverse thrust with consistent scatter for the number of holes tapped raises some arguable points as to why this observation occurs. At two hundred and at four hundred and fifty holes, the thrust was half the mean values found for the other measurement points. From Figure 5.7 (b), the general large increase for forward and reverse thrust (over a non-synchronous attachment) was considered a result of poor synchronisation of the machine spindle axis with the spindle rotation. However, the variation in the mean values of reverse thrust cannot be readily explained, as these significant increases did not correspond to the forward thrust and, with increases in forward and reverse torque. This allows equipment and/or user error to be discounted. Damage to the heel cutting edge would present similar increases in measured torque and thrust, however such increases would be repeated for all holes tapped at later stages and this was not observed.

This observation can be explained by a number of variables, namely; flank cutting on reversal, absence of significant material transfer to the tool/work contact surface causing increased friction, and swarf jamming which can lead to reduced coolant access. A combination of the above cases may lead to galling (wear) and tap seizure reported by Zhang and Chen [38] in difficult-to-cut materials when deep-hole tapping with taps below a nominal diameter of 6 mm.

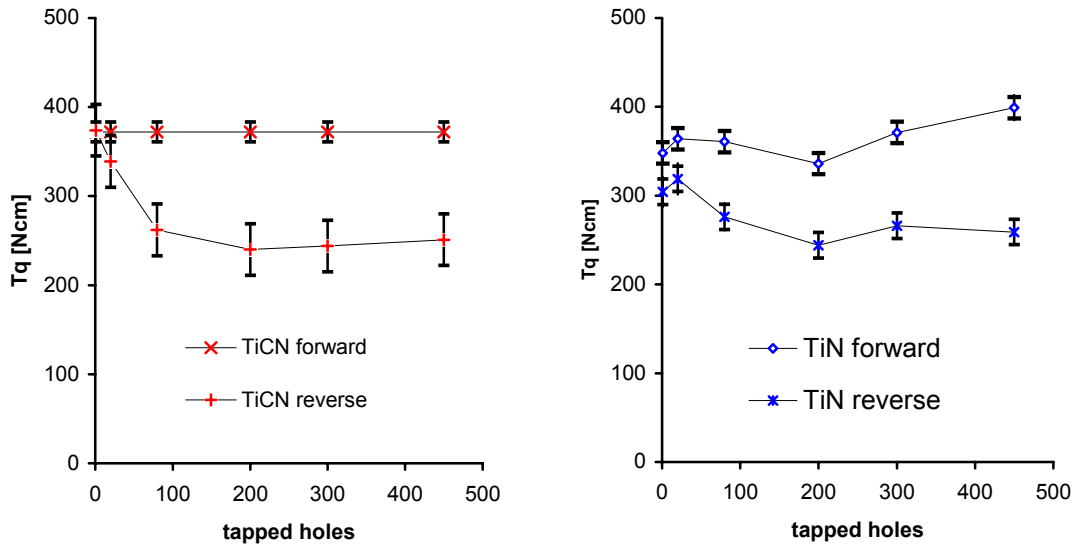


**Figure 5.8.** Torque comparison of TiCN and TiN coated taps for non-synchronous attachment.

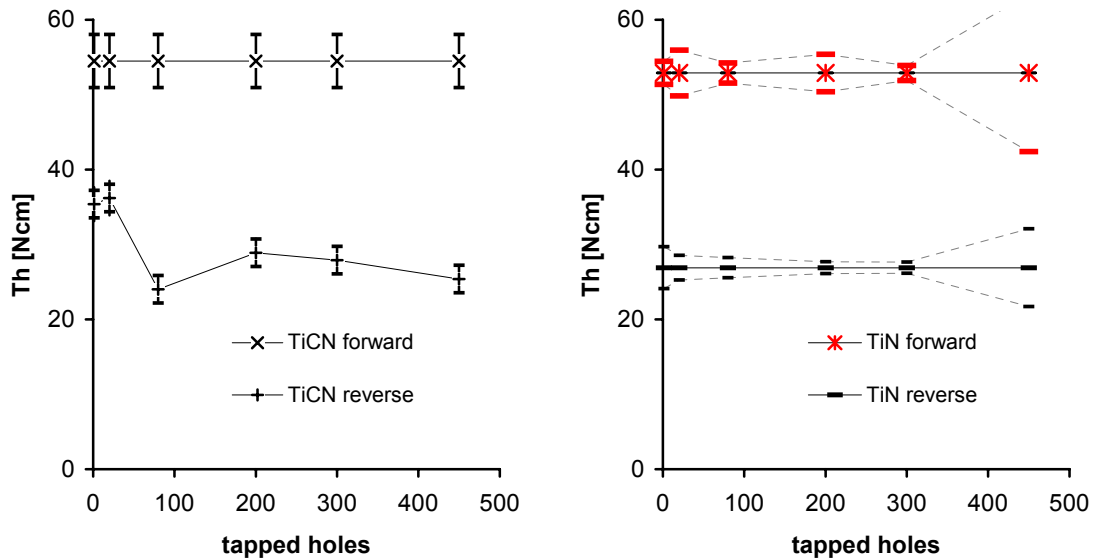


**Figure 5.9.** Thrust comparison of TiCN and TiN coated taps for non-synchronous attachment.

It is evident from the torque graph shown in Figure 5.8, comparing TiCN and TiN coatings using a floating holder, that the TiCN coating provided improved performance for forward and reverse torque. However, the TiN coated tap out performed the TiCN coated tap below eighty holes tapped. After three hundred holes, the TiN coated tap showed inferior performance to the TiCN coated tap for forward torque and thrust.

Figure 5.9 shows the thrust for the TiN coated taps to increase in scatter after three hundred holes. This also corresponded to an increase in the observation of swarf jamming for the TiN coated taps, suggesting cold-welding of the chip to the cutting tool.

### 5.2.3 Analysis of Cutting Tool Wear

The outer diameter (OD) relief from the cutting edge to the trailing edge of the full form teeth of all taps was taken to represent tap wear. A reduction in mean relief values indicate wear. The mean values of the O.D. relief profiles for uncoated, TiN coated and TiCN coated taps after a) new, b) one hole, c) twenty holes, and d) eighty holes are shown in Figure 5.10. The tapping tests were conducted using a non-synchronous tapping attachment.

The relief profile is identified by two vertical lines on each of the measured relief profiles. These vertical lines identify the range over which a gradient was calculated for each slope using CMS software to determine the relief values. The rise and fall of the profiles either side of the two vertical lines represent the stylus engaging and disengaging with the thread land from one flute to the next. Radius profiles, outside of the measured range, showed a change with the number of holes tapped. However, measurements of these changes in radius are not analysed because, firstly, the CMS machine was not designed to measure the radius and, secondly, the stylus was not designed to trace along the rake and heel face.



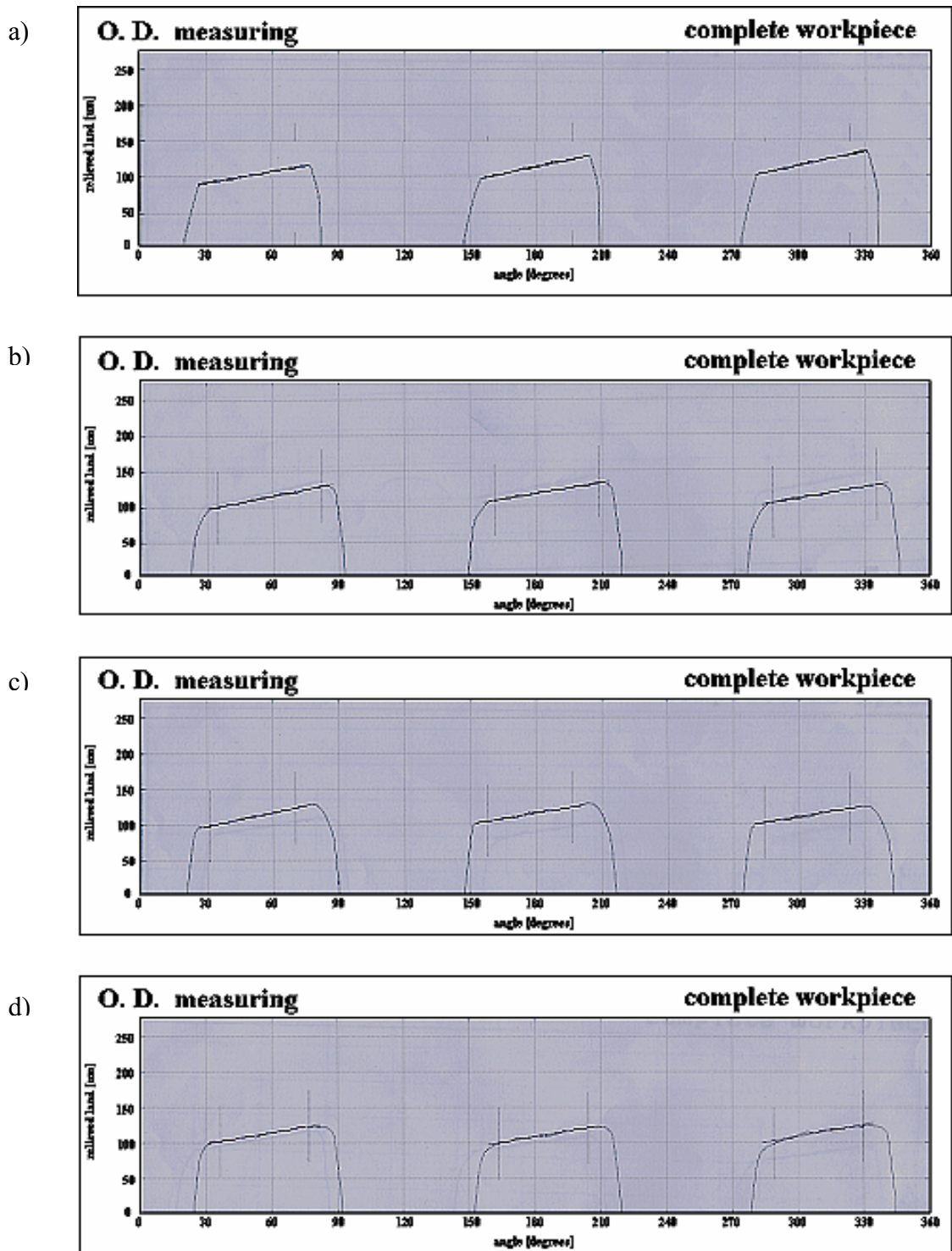


**Figure 5.10.** O.D. relief measurements of an uncoated tap for a) new, b) one hole, c) twenty holes, and d) eighty holes, showing measured relief profiles for three lands on an uncoated tap for an axial floating holder.

**Table 17.** Mean values of outer diameter (O.D.) relief profiles averaged over 5 taps for each surface condition and the three lands for each tap.

Tool surface conditions	Tap Holder	Chosen measurement Intervals (No. of Holes)						
		New	1	20	80	200	300	450
Uncoated	Non-synchronous	19.8	19.1	18.9	18.6	-	-	-
TiN coated	Non-synchronous	21.5	20.6	-	20.4	21.3	22.2	21.3
TiCN coated	Non-synchronous	18.2	20.3	-	21.2	21.2	22.5	21.1
TiCN coated	Synchronous	18.9	19.8	-	20.7	24.3	25.6	25.0

Note: - data not recorded.

**Table 17** lists the mean values of outer diameter (O.D.) relief profiles averaged over 5 taps for each surface condition and the three lands for each tap. It is evident that the wear appears to plateau for the coated taps in that it does not decrease below the minimum value measured during the first hole tapped. This raises an interesting question as to whether the wear is insignificant along the OD relief for coated taps for the number of holes tested, or material transfer on the thread relief surfaces is preventing accurate measurement of relief wear. Importantly, the effect of the material transfer may only impact on tap performance after significant wear has occurred to the PVD coatings allowing the work material to significantly build-up.

A further analysis of the tool/work contact surfaces was carried out using scanning electron microscopy (SEM) with the aim of identifying any material transfer or evidence of built-up edge. Figure 5.11 is an SEM image of a TiCN tap after tapping 450 holes using a synchronous attachment, showing material transfer on the outer diameter relief profile of a thread land, near the heel edge of the flanks.

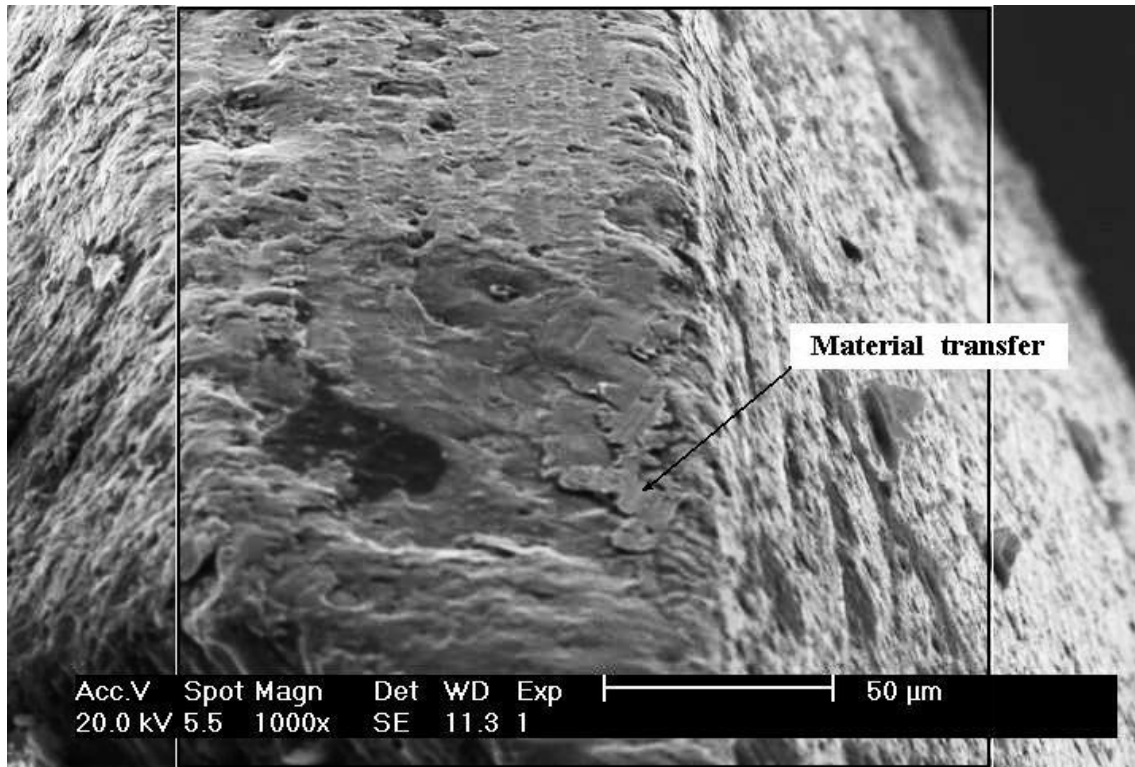
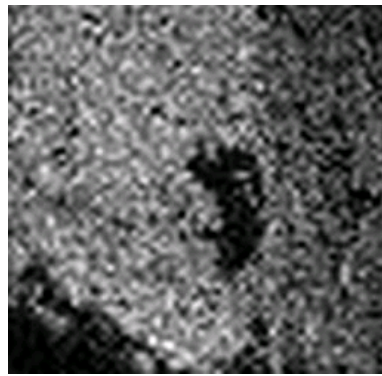


**Figure 5.11.** SEM image of a TiCN coated spiral fluted tap, showing material transfer on the surface of the thread crest near the heel edge of the tap. The box shows XRM selected area.

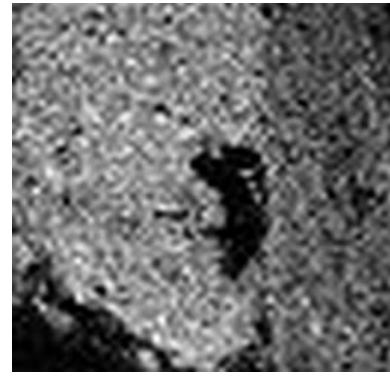
An energy dispersive spectral (EDS) analysis was carried out on the material transfer in order to confirm the origin of the transferred material (see Figure 5.11). Table 18 lists the elements present on the tap surface that were detected by the EDS. The two most abundant elements were titanium and carbon, the bulk of which derives from the TiCN coating. X-ray mapping (XRM) of the elemental composition within the box overlaid on Figure 5.11 was also performed (see Figure 5.12). The result of this analysis was consistent with the interpretation that the TiCN is largely intact with the addition of material transfer from the work material. The remainder of the elements detected are consistent with the particular grade of high-speed steel, namely, M9V (see Chapter 4, Section 4.2.1, Table 3).

**Table 18.** Relative elemental constituents of the selected area detected by the EDS.

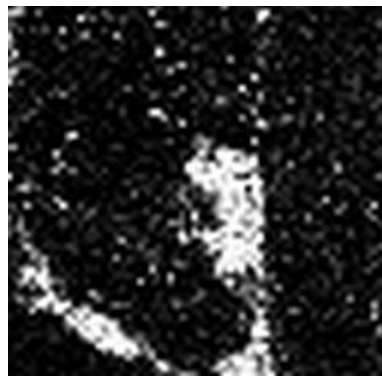
EDS spectra of a TiCN coated tap after 450 holes using the rigid holder.									
Element	Cr	Mn	Fe	Co	Ni	V	Ti	C	Mo
wt.%	0.87	0.14	4.24	0.04	0.38	0.26	29.11	64.83	0.13



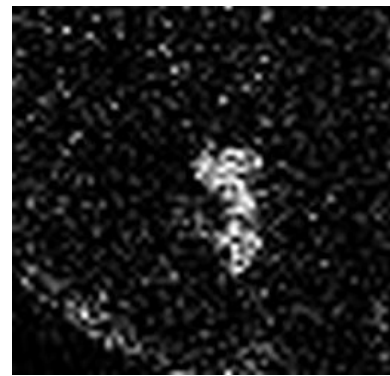
Carbon - C



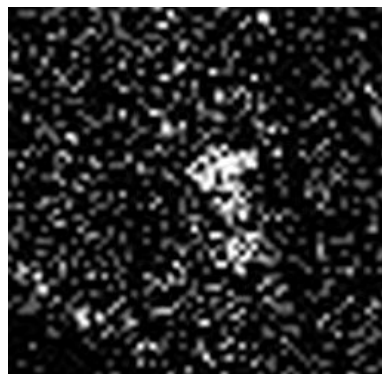
Titanium - Ti



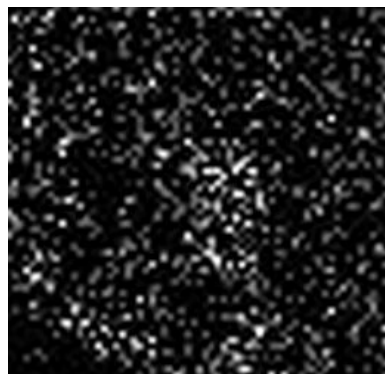
Iron - Fe



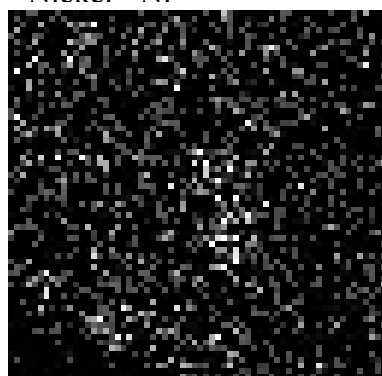
Chromium - Cr



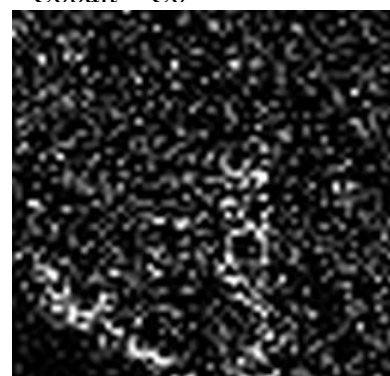
Nickel - Ni



Cobalt - Co



Magnesium - Mn



Molybdenum - Mo

**Figure 5.12.** Relative compositional analyses using X-ray mapping, of the thread crest in the selected area (as shown in Figure 5.11), showing stainless work material transfer (Cr and Ni) and loss of PVD coating at the cutting edges (Fe and Mo).

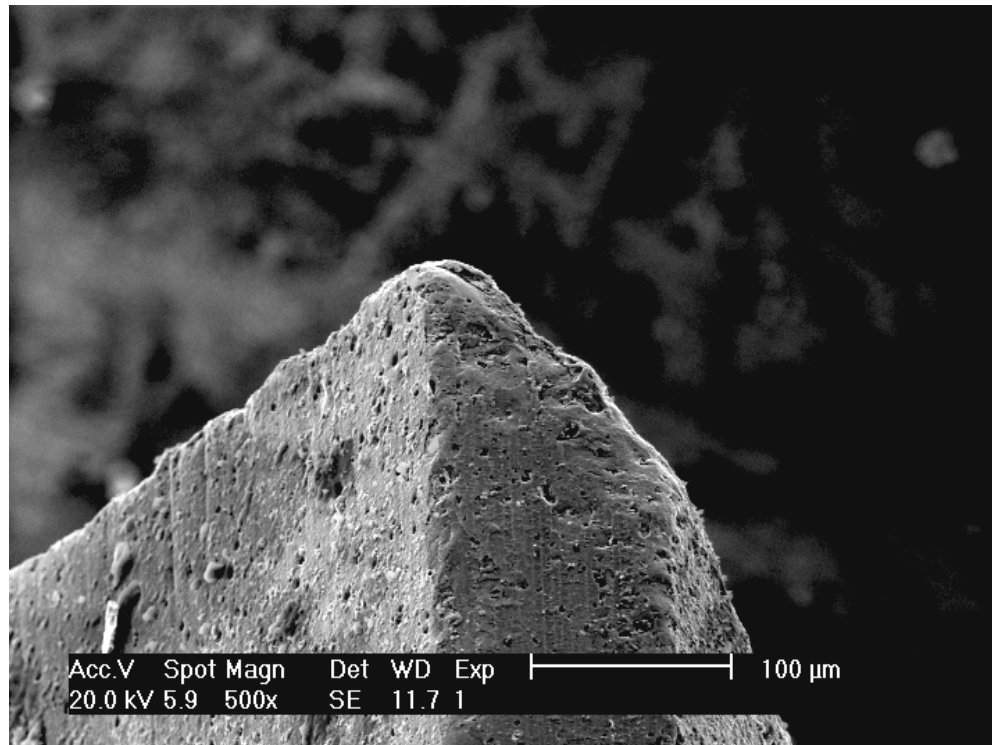


**Figure 5.13.** SEM image of a full form sizing tooth and thread flanks for a new TiCN tap with the leading thread flank to the left and the rake face hidden from view.

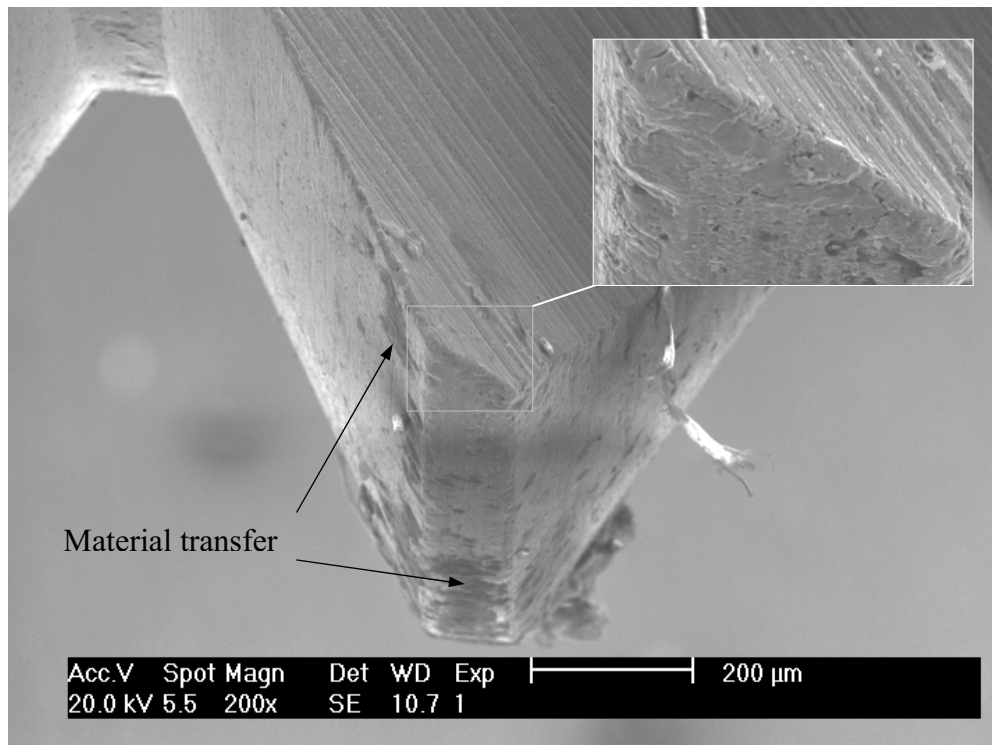


**Figure 5.14.** SEM image of a TiCN tap after 450 holes using a non-synchronous attachment, showing minimal wear to the full-form sizing tooth. Inset: Magn 2000x.

The SEM image in Figure 5.13 shows the condition of a TiCN tap in the as received condition for a full form sizing tooth with some grinding marks from manufacture visible on the leading thread flank. Figure 5.14 is an SEM image of a TiCN coated tap after tapping 450 holes using a non-synchronous attachment, showing minimal wear to a full-form sizing tooth (an equivalent tooth to that shown in Figure 5.13). Material transfer is evident on the flank surfaces and the OD relief profile (thread crest), however, the material transfer on the OD relief profile occurs away from the cutting edge where the relief profile reduces in diameter. This is further evidence for the lack of a decrease in measured O.D. relief shown in

**Table 17.**

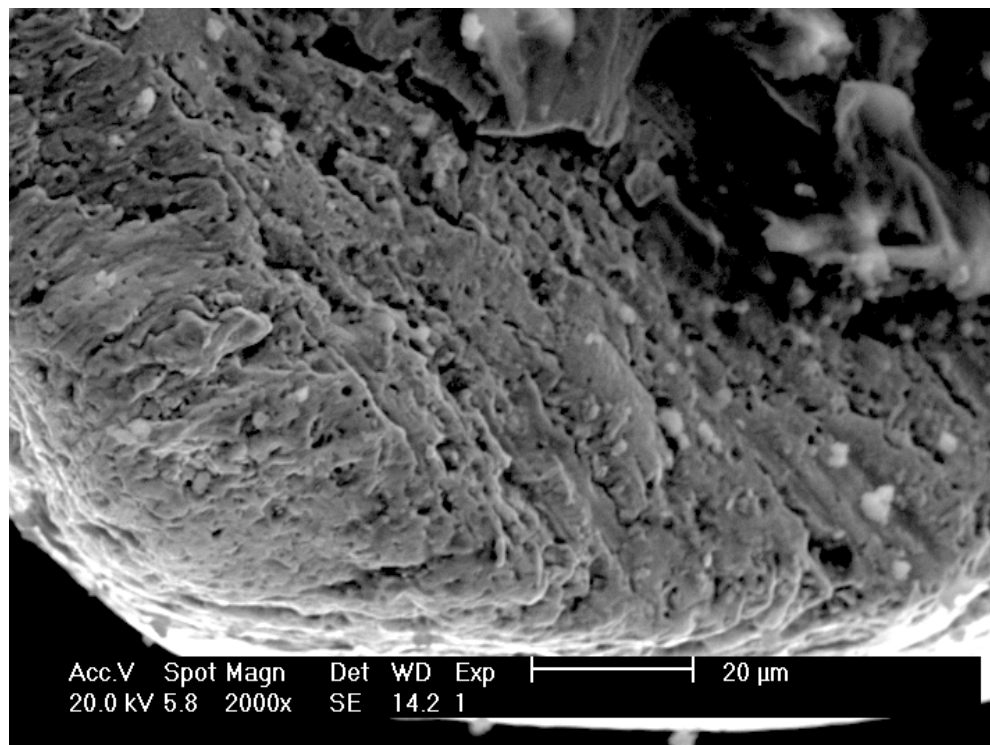


**Figure 5.15.** SEM image of the rake face for a full form tooth of an uncoated tap after eighty holes with an non-synchronous attachment, showing adhesive wear. Magnified 2000x.

Figure 5.15 is an SEM image of the rake face of a full form tooth of an uncoated tap after eighty holes using a non-synchronous tapping attachment, showing adhesive wear



caused by a process of material transfer. Comparing the inset image of Figure 5.14 for a TiCN coated tap after 450 holes with Figure 5.15 of an uncoated tap after eighty holes, each at a magnification of 2000x. It is apparent the uncoated tap experiences adhesive wear at the rake face at a much lower number of holes.

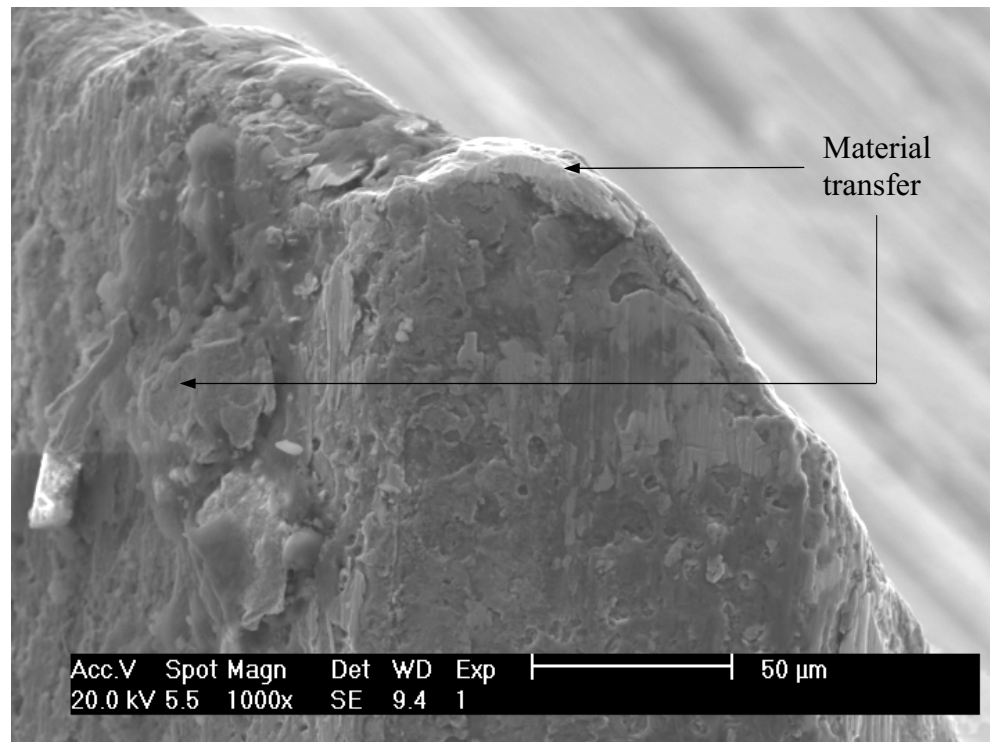


**Figure 5.16.** SEM image of a TiCN tap after 450 holes tapped using the synchronous attachment, showing wear and material transfer to a full form sizing tooth.

The SEM image shown in Figure 5.16 is of a full form sizing tooth of a TiCN tap after tapping 450 holes using a *synchronous* attachment. This shows wear to the cutting edges and material transfer to the thread flanks and thread crest (outer diameter relief land).

It is evident from such images (uncoated and PVD coated) that there is material transfer from the stainless steel work material to the taps. This is probably not surprising given the high levels of high strain deformation known to occur in machining and hence the likelihood of delamination wear occurring [78]. The material transfer has a greater effect on the uncoated taps leading to adhesive wear, whereas, the PVD coated taps are shown to have a thin film of material transfer without evidence of adhesive wear.

#### 5.2.4 Tool Life

Figure 5.17 shows the mean values of the tool life as measured using the go / no-go plug gauge for different tap surface treatments and the type of tapping attachment used. For the taps tested with the non-synchronous tapping attachment, the uncoated taps were observed to catastrophically fail (i.e. fractured) on the forward cutting motion following (after a few holes) a ‘screech’ sound when the tap neared the bottom of the hole. It should be noted that ‘screech’ is a common term used in industry for failure associated with a loud noise. On inspection of the uncoated taps after incidence of screech, it was found that chipping of both the full form teeth and the lead chamfer teeth had occurred. Consequently, the mean tool life as measured by the plug gauge for the uncoated taps was 104 holes with a scatter of  $\pm 21$  holes (see Figure 5.17).

In contrast, the TiN coated taps failed the ‘go’ (undersize) end of the plug gauge without any associated prior screech. In the test, four TiN coated taps did not pass the ‘go’ end of the plug gauge at 450 holes. Consequently, all prior holes tapped were checked with the gauge in order to determine tool life. A feature of the operation of these taps, i.e. TiN and TiCN when using a non-synchronous attachment, was irregular swarf jamming in the flutes after approximately two hundred holes tapped. This was associated with ‘balling’, a term used to describe when a chip remains in the flute of the tap and becomes entangled in the new chips produced. This phenomenon was observed irregularly and for one of the TiN coated taps, up to the point of catastrophic failure (by fracture) at 285 holes. The mean tool life for the TiN coated taps was 366 holes with a scatter of  $\pm 40$  holes (see Figure 5.17), this is a three-fold improvement on the uncoated taps for the same non-synchronous attachment.

The TiCN coated taps for the non-synchronous tapping attachment showed the best performance in threaded hole accuracy, with all five taps gauged to four hundred and fifty holes. This result is in agreement with the result of the torque, thrust and wear analyses, showing the TiCN taps for the non-synchronous attachment to have superior performance for 450 holes tapped in comparison to the uncoated (104 holes) and TiN coated (366 holes) taps.

In contrast, swarf jamming was observed after eighty holes for the TiCN coated taps tested using the *synchronous* attachment, with a corresponding increase in the random incidence of undersize gauge measurements. Consequently, the mean life of the TiCN coated taps using the synchronous attachment was reduced to 266 holes with an



increased scatter of  $\pm 93$  holes (see Figure 5.17). The increased wear to the full form sizing tooth for the synchronous tapping attachment as shown in Figure 5.16, correlates with the results of the tool life as measured by the thread gauge in comparison to the wear of the TiCN coated tap using the non-synchronous attachment shown in Figure 5.15.

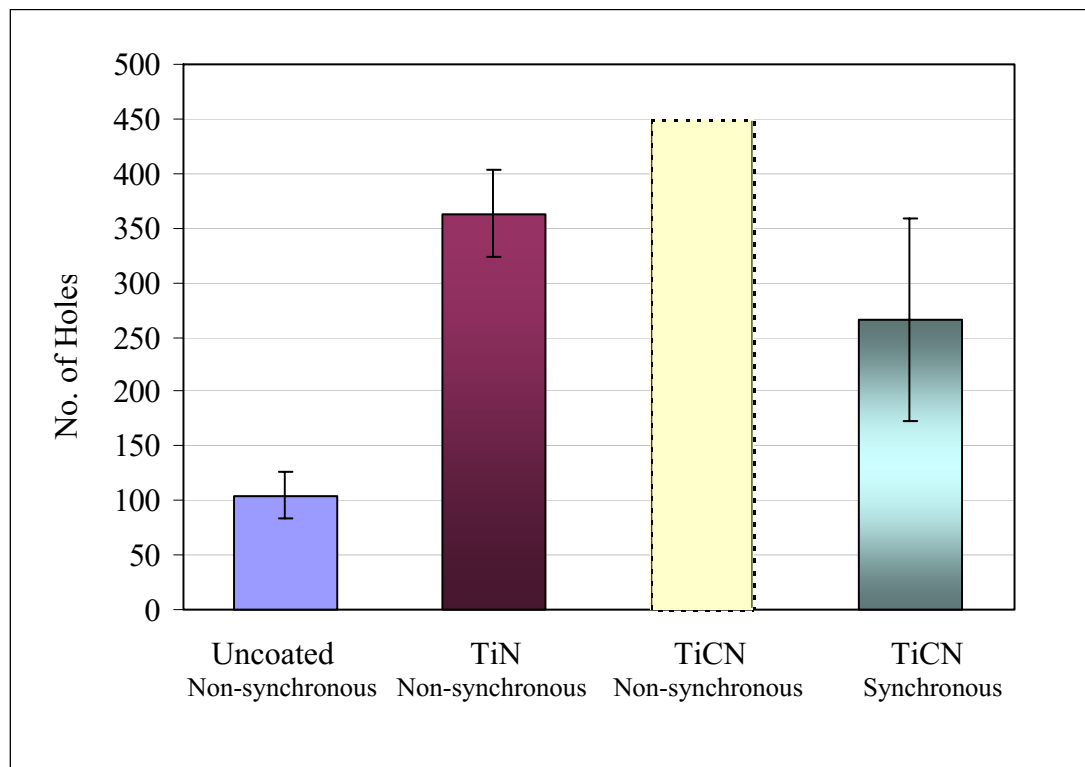
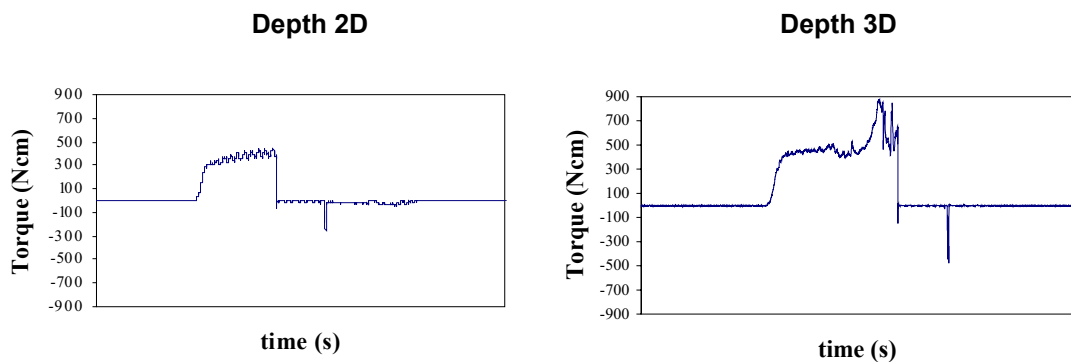


**Figure 5.17.** Histogram showing a comparison of tool life as measured in terms of threaded hole accuracy and surface treatment of spiral flute taps. Non-synchronous and synchronous indicating the type of attachment used.

It is evident from Figure 5.17 that for a *non-synchronous* attachment, the TiCN coated taps out-performed the TiN coated taps and have a significant advantage over uncoated taps when tapping stainless steel. The non-synchronous attachment also provides an advantage over the *synchronous* attachment when comparing TiCN taps of the same design. Further, the tool life results as measured by the go/no-go plug gauge do not compare with the outer tap relief measurements presented earlier (Section 5.2.3, Table 17), as the outcome is obscured for PVD coated taps and therefore, does not provide a quantifiable method to measure tool life in this investigation. This is also consistent with the metallographic analysis showing evidence of material transfer and negligible wear to the outer tap relief for the PVD coated taps.

### 5.3 Deep Hole Tapping

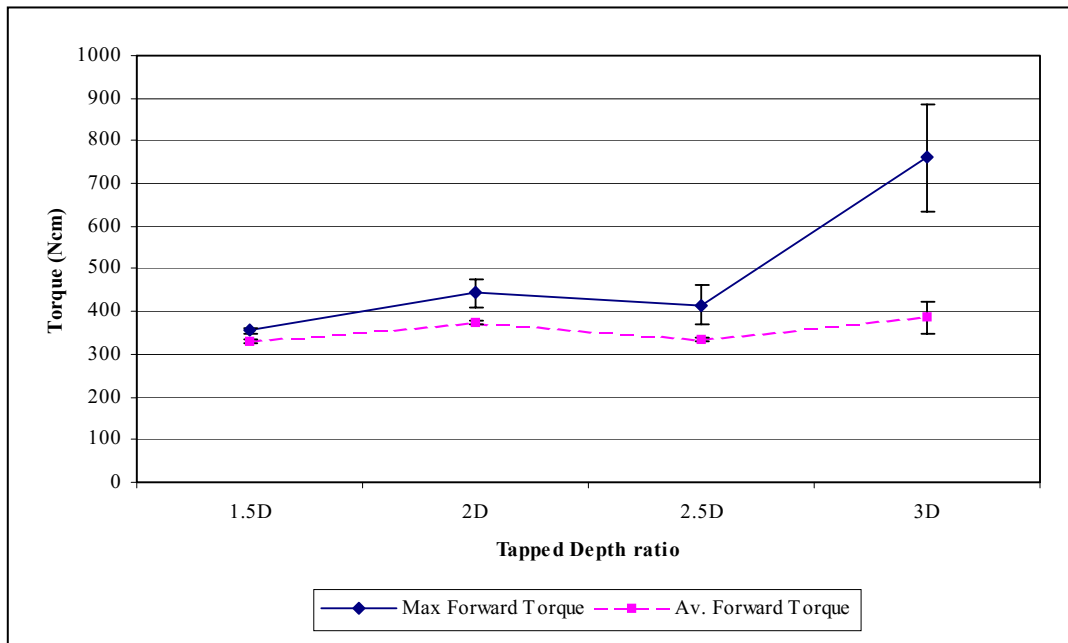
In deep hole tapping, industry publications [39,40] suggest a combination of restricted volume of flute space, restricted lubricant access to the cutting edges of the tap and work hardening of the work material at the chip/tool interface to be the cause of tap failures. The solution of the machine shop engineers using their skilled craft oriented knowledge was to reduce the surface cutting speed when tapping holes greater than 1.5 tap diameters and was supported by the industry publications [39,40]. This is consistent with cutting tool manufacturers electronic catalogues [10-12] that show a drop in cutting speed for increased hole depth, of approximately 50% at a depth of 2.5 times nominal tap diameter or greater for both straight and spiral flute taps. In this study, analysis on the torque and thrust for a range of hole depths at a constant cutting speed of 3 m/min for a non-synchronous attachment, was examined for spiral flute taps. Typical torque charts as a function of time are given for two hole depths of two and three tap diameters respectively showing increased torque with hole depth (see Figure 5.18).



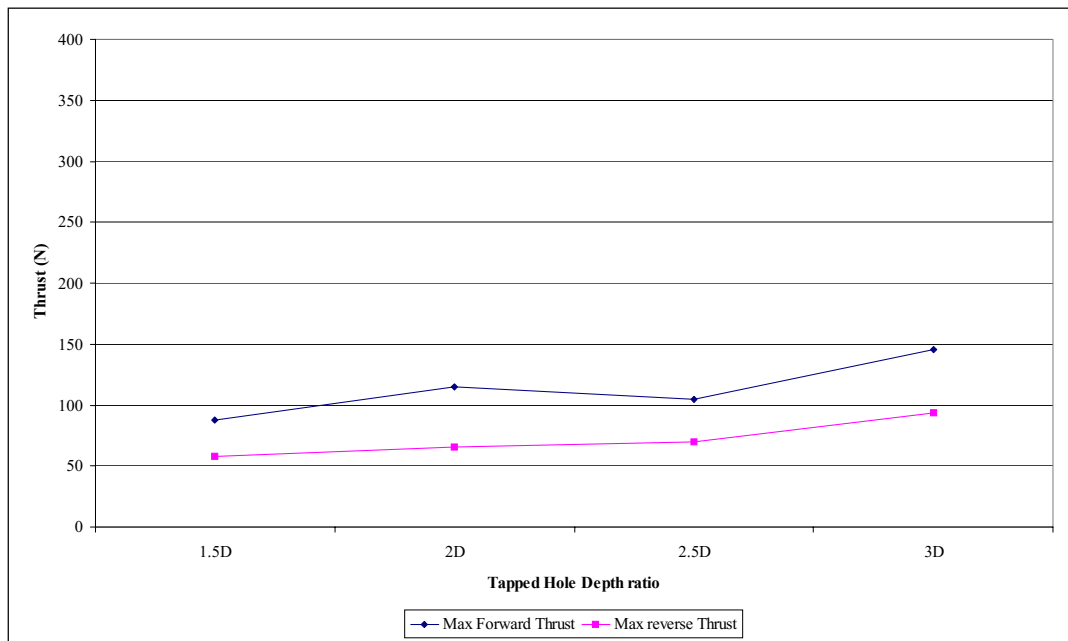
**Figure 5.18.** Typical charts recorded for the torque as a function of time for hole depths 2D and 3D respectively, showing the torque to increase as the tapping progresses to the bottom of the hole.

Figure 5.19 charts the arithmetic mean values of the mean forward torque and maximum forward torque over ten holes with the ratio of threaded hole depth over nominal tap diameter, showing an increase in torque for increased threaded hole depth. The mean forward torque (lower line) showed a linear trend of increasing torque with increased hole depth, however, the maximum forward torque (upper line) shows a significant increase above a tapped hole-depth of 2.5 times the nominal tap diameter (i.e. 2.5D). At 2.5D, there is an approximate 50% increase in maximum torque compared to depth at 1.5D, while at 3D this increases to approximately 150%. Swarf

jamming was not observed during the investigation, however swarf compaction within the flutes cannot be discounted.



**Figure 5.19.** Arithmetic mean values of the mean forward torque and maximum forward torque over ten holes with the ratio of threaded hole depth over nominal tap diameter, showing an increase in torque for increased threaded hole depth.



**Figure 5.20.** Arithmetic mean values of the maximum forward thrust and average reverse thrust over ten holes with the ratio of threaded hole depth over nominal tap diameter, showing an increase in thrust for increased threaded hole depth.

The slight increase in thrust for increased tapped hole depth observed in Figure 5.20, would suggest that swarf compaction within the flutes was impacting on the axial thrust. This is supported by the published literature [4] that indicates as the depth of the tapped hole increases, the swarf-jamming load becomes a dominant factor, while at hole depths less than 1.5 tap diameters, the swarf-jamming load was shown to be random in occurrence. The increase in load with hole depth is consistent with cutting tool manufacturers electronic catalogues [8,10,12] showing increased torque and reduced tool life, however, competing electronic catalogues [9,11] show no change in estimated torque or tool life.

From equation 7, Chapter 2, Section 2.1, the torque is assumed to be independent of cutting speed, thus, reducing cutting speed should not alter the torque, however, it allows more time for lubricant to gain access to the cutting edges and in theory reduce the torque by reducing friction at the tool/chip interface. The mechanistic model by Cao and Sutherland [4] accounts for cutting speed changes in the prediction of tapping loads, but only minor changes in loads were predicted and found. From an earlier exploratory study [79] with the local cutting tool supplier, the effect of reduced cutting speed on the measured torque for increased tapped hole depth was investigated, see Figure 5.21. The same tap designs and work materials used throughout this investigation, namely, M6 R45VA taps and 316 stainless steel, were also used for this test. As only one tap was used for each depth and speed combination, the results can only be considered a qualitative guide. The relationship established from the skilled craft oriented knowledge shown in Chapter 3, Section 3.3.4 , Figure 3.4 was used to determine the reduction in cutting speed with increased hole depth.

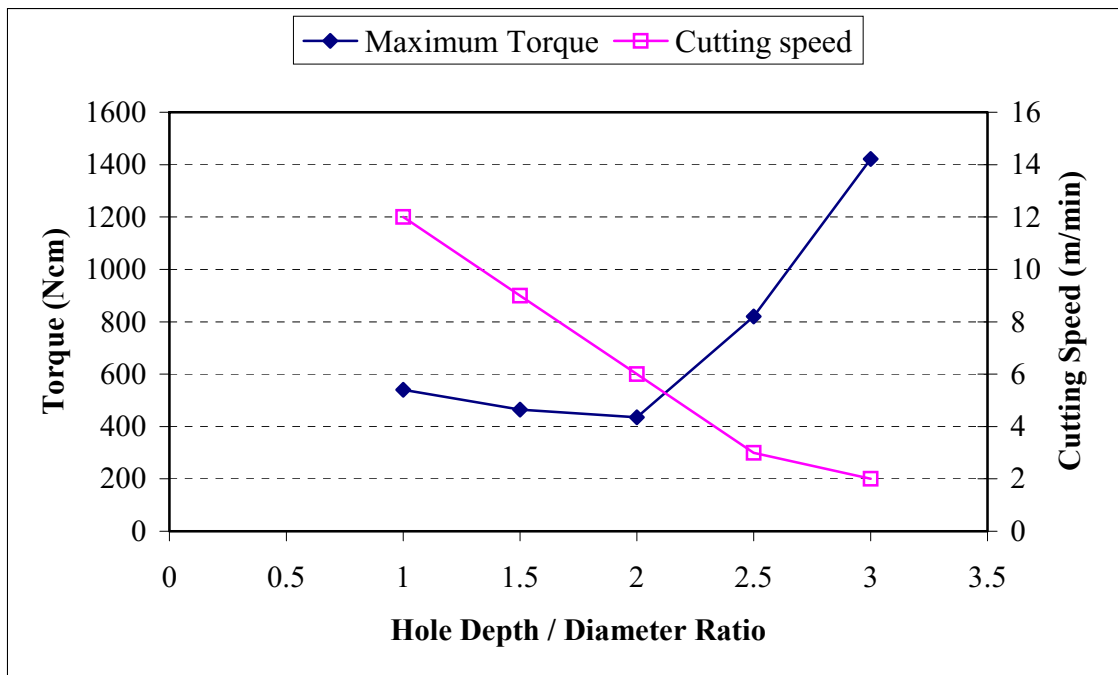


**Figure 5.21.** Charts the qualitative trend in forward torque as a function of reduced tapping speed versus the ratio of threaded hole depth over nominal tap diameter, showing that after a depth of two tap diameters, reducing the cutting speed does not prevent an increase in torque [79].

It was observed that, tapping at a depth of two tap diameters or greater, the reduction of cutting speed did not prevent an increase in torque. This is in agreement with the cutting tool manufacturers electronic catalogues [8,10,12] showing increased torque with hole depth, however, these catalogues appear to underestimate the significant increase in torque as observed in the above studies.

It is proposed that the largest gains in tap performance for tapping two diameters and greater, will be from improved coolant access to the cutting edges. Higher coolant pressure, increased flute volume and through tap coolant may provide the method for improved deep-hole tapping.

#### 5.4 Tool Rigidity

Tool rigidity has been investigated to determine if a decrease in tap diameter and inherent torsional strength will decrease the maximum cutting speed capability of the tap. In particular, it has been observed that small taps (below M6) fail more frequently during blind-hole tapping due to several factors [48]. From Figure 5.22, it is evident small diameter taps of less than M6 tend to fail at significantly lower surface cutting speeds. Interestingly, the M5 diameter tap broke at a lower cutting speed than the M4 diameter tap. Testing of M5 diameter taps from different production batches and for different surface treatments did not result in an improvement.

From Figure 5.22, it is evident that the M6 diameter tap failed at significantly higher cutting speed than the smaller taps. However, the recommended cutting speed range for this style of tap in the blind hole tapping of austenitic stainless steel is 3.2 - 8.0 mm/min for the range of 1 - 8 mm diameter taps respectively. At the recommended speeds shown in Figure 5.22, a reduction factor for taps smaller than M6 is not required. While at the upper limit of 8.0 m/min, the M3 diameter taps and smaller are shown closer to their maximum torsional strength. From the results, it is clear that taps of larger diameter than M6 can be run at higher speeds. Further statistical testing is required to establish a reliable equation for a speed reduction factor for taps below M6 diameter.

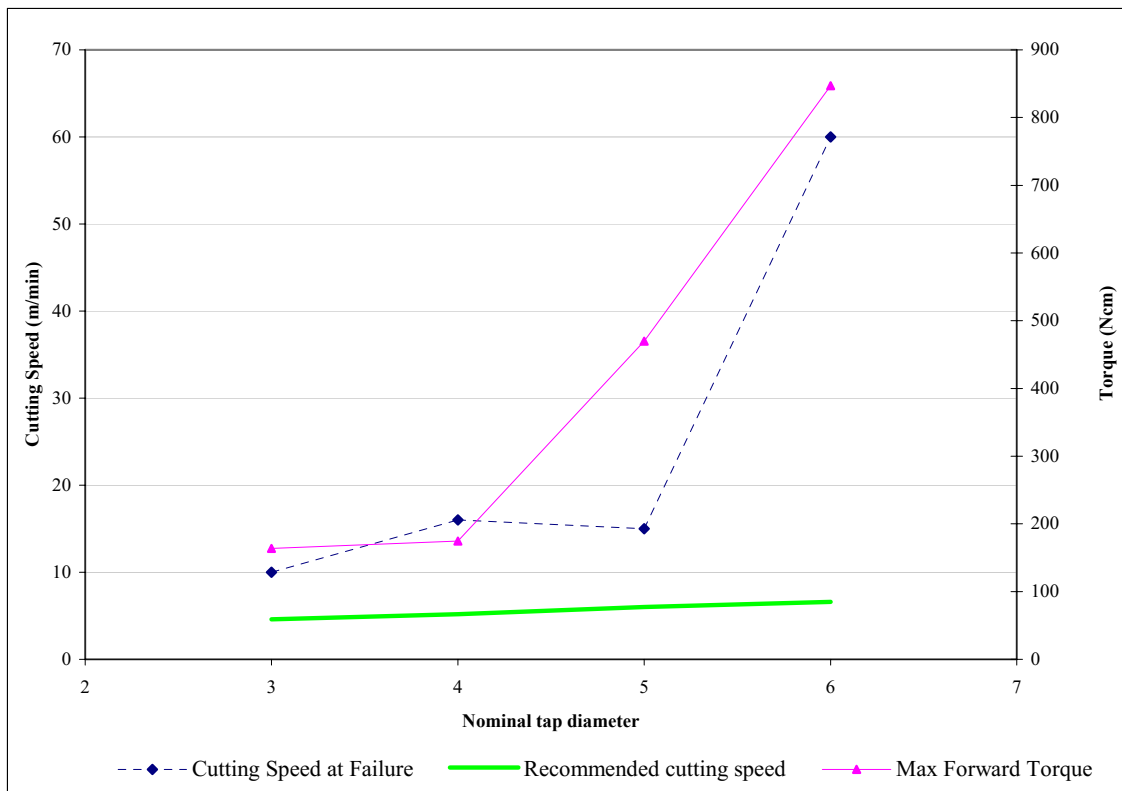


**Figure 5.22.** Chart of the maximum torque and cutting speed at thread failure of a range of tap sizes for a tapped depth of 2D, showing the trend of increased cutting speed capability of taps larger than 5 mm.

The database has been designed with the ability to set recommended cutting speeds for individual taps or for a range of taps. A second option allows for an equation to be incorporated into the modification of the cutting speed according to the tap diameter selected. The initial database set-up using the relationship established in Chapter 3, Section 3.3.5 by knowledge engineered interview process does not reduce the cutting speed as found by this experiment. The failure of the M5 tap at a lower cutting speed than the M4 diameter tap requires a different relationship or method to alter the speed. Modification of the craft oriented rule was made to recommended a cutting speed of 10 m/min for M6 and above to provide a safe operating speed and allow a 50% speed reduction factor for all taps below M6, positioning them in the mid range of the cutting speed capability shown in Figure 5.22. This allows all diameter taps to be recommended with a conservative starting speed without risk of cutting tool failure.

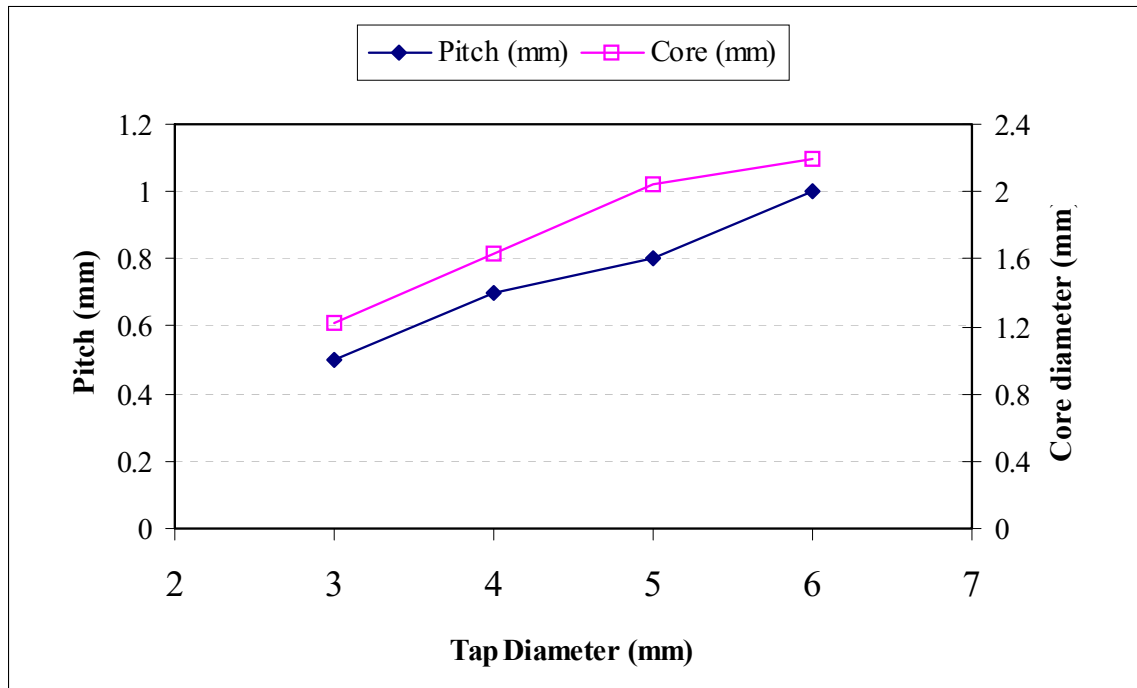


**Figure 5.23.** Chart of the pitch and core size versus tap diameter, showing divergence between the pitch and core at the 5.0 mm tap diameter.

The M5 diameter tap was expected to fail at a higher surface cutting speed than that of the M4 diameter tap. The maximum torque at failure was higher than the M4 diameter tap as expected for a larger diameter tap having increased torsional strength. The cutting speed result for the M5 tap was retested with taps from different batches and different surface treatments and again the taps failed at a similar cutting speed of 15.0m/min. A comparison of tap features, namely, tap core diameter and the tap pitch, were charted in Figure 5.23 to ascertain if they showed an influence on the measured results of the M5 diameter tap. Interestingly, Figure 5.23 shows a divergence between the two features at the M5 diameter tap. Plotting the ratio of the pitch to the core diameter versus the tap diameter (see Figure 5.24) highlights this divergence for the M5 diameter tap.



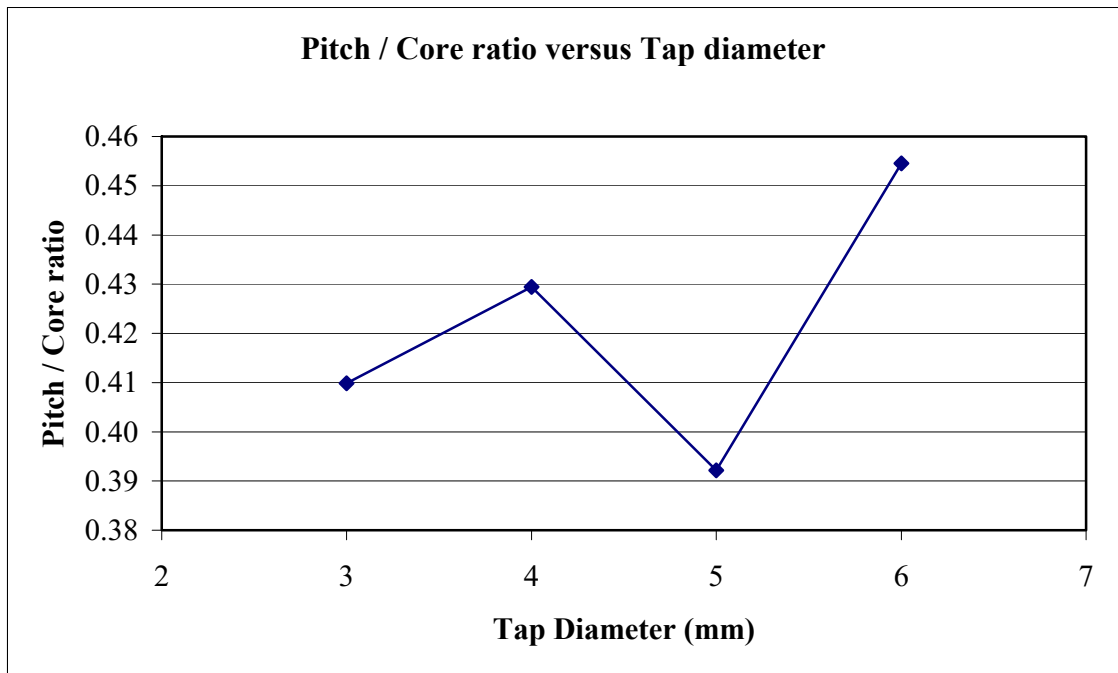


**Figure 5.24.** Chart of the pitch core ratio versus tap diameter, showing divergence between the pitch and core at the 5.0 mm tap diameter.

This effect is counter intuitive with respect to the core diameter of the tap, as the M5 diameter tap is shown with an increased (relative pitch/core ratio) core diameter, which one would expect to increase the strength of the tap in relation to the nominal tap diameter. Further investigation of the effect the Pitch to Core ratio on tap strength at this nominal tap diameter is recommended to improve performance. Time and manufacturing constraints have prevented further study of this observation.

## 5.5 Metal Machining Conclusions

The measured wear of the O.D. relief (thread crest) of the uncoated taps observed by SEM, corresponded with adhesive wear to the rake face of the full form teeth, with evidence of chipping on the lead chamfer teeth after tapping eighty holes. Material transfer was not directly observed on the SEM images of an uncoated tap after tapping eighty holes. The taps passed the plug gauge test until the taps emitted a screech sound over a few holes, at which point they failed they tapped undersize with some failing by fracture.

The uncoated taps showed a short period of improved performance below eighty holes tapped compared to the TiCN taps, believed to be from increased material transfer to the relief face surfaces and cutting edge of the uncoated tap. Further, reduced material transfer at a low number of holes means there is increased contact of the PVD coating with the work material. This asperity contact between the work material and PVD coated taps is thought to cause higher friction thus high torque compared to the uncoated taps at or less than 20 holes tapped. The high carbon stoichiometry of the TiCN coated taps is also the likely cause of the increased torque measured compared to the TiN coated taps.

The poor heat conductivity of stainless steels in comparison to plain carbon steels has been well established to cause increased temperatures localised to the tool / chip interface [14]. Comparing the uncoated taps over eighty holes with the TiN and TiCN coated taps for a non-synchronous attachment, the improved performance of the coatings for torque and thrust for a larger number of holes tapped was evident.

Measured O.D. relief profiles of the PVD coated taps have not shown a pattern of wear for this feature over four hundred and fifty holes tapped and this was confirmed by SEM observation showing minimal wear to the coating. SEM analysis showed evidence of material transfer to the PVD coated taps that can disguise the true O.D. relief measurement of the tap. The variability in measured O.D. relief for the PVD coated taps was attributed to material transfer. From these results, it is suggested the O.D. relief tap feature, is unsuited to measuring wear of PVD coated taps when the addition of work material by material transfer, is greater than measurable wear. Also, the cutting edges suffer significant wear in comparison with the O.D. relief, having greater effect on the measured torque and thrust values. Further investigation is required to establish

if the O.D. relief feature was in a plateau stage of wear for the PVD coated taps and if measurable wear would present before failure of the cutting edges.

SEM analysis of the PVD coated taps comparing attachment types, has shown for the synchronous attachment, abrasive wear on the chamfer lead teeth and evidence of work material transfer on the full form teeth after four hundred and fifty holes tapped. This analysis combined with the results (450+ holes for non-synchronous and 266±93 holes for synchronous), shows a clear advantage for the non-synchronous attachments to reduce the forces and wear for TiCN taps in comparison with the synchronous attachment. The experimental investigation has clarified the effects of CNC controlled machine tools with synchronous and non-synchronous attachments amongst conflicting reports published in engineering literature [55,57,58] that suggest performance benefits for both methods.

The performance benefits of PVD coatings in this study have confirmed previous research [51] in tapping with different work materials on the benefits of such coatings to tool performance. In thread tapping, this advantage has proven to be increased wear resistance to the final sizing teeth of the thread tap for the cutting edges and the outside diameter and thread flank relief surfaces. The improved performance of TiCN coatings, over TiN and uncoated taps in the work materials tested was attributed to the sp<sup>2</sup> carbon bonding of the TiCN coating providing a metal stabilised carbon structure [77] to reduce friction.

In the deep hole tapping experiment, swarf jamming was not observed for any of the hole depths tapped, however swarf compaction in the flutes was the likely cause of the marginal rise in axial thrust. Importantly, the effect of swarf compaction in the flutes contributes to reduced coolant access and work hardening of the chip at the tool/chip interface. This increases the forces on the cutting teeth, leading to increased wear processes of the cutting edges and subsequent tool failure.

Taps of 5 mm in diameter or smaller, were found to fail at a cutting speeds significantly lower than a 6 mm diameter tap. Although the recommended surface cutting speed is not dependent (the RPM changes) on tap diameter, the torsional rigidity and tap features, such as core diameter and pitch, were found to vary between taps of the same design but different diameters. An empirical relationship for surface cutting speed reduction to account for reduced tap diameter was not found due to the 5 mm diameter taps not performing to expectation.

## Overall Discussion

---

The database compiled in this study is an expert system that provides end-users in manufacturing with a user friendly system to make intelligent cutting tool selections using a *knowledge engineered* approach based on *skilled craft oriented knowledge*. The review of the published literature in this field [1,8-13,15,23-34] revealed that the approach had many advantages, the key ones being the utilisation and transfer of expert knowledge, cost and flexibility. The review also highlighted the difficulty of incorporating metal cutting models and other predictive models into a database required to cater for many different cutting tools and application conditions. The predictive models reviewed were not able to encompass the wide range of variables encountered in practical metal machining. Consider, for example, the many process variables encountered in tapping. There are a large number of tap designs for one size tap plus the performance variations in different work materials and in different types of machine set-up. This highlights the economic penalty of testing and / or training such models, if valid performance prediction is to be attained. This complexity of establishing performance predictions reinforces the conclusions reported by Armarego et al. [15] that such an ‘all encompassing’ predictive model remains to be seen.

Expert systems based on the *knowledge engineered* approach, utilise skilled craft oriented knowledge codified into software to provide the sort of recommendations in both cutting tool performance and cutting tool selection that one might expect from consultation with a cutting tool engineer. The advantage of this approach is the ability to modify the skilled craft oriented rules to include empirical relationships or include data from predictive models for specific conditions within the database as new knowledge is acquired. A review of expert systems [8-12] revealed this to be the most common approach used to provide intelligent cutting tool selection and performance recommendation with a study of one expert system [8] revealing the use of Taylor-like forms of empirical equations to provide performance values.

Thus, the *knowledge engineered* approach was the one adopted to set up a working expert system for selection, recommendation and performance of cutting tools supplied by a local manufacturer. In keeping with the findings of the review, it was decided to

interrogate the expert system in the specific area of tapping of austenitic stainless steel in order to challenge by experiment, skilled craft oriented knowledge in this area. The following four areas were selected for investigation:

- Comparison of PVD coated (TiN and TiCN coatings) with uncoated taps with respect to tap performance measures.
- Comparison of synchronous and non-synchronous tapping attachments.
- The effects of increasing the tapped hole depth on the torque and thrust and the effect of reducing cutting speed with increased hole depth.
- The effect of reducing the tap diameter on the recommended cutting speed.

Comparing the results of the first experiment with the published expert systems (see Chapter 2, Section 2.2, Figure 2.5), it is evident that the results are consistent with the recommendations of the cutting tool manufacturers with respect to the number of holes tapped compared to the type of surface treatment. Only three of the four cutting tool manufacturers recommend both TiN and TiCN coatings. Of the three, two show TiCN to have a greater tool life than TiN when tapping austenitic stainless steel. This is in agreement with the results of the current investigation. The experimental result was successfully incorporated into the database and used to establish a preferential sort order of taps recommended to an end-user. The uncoated taps having an average tool life of 80 holes, TiN taps an average of 360 holes and TiCN taps still performing at 450 holes. The forward cutting torque was shown to increase with the number of holes tapped for the uncoated and TiN coated taps, however, it remained at a plateau for the TiCN coated taps. For stainless steel thread tapping, the order of preference used for the database was TiCN, TiN followed by uncoated taps.

The second experiment provided qualitative information on the effects of using different types of tapping attachments on performance. The results revealed that the non-synchronous attachment provided the best performance in terms of thrust, torque and tool life. The tool life results showed the synchronous attachment to reduce tool life by nearly half the measured number of holes for the non-synchronous attachment (266±93 holes to 450+ holes respectively). These results are difficult to quantify in an empirical rule for performance recommendation and is further complicated by the tapping conditions and machine set-up for different end-users.

The solution for use of these results in the database was to provide for taps designed specifically for synchronous attachments (the poorer performing) to overcome the deficiencies discussed, such as, improved coolant access and chip disposal. The results confirmed the need for taps to be designed with reduced friction and also for accurate machine tool synchronisation. As such, the database provides a selection choice for the two tap designs suitable for each attachment and sorts these two tap designs preferentially for each attachment choice.

The third set of experiments, showed that increasing the tapped hole depth by two tap diameters or greater gave significant increases in torque (up to 150% at 3D). The craft oriented rule established for the database for reducing cutting speed was compared with the measured torque results. The results showed that the maximum torque increased in a similar trend to the increases observed when keeping the speed constant while increasing hole depth. The results of both experiments indicated that adopting slower cutting speeds did not significantly reduce torque and therefore lubricant access is not necessarily improved. The rules established by the craft oriented approach were included on the recommendation of the skilled craft oriented experts, until more testing to evaluate this relationship with respect to the number of holes tapped provides usable qualitative information.

The final experiment was to establish the relationship between torsional strength of a tap as a function of decreasing tap diameter, which was revealed to be a common problem when blind-hole thread tapping in difficult to machine work materials [48]. For the range of taps tested, tap breakage and/or thread failure was found to occur in an exponential-like pattern with cutting speed. However, the M5 diameter tap fell outside of this trend. Further investigation of the M5 diameter tap revealed that the design features did not reduce proportionally as was the case for the smaller tap diameters, preventing the skilled craft oriented rule from being validated. This craft oriented relationship established in Chapter 3, Section 3.3.2, Figure 3.5 holds for taps below M6 diameter provided the initial recommended cutting speed value remains less than or equal to 8.0 m/min for M6 and larger diameter taps. Then the recommended cutting speeds for the smaller diameter taps fall midway of the maximum cutting speed at which failure occurred and still lie in the recommended speed range of 3 – 8 m/min. Further investigation of the M5 tap features are required to allow an improved tap to be designed to validate this approach with respect to the skilled craft oriented knowledge.

## Conclusions

---

Over the period of this investigation an expert system based on the knowledge engineered approach was set up for the selection and performance assessment of cutting tools as supplied by a local manufacturer. This approach was adopted following a review of the literature and the realization that the key strength of the approach was its flexibility to modify skilled craft oriented rules and include data from predictive models for specific conditions as new knowledge emerges.

An investigation into tapping of austenitic stainless steels was undertaken to develop part of a larger expert system. The following key findings were obtained and incorporated into the expert system where appropriate:-

- The PVD TiCN coated taps out performed the PVD TiN coated taps, which in turn had significantly improved performance over the uncoated taps when tapping austenitic stainless steel. Consequently the TiCN coated taps were recommended for tapping in austenitic stainless within the expert system. Improvement of the TiCN over the TiN taps was assumed attributed to  $sp^2$  carbon bonding at the surface of the coating providing reduced friction and tribological wear resistance to rubbing. The higher torque observed for the PVD coated taps compared with the uncoated taps was attributed to be from the lower coefficient of friction associated with the coatings allowing the taps to cut closer to size. Thus, there is more asperity contact between the tap and work material leading to high measured torque.
- A key finding was that metallographic analysis showed evidence of material transfer on the taps. The uncoated taps showed adhesive wear on the cutting edges leading to early tool failure with wear being measured by the outer diameter (O.D.) relief. Material transfer was observed on the PVD coated (TiCN and TiN) taps, however, evidence of adhesive wear was not observed. Material transfer and lack of significant wear prevented reliable measurement of the O.D. relief of the PVD coated taps. Wear processes of the PVD coatings were assumed attributed to thin film rubbing tribological wear.

- The non-synchronous tapping attachment showed a major performance benefit over the synchronous tapping attachment. It was found that machine synchronisation was the main cause for the performance difference when using a CNC machine tool with spindle / feed synchronisation capability. Machine tool set up conditions and synchronisation accuracy can vary with the end-user, this prevented quantification of empirical rules within the expert system. However, the expert system was modified to allow for taps designed specific to the attachment type and sorts them in order of preference depending on which is selected. For synchronous tapping, attachments with a small amount of axial movement are recommended to account for poor synchronisation.
- The results of the deep-hole tapping test confirmed that torque increases with tapped hole depth due to restricted lubricant access as a result of swarf compaction within the flutes at a depth of 2.5 tap diameters and greater. This lead to higher stresses at the cutting edges and work hardening of the chip at the chip/tool interface. The reduction of surface cutting speeds to allow more coolant access, had a minimal effect on cutting torque, however reduced cutting speeds remain as a recommendation to reduce the problem of swarf compaction. Swarf jamming (in which, the tap seizes in the hole) was not observed to be the cause of tap failure when deep hole tapping using spiral fluted taps. A redesign of tap features and further investigation is required. An outcome of this investigation is that the local manufacturer has implemented a program to introduce coolant through the body of the taps to exit near the cutting edges.
- The effect of tap rigidity on cutting speed was found to be significant for taps less than 6 mm in diameter. However, a skilled knowledge rule was not validated due to a 5 mm tap being inferior to both the 4 mm and 6 mm taps in performance. Further redesign of the 5 mm tap is recommended to improve the performance with respect to the 4 mm and 6 mm taps. The expert system utilised the knowledge rule established from the skilled craft oriented engineers, however, the rule is restricted to a maximum cutting speed at and above the speed used for the 6 mm diameter tap. This ensures a conservative recommended surface cutting speed for taps below 6 mm in diameter.



## **Future Work**

---

Further studies on tooling characteristics, machining techniques, work-piece materials and coatings are recommended for inclusion into the database. Importantly, broader studies are needed on advanced surface engineered coatings that aim to reduce friction. This is particularly important in the area of tapping due to the high rubbing contact between the tap and work-piece material.

## References

---

- [1] E.M. Trent, P.K. Wright, "Metal Cutting", 4<sup>th</sup> edition, Butterworth Heinmann, USA, pp372-408, 2000.
- [2] S. J. Dowey, "Advanced On-line and Off-line Process Control for Surface-Engineered Applications", Phd Thesis, University of Hull, October 1999.
- [3] F.W. Taylor, Trans. A.S.M.E., v28, pp21, 1907.
- [4] O.A. Meezentsev, R. Zhu, R.E. DeVor, S.G. Kapoor, W.A. Kline, "Use of radial forces for fault detection in tapping", Int. J. Machine Tools and Manufacture, v42, pp479-488, 2002.
- [5] W. Li, D. Li, J. Ni, "Diagnosis of tapping process using spindle motor current", Int. J. Machine Tools and Manufacture, v43, pp73-79, 2003.
- [6] T.I. Liu, E.J. Ko, J.L. Sha, "Diagnosis of tapping operations using AI approach", Journal of Material Shaping Technology, v9, pp39-46, 1991.
- [7] A.P.S. Dogra, S.G. Kapoor, R.E. DeVor, "Mechanistic model for tapping process with emphasis on process faults and hole geometry", Proceedings of ASME MED10, Nov 14-Nov 19, pp271-283, 1999.
- [8] Titex Electronic Catalog v.5.0, 2000, D-60489 Frankfurt am Main, Germany.
- [9] Dormer Product Selector 2001, S20 3RW, Dormer Tools, Sheffield, England.
- [10] EMUGE-FRANKEN Tool Finder TF v.2.0, D-91207 Lauf, Germany.
- [11] OSG Electronic Catalogue, <http://www.osgnet.com/select/taps/english/>.
- [12] CCS Prototyp Electronic Catalogue v.4, 1996.
- [13] B. Y. Lee, H. S. Liu, Y. S. Tarng, "An Abductive Network for predicting Tool Life in Drilling", IEEE Transactions on Industry Applications, v35 (1), pp190-195, 1999.
- [14] "Technical Handbook of Stainless Steels", Atlas Steels Pty. Ltd, revised November 2000.
- [15] E.J.A. Armarego, D. Ostafiev, S.W.Y. Wong, S. Verezub, "An Appraisal of Empirical Modelling and Proprietary Software Databases for Performance

- 
- Prediction Machining Operations”, 4<sup>th</sup> CIRP International Workshop on Modelling Machining Operations, August 2000, UNSW, Australia.
- [16] I. Finnie, “Review of the Metal Cutting Analyses of the Past Hundred Years”, American Society of Mechanical Engineers, Mechanical Engineering, v78, pp715, 1956.
- [17] A.G. Kosilova, R.K. Mescheryakov, “Technological Machining Handbook”, Machinostroeniye, Moscow, 1985.
- [18] X. Ai, Q. Tao, S. Xiao, “Metal Cutting Conditions Handbook”, Mechanical Industry Press, China, 1966.
- [19] X. Ai, S. Xiao, “Metal Cutting Conditions Handbook”, Mechanical Industry Press, China, 1985.
- [20] ASME Research Committee on Metal Cutting Data and Bibliography, “Manual on Cutting Metals with Single-Point Tools”, 2<sup>nd</sup> edition, American Society of Engineers, 1952.
- [21] Sutton Pty. Ltd. Printed Catalogue, 1999.
- [22] Prototyp Pty. Ltd. Printed Catalogue 1998.
- [23] S.M. Wu, “Tool life testing by response surface methodology”, parts I and II, Trans. ASME v86, pp105-116, 1964.
- [24] I.A. Choudhury, M.A. El-Baradie, “Tool-life prediction model by design of experiments for turning high strength steel (290 BHN)”, Journal of Materials Processing Technology, v77, pp319-326, 1998.
- [25] E.O. Ezugwu, S.J. Arthur, E.L. Hines, “Tool-wear prediction using artificial neural networks”, Journal of Materials Processing Technology, v49, pp255-264, 1995.
- [26] R.G. Silva, R.L. Reuben, K.J. Baker, S.J. Wilcox, “Tool wear monitoring of turning operations by neural network and expert system classification of a feature set generated from multiple sensors”, Mechanical Systems and Signal Processing, v12 (2), pp319-332, 1998.

- 
- [27] R.G. Silva, K.J. Baker, S.J. Wilcox, R.L. Reuben, "The adaptability of a tool wear monitoring system under changing cutting conditions", *Mechanical Systems and Signal Processing*, v14 (2), pp287-298, 2000.
- [28] B.Y. Lee, Y.S. Tarn, H.R. Lii, "An investigation of modelling of the machining database in turning operations", *Journal of Materials Processing Technology*, v105, pp1-6, 2000.
- [29] A.G. Ivakhnenko, "Polynomial theory of complex systems", *IEEE Trans. Syst. Man Cybernetics*, v1 (4), pp364-378, 1971.
- [30] H. Wiklund, "Bayesian and regression approaches to on-line prediction of residual tool life", *Quality and Reliability Engineering International*, v14, pp303-309, 1998.
- [31] E.J. Armarego, H. Zhao, "Predictive Force Models for Point-Thinned and Circular Centre Edge Twist Drill Designs", *Annals of the CIRP*, v45, 1, pp65-70, 1996.
- [32] H.T. Huang, C.I. Weng, C.K. Chen, "Prediction of Thrust and torque for Multifacet Drills (MFD)", *J. of Engineering for Industry*, v116, pp1-7, 1994.
- [33] T. Cao, J.W. Sutherland, "Investigation of thread tapping load characteristics through mechanistic modelling and experimentation", *Int. J. Machine Tools and Manufacture*, v42, pp1527-1538, 2002.
- [34] M. Elhachimi, S. Torbaty, P. Joyot, "Mechanical modelling of high speed drilling. 1: predicting torque and thrust", *Int. J. Machine Tools and Manufacture*, v39, pp553-568, 1999.
- [35] E.J. Armarego, "Cutting with Double Edge Tools: Symmetrical Triangular Cuts", *International Journal of Machine Design Research*, v7, pp23, 1967.
- [36] W.E. Henderer, "On the Art of Tapping Metals", Ph.D Dissertation, The University of Vermont, 1976.
- [37] N. Gane, "The Tapping of Screw Threads", CSIRO Division of Manufacturing Technology, Melbourne, Report No. MTM 96, v1-2, 1984.
- [38] D.E.Y. Zhang, D.C. Chen, "Relief-face friction in vibration tapping", *International Journal of Mechanical Science*, v40, n12, pp1209-1222, 1998.
-

- 
- [39] L. Carrol, "Tapping the Deep Hole – It can be done, but it takes specific tools and special measures", *Cutting Tool Engineering*, v47, n5, August 1995.
- [40] P. Fretty, "Going Deep – Deep-hole tapping takes on a new dimension when the workpiece material is aerospace-grade titanium", *Cutting Tool Engineering*, v53, n1, January 2001.
- [41] H.W. Lo, S. Kaldor, P.K. Venuvinod, "A 'Broad-Brush' approach to the selection of general purpose cutting tool geometry for maximum tool life", *Int. J. Machine Tools and Manufacture*, v38 (1-2), pp1-14, 1998.
- [42] K.Hashmi, M.A. El-Baradie, M. Ryan, "Fuzzy-logic based intelligent selection of machining parameters", *Journal of Materials Processing Technology*, v94, pp94-111, 1999.
- [43] K.Hashmi, I.D. Graham, B. Mills, "Fuzzy logic based data selection for the drilling process", *Journal of Materials Processing Technology*, v108, pp55-61, 2000.
- [44] G.E. D'Errico, "Fuzzy control systems with application to machining processes", *Journal of Materials Processing Technology*, v109, pp38-43, 2001.
- [45] Metcut Research Associates, "Machining Data Handbook", 3<sup>rd</sup> edition, v1-2, Cincinnati, 1980.
- [46] E.J.A. Armarego, S.W.Y. Wong, "An Appraisal of a Drilling Performance Database within a Proprietary Machining Software Package", Research Report 2000/MP/1, Manufacturing Science Group, Department of Mechanical and Manufacturing Engineering, University of Melbourne.
- [47] E.J.A. Armarego, S. Verezub, "The Influence of Tool Surface Coatings on the Cutting Action, Friction and Performance of various machining Operations", The 12<sup>th</sup> International Federation of Heat Treatment and Surface Engineering Congress, v1 29<sup>th</sup> Oct- 2<sup>nd</sup> Nov 2000, Melbourne.
- [48] S. Patil, S. S. Pande, S. Somasundaram, "Some Investigations on Vibratory Tapping Process", *Int. Journal of Machine Tools Manufacturing*, v27 (3), pp343-350, 1987.

- 
- [49] J.E. Williams, E.F. Smart, D.R. Milner, "The Metallurgy of Machining -Parts I, II and III", *Metallurgia*, v81, 1970.
- [50] V.V. Matveev, "Torque Deformation of taps", *Machines and Tooling*, v42, n6, 1970.
- [51] S. G. Harris. "Improved Performance of Metal Cutting Tools by Advanced Physical Vapour Deposited Coatings: Applications in the Automotive Industry", Masters Thesis, School of Engineering and Science, Swinburne University of Technology, Australia, 2001.
- [52] ASME B94.9-1999, "Taps: Ground and cut threads (inch and metric sizes). An American national standard", The American society of mechanical engineers, 1999.
- [53] B. Kennedy (ed.), "Whats on Tap", *Cutting Tool Engineering*, v54 (5), May 2002.
- [54] D. Ridenour, P. Matysiak, "Speed Tapping – Users discover the technology they need to boost tapping rpm", *Cutting Tool Engineering*, v50, n5, August 1998.
- [55] A. Krenick, "Rigid Rules", *Cutting Tool Engineering*, v48, n5, August 1996.
- [56] P. Zierhut, "New Twists on Threading", *Cutting Tool Engineering*, v48, n5, August 1996.
- [57] D. Moore, "Driving the Tap", *Cutting Tool Engineering*, v47, n5, August 1995.
- [58] D. Esford, "Thread Heads – How the pros tap a lot of holes at high speeds", *Cutting Tool Engineering*, v52, n1, January 2000.
- [59] F. Mason, "Threading your way through thread gaging", *Society of Manufacturing Engineers, Manufacturing Engineering*, v116, n4, pp37, April 1996.
- [60] B.F. von Turkovich, W.E. Henderer, "On the Tool Life of High Speed Steel Tools", *Annals of the CIRP*, v27, n1, 1978.
- [61] E.D. Doyle, "Fractographic Study of the Failure of High Speed Steel Taps using the Scanning Electron Microscope", *Harold Armstrong Conference in Production Science in Industry*, Melbourne, Australia, 1971.
-

- 
- [62] Audy J., Harris S.G., Audy K., Brinkles H., Doyle E.D., McKenzie D.R., “Performance evaluation of cathodic arc evaporated (cae) TiAlCrN coated general purpose twist drills when dry machining grey cast iron”, 5<sup>th</sup> Int. Conf. On behaviour of materials in Machining, 11-14<sup>th</sup> November, England, Chester, 2002.
- [63] E. D. Doyle, S. K. Dean, “Effect of Axial Forces on Dimensional Accuracy During Tapping”, Int. Journal of Machine Tool Design and Research, v14, pp325-333, 1974.
- [64] Tapmatic Corporation, “New SynchroFlex – The rigid tap driver that does more than just hold a tap”, printed product brochure,  
[http://www.tapmatic.com/pdfs/NewSynchroflex10\\_01.pdf](http://www.tapmatic.com/pdfs/NewSynchroflex10_01.pdf)
- [65] V.V. Matveev, “Determining Thrust in Tapping”, Machines and Tooling, v41, n5, pp44-46, 1970.
- [66] A.A. Grudov, “The Influence of Cutting Speed and Tap Wear on Torque”, Machines and Tooling, v34, n1, 1966.
- [67] G. Lorenz, “On Tapping Torque and Tap Geometry”, Annals of the CIRP v29 (1), 1980.
- [68] M. Routio, M. Säynätjoki, “Tool wear and failure in the drilling of stainless steel”, Journal of Materials Processing Technology, v52, pp35-43, 1995.
- [69] A.A. Grudov, “Composite Radial Relief Taps for Blind Holes”, Machines and Tooling, v39, n6, pp34-37, 1968.
- [70] Filemaker Pro 5.1 Developer database software, Filemaker Inc. subsidiary of Apple Computer Inc.
- [71] ERASTEEL 2003 website, <http://www.erasteel.com/us/produits/hss.php>
- [72] Audy J., “Development of Metal Machining Process Parameters and the Development of Adaptive Control”, PhD Thesis, Gartrell School of Mining, Metallurgy and Geology, The University of South Australia, p. 23, June 1996.
- [73] E.J.A. Armarego, “Machining performance prediction for modern manufacturing”, Proceedings of 7<sup>th</sup> Int. Conference on Production and Precision

---

Engineering and 4<sup>th</sup> Int. Conference on High Technology, Chiba, Japan, pp. k52, 1994.

[74] Operating Instructions Quartz 4 component dynamometer Type 9272, Kistler Instrument AG, CH-8408 Winterthur, Switzerland, 2000.

[75] D. Camino, A. H. S. Jones, D. Mercs, D. G. Teer, "High performance sputtered carbon coatings for wear resistant applications", *Vacuum*, v.52, pp125-131, 1999.

[76] V. C. Fox, A. Jones, N. M. Renevier, D. G. Teer, "Hard lubricating coatings for cutting and forming tools and mechanical components", *Surface and coatings technology*, v.125, pp347-353, 2000.

[77] D.R. McKenzie, "Tetrahedral bonding in amorphous carbon", *Rep. Prog. Phys.*, v.59, pp1611-1664, 1996.

[78] N.P. Suh, "The delamination theory of wear", *Wear*, v.25, pp111-124, 1973.

[79] J. Boyd, T. vom Braucke, J. Audy, "Preliminary investigations of the measured thrust and torque trends when drilling and tapping type 316 stainless steel workpiece material", Internal report II, Sutton Tools, August 2002.



## Appendix 1 – Taps Database Specification

Taps sorting algorithm	
Order in sorting process	Sort type
1.	Material Group
2.	If(suitableRatio <= 1.5) then SortBy: maxRatio: low -> high Else SortBy: maxRatio: high -> low /if
3.	Speed (Vc): high -> low
4.	Coating Type per material group
5.	Attachment Type: If (type = synch) then SortBy: synch: high -> low Else Find: non-synch
Note:	$\text{SuitablRatio} = \frac{\text{thread\_depth\_specified\_in\_search}}{\text{diameter\_specified\_in\_search}}$

Taps Calculation algorithm for Speed (Vc) and Torque (Md)	
Calculation order	Calculation type
1.	$V_{c_{rec}} = V_c \cdot gTDmod \cdot S_f \cdot F_f$
2.	Depth Factor = gTDmod
3.	Strength Factor = $S_f$
4.	Torque Md: $M_D = k_{c1.1} \cdot h_m^{(1-mc)} \cdot \frac{D.P.Z}{40} \cdot T_d^{kt} \cdot T_a$
Note:	$F_f$ : Surface treatment (finish) factor included for future potential use.

## Appendix 2 – Statistical Data

**Table A.** Statistical analysis of max torque and thrust data up to eighty holes for all taps.

Holes	Statistical results for $T_q$ forward	Meaning
1	Bartlett test passes at 95%C.L. Chisqr = 3.519; Chisqr tab = 5.99, thus Anova fails at 95% and higher C.L. Fvalue = 13.49; Fstat = 3.89, thus	Variances same = 24.9 Means different = 301 for uncoated taps 348 for TiN coated taps 383 for TiCN coated taps
20	Bartlett test passes at 95%C.L. Chisqr = 1.27; Chisqr tab = 5.99, thus Anova passes at 95% C.L. Fvalue = 1.24; Fstat = 3.89, thus	Variances same = 25.67 Means same = 369.53
80	Bartlett test passes at 95%C.L. Chisqr = 4.34; Chisqr tab = 5.99, thus Anova passes at 95% C.L. Fvalue = 3.37; Fstat = 3.89, thus	Variances same = 39.59 Means same = 380.86
Holes	Statistical results for $T_h$ forward	Meaning
1	Bartlett test passes at 95%C.L. Chisqr = 5.26; Chisqr tab = 5.99, thus Anova passes at 95% C.L. Fvalue = 1.56; Fstat = 3.89, thus	Variances same = 7.35 Means same = 50.93
20	Bartlett test passes at 95%C.L. Chisqr = 2.79; Chisqr tab = 5.99, thus Anova passes at 95% C.L. Fvalue = 0.05; Fstat = 3.89, thus	Variances same = 8.9 Means same = 57.26
80	Bartlett test fails at 95%C.L. Chisqr = 6.83; Chisqr tab = 5.99 Welch test passes at 95%C.L. Fvalue = 2.09; Fstat = 4.96, thus	Variances different = 10.5 for uncoated taps 2.7 for TiN coated taps 4.5 for TiCN coated taps Means same = 53.3
Holes	Statistical results for $T_q$ reverse	Meaning
1	Bartlett test passes at 95%C.L. Chisqr = 3.99; Chisqr tab = 5.99, thus Anova fails at 95% C.L. Fvalue = 4.39; Fstat = 3.89, thus Anova passes at 97.5%C.L Fvalue = 4.39; Fstat = 5.1, thus	Variances same = 58.3 Means different = 266 for uncoated taps 304 for TiN coated taps 374 for TiCN coated taps Means same = 314
20	Bartlett test passes at 95%C.L. Chisqr = 0.408; Chisqr tab = 5.99, thus Anova passes at 95% C.L. Fvalue = 2.43; Fstat = 3.89, thus	Variances same = 37.4 Means same = 315.4
80	Bartlett test passes at 95%C.L. Chisqr = 1.58; Chisqr tab = 5.99, thus Anova passes at 95% C.L. Fvalue = 0.45; Fstat = 3.89, thus	Variances same = 31.7 Means same = 272.7
Holes	Statistical results for $T_h$ reverse	Meaning
1	Bartlett test fails at 95%C.L. Chisqr = 6.83; Chisqr tab = 5.99 Welch test passes at 95%C.L. Fvalue = 2.96; Fstat = 5.47, thus Bartlett test passes at 97.5%C.L. Chisqr = 5.26; Chisqr tab = 5.99, thus	Variances different = 1.1 for uncoated taps 5.6 for TiN coated taps 4.5 for TiCN coated taps Means same = 30.8 Variances same = 4.2
20	Bartlett test passes at 95%C.L. Chisqr = 4.73; Chisqr tab = 5.99, thus Anova fails at 95% C.L. Fvalue = 10.4; Fstat = 3.89, thus Anova fails at 97.5%C.L. Fvalue = 10.4; Fstat = 5.1 Anova passes at 99.9% C.L. Fvalue = 10.4; Fstat = 12.9, thus	Variances same = 2.8 Means different = 29 for uncoated taps 29.6 for TiN coated taps 36.2 for TiCN coated taps Means same = 31.6
80	Bartlett test passes at 95%C.L. Chisqr = 2.88; Chisqr tab = 5.99, thus Anova fails at 95% C.L. Fvalue = 7.19; Fstat = 3.89, thus Anova fails at 97.5%C.L. Fvalue = 7.19; Fstat = 5.1 Anova passes at 99.9% C.L. Fvalue = 7.19; Fstat = 12.9, thus	Variances same = 2.4 Means different = 29 for uncoated taps 25 for TiN coated taps 24 for TiCN coated taps Means same = 26.5

**Table B.** Maximum torque and thrust data of TiCN taps for attachment comparison statistics up to four hundred and fifty holes tapped. Data was analysed by the same process as Table A.

Holder Type	Tap number	Maximum Torque (Ncm)											
		Forward						Reverse					
		1h	20h	80h	200h	300h	450h	1h	20h	80h	200h	300h	450h
Floating	T1_01C	411	399	363	356	389	376	477	378	333	310	280	374
	T1_02C	361	363	342	325	337	371	363	297	226	241	291	227
	T1_03C	331	366	367	359	374	398	292	352	248	228	267	228
	T1_04C	408	424	389	354	388	394	310	369	256	195	248	249
	T1_05C	404	369	356	339	370	380	428	302	247	231	135	182
Rigid	T3_01B	405	377	337	366	365	366	394	347	265	226	233	188
	T3_02B	409	360	359	-	-	-	444	261	244	-	-	-
	T3_03B	421	376	360	383	-	-	376	271	267	223	-	-
	T3_04B	458	366	315	393	352	436	414	305	277	305	349	278
	T3_05B	418	341	321	360	354	391	360	319	277	480	267	156
Holder Type	Tap number	Maximum Thrust (N)											
		Forward						Reverse					
		1h	20h	80h	200h	300h	450h	1h	20h	80h	200h	300h	450h
Floating	T1_01C	57	46	60	67	60	45	41	41	23	30	22	28
	T1_02C	48	45	60	56	52	45	29	34	27	26	34	26
	T1_03C	44	58	49	58	61	55	34	35	23	26	27	27
	T1_04C	47	71	58	68	52	50	35	38	23	37	29	22
	T1_05C	43	71	57	51	55	45	38	33	24	27	28	26
Rigid	T3_01B	144	210	221	193	210	187	372	723	615	391	625	344
	T3_02B	161	159	111	-	-	-	367	515	507	-	-	-
	T3_03B	122	171	161	163	-	-	273	699	550	359	-	-
	T3_04B	151	220	232	195	229	162	322	701	602	359	705	411
	T3_05B	199	298	249	203	162	139	342	773	586	456	581	375

Note: - tap failure, data not recorded.

---

## **Appendix 3 – Database URL**

### Internet database – Expert System version 1

A prototype version was created on CD-ROM, however significant improvements to the operation of the database were made during and after the conversion from the database software to the Internet/website version. This improvement over the prototype version was in part, due to the limitations of the database software in handling large amounts of data. The 2004 website address presented below, hosts a functioning version of the original database and is subject to change by the owner.

<http://www.sutton.com.au/page.swhtml?page=expertToolSystem>